5. EXPLANATORY NOTES[1]

Shipboard Scientific Party[2]

INTRODUCTION

Information assembled in this chapter will help the reader understand the basis for our preliminary conclusions and will also enable the interested investigator to select samples for further analysis. This information concerns only shipboard operations and analyses described in the site reports in the Leg 201 *Proceedings of the Ocean Drilling Program, Initial Reports* volume. Methods used by various investigators for shore-based analyses of Leg 201 samples will be described in the individual contributions published in the Leg 201 *Scientific Results* volume and in publications in various professional journals.

Authorship of Site Chapters

The separate sections of the site chapters were written by the following shipboard scientists (authors are listed in alphabetical order, no seniority is implied):

Leg summary and principal results: Shipboard Scientific Party
Background and objectives: D'Hondt, Jørgensen
Operations: Miller, Storms
Lithostratigraphy: Aiello, Meister, Naehr, Niitsuma
Biogeochemistry: Blake, Dickens, Hinrichs, Holm, Jørgensen, Mitterer, Solis Acosta, Spivack
Microbiology: Cragg, Cypionka, Ferdelman, House, Inagaki, Jørgensen, Naranjo Padilla, Parkes, Schippers, Smith, Teske, Wiegel
Physical properties: Bekins, Ford, Gettemy, Niitsuma, Skilbeck
Downhole tools: Bekins, Dickens
Downhole logging: Guèrin
Observer (Ecuadorian): Naranjo Padilla
Observer (Peruvian): Solis Acosta

[1]Examples of how to reference the whole or part of this volume.
[2]Shipboard Scientific Party addresses.

Drilling Operations

Two standard coring systems were used during Leg 201, the advanced hydraulic piston corer (APC), and the extended core barrel (XCB). These standard coring systems and their characteristics are summarized in the "Explanatory Notes" chapters of various previous *Initial Reports* volumes as well a number of *Technical Notes*. Most cored intervals were ~9.5 m long, which is the length of a standard core barrel. In other cases the drill string was drilled, or "washed ahead," without recovering sediments to advance the drill bit to a target depth where core recovery needed to resume.

Drilled intervals are referred to in meters below rig floor (mbrf), which are measured from the kelly bushing on the rig floor to the bottom of the drill pipe, and meters below seafloor (mbsf), which are calculated from the length of pipe deployed less estimated seafloor depth. When sediments of substantial thickness cover the seafloor, the mbrf depth of the seafloor is determined with a mudline core, assuming 100% recovery for the cored interval in the first core. Water depth is calculated by subtracting the distance from the rig floor to sea level from the mudline measurement in mbrf. This water depth usually differs from precision depth recorder measurements by a few to several meters. The mbsf depths of core tops are determined by subtracting the seafloor depth (mbrf) from the core top depth (mbrf). The resulting core top datums in mbsf are the ultimate reference for any further depth calculation procedures.

Drilling Deformation

When cores are split, many show signs of significant sediment disturbance, including the concave-downward appearance of originally horizontal bedding, haphazard mixing of lumps of different lithologies (mainly at the tops of cores), fluidization, and flow-in. Core deformation may also occur during retrieval because of changes in pressure and temperature as the core is raised and during cutting and core handling on deck.

Curatorial Procedures and Sample Depth Calculations

Numbering of sites, holes, cores, and samples follows the standard Ocean Drilling Program (ODP) procedure (Fig. F1). A full curatorial identifier for a sample consists of the leg, site, hole, core number, core type, section number, and interval in centimeters measured from the top of the core section. For example, a sample identification of 201-1225A-1H-1, 10–12 cm, represents a sample removed from the interval between 10 and 12 cm below the top of Section 1, Core 1 (H designates that this core was taken with the APC system) of Hole 1225A during Leg 201. Cored intervals are also referred to in "curatorial" mbsf. The mbsf depth of a sample is calculated by adding the depth of the sample below the section top and the lengths of all higher sections in the core to the core top datum measured with the drill string.

A sediment core from less than a few hundred mbsf may, in some cases, expand upon recovery (typically 10% in the upper 300 mbsf), and its length may not necessarily match the drilled interval. In addition, a coring gap is typically present between cores. Thus, a discrepancy may exist between the drilling mbsf and the curatorial mbsf. For instance, the curatorial mbsf of a sample taken from the bottom of a

F1. Coring and depth intervals, p. 67.
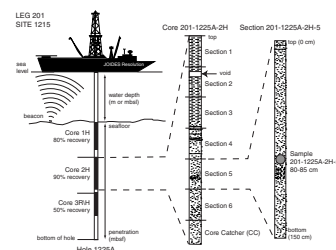
core may be larger than that of a sample from the top of the subsequent core, where the latter corresponds to the drilled core-top datum.

If a core has incomplete recovery, all cored material is assumed to originate from the top of the drilled interval as a continuous section for curation purposes. The true depth interval within the cored interval is not known. This should be considered as a sampling uncertainty in age-depth analysis and correlation of core facies with downhole log signals.

Core Handling and Analysis

To ensure as little damage as possible to the microbial communities present in cores, a unique core processing strategy was established for Leg 201. Since microorganisms existing at deepwater seafloor temperatures (2°–4°C) can be acutely sensitive to elevated temperature (>10°C) and oxygen, we recognized a critical need to prevent thermal equilibration and exposure of the cores to oxygen after recovery. To minimize equilibration of the cores, we modified the standard coring practice of shelving a recovered core barrel on the rig floor while a new core barrel is deployed and a joint of pipe is added. The core barrel was extracted from the drill string and immediately transferred to the catwalk and marked by the ODP curatorial staff into 1.5-m sections. Shipboard microbiologists identified one or more 1.5-m sections (hereafter referred to as the MBIO sections) for rapid microbiological processing. Once the MBIO sections were selected, they were labeled with a red permanent marker with orientation and section number and removed from the core. Ends of the removed sections were covered with plastic caps but not sealed, and the sections were carried into the hold refrigerator, which was set to ~4°C and served as a microbiology cold room. After some modifications to the cooling unit and installation of plastic sheets across the door to dampen air exchange, thermal loggers indicated an ambient temperature in the cold room of ~6°C. Multiple sections were moved to the cold room in order to ensure that sufficient undisturbed material was available for microbiology and coupled geochemistry sampling. Microbiology and geochemistry samples were rapidly extracted, as described in "Whole-Round Core Sampling in the Cold Room," p. 16, in "Core Handling and Sampling" in "Introduction and Background" in "Microbiology." Unsampled microbiological subsections and the remainder of the core on the catwalk were processed according to the ODP standard core handling procedures as described in previous *Initial Reports* volumes and the Shipboard Scientist's Handbook (with minor modifications). In brief, prior to sectioning, an infrared (IR) camera was passed along the length of the core, capturing a thermally calibrated image (see "Infrared Thermal Imaging," p. 42, in "Physical Properties"). Routine shipboard safety and pollution prevention samples were collected on the catwalk (see "Biogeochemistry," p. 9). The core was then cut into nominally 1.5-m sections. The remaining cut sections were transferred to the core laboratory for further processing.

Whole-round core sections not used for microbiological sampling were run through the multisensor track (MST), and thermal conductivity measurements were performed (see "Physical Properties," p. 41). The cores were then split into working and archive halves (from bottom to top); investigators should be aware that older material may have been transported upward on the split face of each section. When short pieces of sedimentary rock were recovered, the individual pieces were split with the rock saw and placed in split liner compartments created by sealing spacers into the liners with acetone.

Coherent and reasonably long archive-half sections were measured for color reflectance using the archive-half multisensor track (AMST) (see "Color Reflectance Spectrophotometry," p. 8, in "Lithostratigraphy). Visual descriptions were prepared of the archive halves, augmented by smear slides and thin sections (see "Lithostratigraphy," p. 4), and the archive halves were photographed with both black-and-white and color film. Close-up photographs were taken of particular features for illustrations in site chapters, as requested by individual scientists. All sections of core not removed for microbiological sampling were additionally imaged using a digital imaging track system equipped with a line-scan camera.

The working half of each core was sampled for shipboard analysis, such as physical properties, carbonate, and bulk X-ray diffraction (XRD) mineralogy, and for shore-based studies. Both halves of the core were then put into labeled plastic tubes, sealed, and placed in cold storage space on board the ship. At the end of the leg, the cores were transferred from the ship into refrigerated containers and shipped to the ODP Gulf Coast Core Repository in College Station, Texas.

LITHOSTRATIGRAPHY

This section outlines the procedures followed to document the basic lithostratigraphy of the deposits recovered during Leg 201, including core description, XRD, color spectrophotometry, digital color imaging, and smear slide description. Only general procedures are outlined, except where they depart significantly from ODP conventions.

Age Assignments

All seven sites drilled during Leg 201 were located very close to sites drilled during previous cruises. The biostratigraphic and magnetostratigraphic age framework presented in the site chapters follows those of the previous legs. The ages of biostratigraphic and magnetostratigraphic events are those of Berggren et al. (1995a, 1995b).

Visual Core Descriptions

Information from macroscopic description of each core was recorded manually for each core section on visual core description (VCD) forms. A wide variety of features that characterize the sediment were recorded, including lithology, sedimentary structures, color, and sediment deformation. Compositional data were obtained from smear slides. The color (hue and chroma) of the sediments was determined by color spectrophotometry (see "Color Reflectance Spectrophotometry," p. 8). This information was condensed and entered into AppleCORE (version 8.1b) software, which generates a simplified one-page graphical description of each core (barrel sheet) (Fig. F2). Barrel sheets are presented with split-core photographs (see the "Core Descriptions" contents list). The lithologies of the recovered sediments are represented on barrel sheets by symbols in the column titled "Graphic Lithology" (Fig. F3). Primary sedimentary structures, bioturbation parameters, soft-sediment deformation, structural features, and drilling disturbance are indicated in columns to the right of the graphic log. The symbols are schematic but are placed as close as possible to their proper stratigraphic position. For exact positions of sedimentary features, more detailed VCDs can be ob-

F2. Example of a VCD form, p. 68.
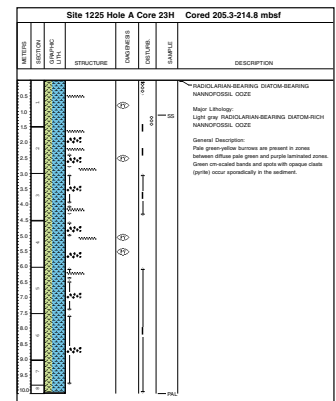
F3. Patterns and symbols used in barrel sheets, p. 69.
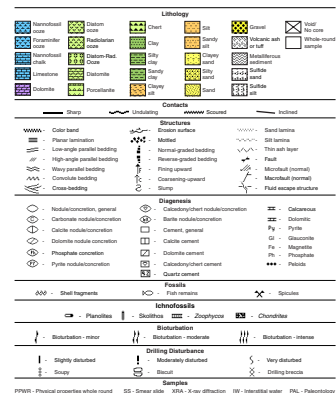
tained from ODP. Deformation and disturbance of sediment resulting from the coring process are illustrated in the "Drilling Disturbance" column. Blank regions indicate the absence of coring disturbance. Locations of samples taken for shipboard analysis are indicated in the "Samples" column. A summary lithologic description with sedimentologic highlights is given in the "Description" column of the barrel sheet. This description provides information about the major sediment lithologies, important minor lithologies, and an extended summary description of the sediments, including color, composition, sedimentary structures, trace fossils identified and extent of bioturbation, and other notable characteristics. Descriptions and locations of thin, interbedded, or minor lithologies that could not be depicted in the "Graphic Lithology" column are also presented in "Description," where space permits.

Lithologic Classification

The sediment classification scheme used during Leg 201 is descriptive and follows the ODP classification scheme (Mazullo et al., 1988), with some simplifying modifications for sediments that are mixtures of siliciclastic and biogenic components (Fig. F4). Classification is based primarily on macroscopic description of the cores and examination of smear slides. During Leg 201, the total calcium carbonate content of the sediments (see "Biogeochemistry," p. 9) and XRD determined on board were also used to aid in classification.

Composition and texture are the criteria used to define lithology. Textural names for the siliciclastic sediment components are derived from the Udden-Wentworth (Wentworth, 1922) grain size scale (Fig. F5). The term clay is used only for particle size and is applied to both clay minerals and other siliciclastic material <4 µm in size. Genetic terms such as pelagic, neritic, hemipelagic, and debris flow do not appear in this classification.

The principal name applied to a sediment is determined by the component or group of components (e.g., total biogenic carbonate) that comprise(s) >60% of the sediment or rock, except for subequal mixtures of biogenic and siliciclastic material. The main principal names are as follows.

Siliciclastic Sediments

If the total siliciclastic content is >60%, the main name is determined by the relative proportions of sand, silt, and clay sizes when plotted on a modified Shepard (1954) classification diagram (Fig. F4A). Examples of siliciclastic principal names are clay, silt, sand, silty clay, sandy clay, clayey silt, sandy silt, clayey sand, and silty sand.
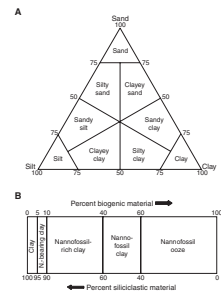
Biogenic Sediments

If the total biogenic content is >60% (i.e., siliciclastic material <40%), then the principal name applied is ooze (Fig. F4B). Biogenic components are not described in textural terms. Thus, a sediment with 65% sand-sized foraminifers and 35% siliciclastic clay is called clay-rich foraminifer ooze, not clay-rich foraminifer sand.

Mixed Sediments

In mixtures of biogenic and nonbiogenic material where the biogenic content is 40%–60% (termed "mixed sediments" in the ODP classification), the name consists of two parts: (1) a major modifier(s) consisting of the name(s) of the major fossil group(s), with the least

F4. Classification of siliciclastic sediments, p. 70.

F5. Grain-size classification diagram, p. 71.

common fossil listed first, followed by (2) the principal name appropriate for the siliciclastic components (e.g., foraminifer clay) (Fig. **F4B**).

If any component (biogenic or siliciclastic) represents between 10% and 40% of a sediment, it qualifies for minor modifier status and is hyphenated with the suffix -rich (e.g., nannofossil-rich clay). When a component makes up only 5%–10% of the sediment, it can be indicated with a minor modifier that consists of the component name hyphenated with the word "bearing" (e.g. nannofossil-bearing clay). Where two minor components are present, the most abundant accessory component appears closest to the principal name. Major and minor modifiers are listed in order of increasing abundance before the principal name.

Examples

15% foraminifers, 40% nannofossils, and 45% clay = foraminifer-rich nannofossil clay,

5% diatoms, 10% radiolarians, and 85% clay = diatom- and radiolarian-bearing clay, and

10% diatoms, 35% silt, and 55% foraminifers = diatom-bearing silt-rich foraminifer ooze.

Induration

The following classes of induration or lithification were adopted and modified from ODP Leg 188 (Shipboard Scientific Party, 2001). They were separated into three classes for biogenic sediments and two classes for nonbiogenic sediments. For biogenic sediments and sedimentary rocks, the three classes of induration are

Soft: sediment has little strength and is readily deformed under pressure of a finger or broad-blade spatula:
   Ooze: unconsolidated calcareous and/or siliceous biogenic sediment;

Firm: partly lithified sediments that are readily scratched with a fingernail or the edge of a spatula:
   Chalk: semi-indurated biogenic sediment composed predominantly of calcareous biogenic grains;
   Diatomite: semi-indurated biogenic sediment composed predominantly of diatoms; and
   Radiolarite: semi-indurated biogenic sediment composed predominantly of radiolarians;

Hard: well-lithified and cemented sediment that is resistant or impossible to scratch with a fingernail or the edge of a spatula:
   Limestone: a white or gray indurated calcareous biogenic sediment;
   Porcelanite: a dull white porous indurated siliceous biogenic sediment; and
   Chert: a lustrous conchoidal fractured indurated siliceous biogenic sediment.

For nonbiogenic clastic sediments, the two classes of induration are

Soft: Gravel, sand, silt, clay; sediment core can be split with a wire cutter; and

Hard: Conglomerate, sandstone, siltstone, claystone; cannot be compressed with finger pressure, or core must be cut with a band saw or diamond saw.

Special Rock Types

The definitions and nomenclatures of special rock types were adopted and modified from ODP Legs 112 and 138 (Shipboard Scientific Party, 1988, 1992) and adhere as closely as possible to conventional terminology. Three special rock types were especially important during Leg 201: authigenic carbonates, phosphates, and metalliferous sediments.

Carbonates and Phosphates

Authigenic minerals are indicated in the "Diagenesis" column of the core description forms (barrel sheets). Carbonates (calcite and dolomite) are present as beds and nodules. In cases where it was possible to clearly identify the carbonate mineralogy, symbols for the respective carbonate minerals were used. The degree of lithification is noted in the core description as friable where the rock showed only partly lithification or lithified where fully cemented. Phosphate-rich sediments were also present, designated by a "Ph" in the "Lithologic Accessories" column (distinct from "P," which is commonly used during ODP legs to designate pyrite). In accordance with the terminology used during Leg 112, two different types of phosphatic materials are distinguished. F-phosphate is the designation given to friable, generally light-colored lenses and layers of fine-grained carbonate fluorapatite (francolite). The term D-phosphate is used for those phosphatic peloids, nodules, gravels, and phosphatic hardgrounds composed mainly of dense, hard, dark-colored francolite. The term "phosphorite" is restricted to layers composed mainly of phosphatic grains.

Metalliferous Sediments and Metal-Rich Oxides

Metalliferous sediments are composed of fine-grained granular sulfides, oxides, and hydroxy oxides rich in iron and other transition elements. They may be present near or within basement rocks in the sedimentary section or as dispersed grains as a minor component of other sediments. In the former instance, the metal-rich sediments may include both primary precipitates and altered crystalline phases. They may also include X-ray amorphous semiopaque oxides. Metalliferous sediments are generally distinguished from other fine-grained nonbiogenic sediments on the basis of their chemistry (e.g., Fe [10 wt% on a carbonate-free basis]; [(Fe + Mn)/Ti] [25]). In the absence of such information at the time the cores were described, we distinguished this sediment lithology on the basis of color, opaque mineral content of smear slides, and/or presence at the base of the sediment column.

Other metal-rich oxides, such as dispersed or nodular manganese oxides, are also present in equatorial Pacific sediments. They may be present near the sediment surface or may lie buried within the sediment. They are distinguished by color, mineralogy, and, in the case of nodules, by their physical appearance.

Smear Slide Analysis

Petrographic analysis of the sand- and silt-sized components of the sediment was primarily conducted by smear slide description. The

slides were fixed by ultraviolet (UV) curing using Norland optical adhesive immersion medium. Alternatively, some of the slides were prepared with heat cure medium. Tables summarizing data from smear slides are available (see "Smear Slides" for each site in the "Core Descriptions" contents list). These tables include information about the sample location, whether the sample represents a dominant (D) or a minor (M) lithology in the core, and the estimated percentage ranges of sand, silt, and clay, together with all identified components. We emphasize here that smear slide analysis provides only crude estimates of the relative abundances of detrital constituents. The mineral identification of finer-grained particles can be difficult using only a petrographic microscope, and sand-sized grains tend to be underestimated because they cannot be evenly incorporated into the smear. The presence of authigenic minerals such as manganese oxides, pyrite, or carbonates was especially noted. The mineralogy of smear slide components was validated by XRD. The relative proportions of carbonate and noncarbonate materials estimated from smear slides were validated by chemical analysis of the sediments (see "Biogeochemistry," p. 9).

X-Ray Diffraction

XRD was used to support and verify the observations of the smear slide analysis to identify small-scale compositional changes, potential authigenic minerals, and to detect main silica phases. Each sample was freeze-dried, ground, and mounted with a random orientation into an aluminum sample holder. For the measurements, a Philips PW-1729 X-ray diffractometer with a CuK$_\alpha$ source (40 kV and 35 mA) and Ni filter was used. Peak intensities were converted to values appropriate for a fixed slit width. The goniometer scan was performed from 2° to 40°2θ at a scan rate of 1.2°/min (step = 0.01° and count time = 0.5 s). Diffractograms were peak-corrected to match the (100) quartz peak at 4.26 Å. Common minerals were identified based on their peak position and relative intensities in the diffractogram using an interactive software package (MacDiff version 4.1.1).

Color Reflectance Spectrophotometry

In addition to visual estimates of the color, reflectance of visible light from soft sediment cores was routinely measured using a Minolta spectrophotometer (model CM-2002) mounted on the AMST. The AMST measures the archive half of each core section and provides a high-resolution stratigraphic record of color variations for visible wavelengths (400–700 nm). Freshly split cores were covered with clear plastic wrap and placed on the AMST. Measurements were taken at 2.0-cm spacing. The AMST skips empty intervals and intervals where the core surface is well below the level of the core liner but does not recognize relatively small cracks or disturbed areas of core. Thus, AMST data may contain spurious measurements that should, to the extent possible, be edited out of the data set before use. Each measurement recorded consists of 31 separate determinations of reflectance in 10-nm-wide spectral bands from 400 to 700 nm. Additional detailed information about measurement and interpretation of spectral data with the Minolta spectrophotometer can be found in Balsam et al. (1997, 1998) and Balsam and Damuth (2000).

Digital Color Imaging and Image Analysis

Systematic high-resolution line-scan digital images of the archive-half core were obtained using the GEOTEK X-Y digital imaging system (DIS). The DIS system was calibrated for black-and-white imaging approximately every 12 hr.

After cores were visually described, they were placed in the DIS and scanned. A spacer holding a neutral gray color chip and a label identifying the section was placed at the base of each section and scanned along with each core. Output from the DIS includes a Windows bitmap (.bmp) file and a Mr.Sid (.sid) file for each section scanned. The bitmap file contains the original data with no compressional algorithms applied, whereas the Mr.Sid files apply extensive compressional algorithms.

Additional postprocessing of data was done to achieve a medium-resolution JPEG image of each section and a composite JPEG image (stored as a Microsoft PowerPoint slide) of each core, which is comparable to the traditional photographic image of each core. The JPEG image of each section was produced by an Adobe Photoshop batch job that opened the bitmap file, resampled to a width of 0.6 in at a resolution of 300 pixels/in, and saved the result as a maximum-resolution JPEG.

BIOGEOCHEMISTRY

Interstitial Water Samples

Shipboard interstitial water (IW) samples were obtained from 5- to 30-cm-long whole-round intervals that were cut according to two general procedures. One set of IW intervals was cut on the catwalk, capped, and taken to the laboratory for immediate processing; the other set was cut from ends of shared microbiology cores that were subsampled in the walk-in refrigerator, usually within an hour of removal from the catwalk. During high-resolution sampling, when there were too many IW intervals to process immediately, the capped whole-round intervals were stored temporarily in a freezer or refrigerator. Cores with high contents of hydrogen sulfide were processed and stored temporarily in a fume hood.

After extrusion from the core liner, the surface of each whole-round interval was carefully scraped with a spatula to remove potential contamination. Sediments were then placed into a titanium squeezer, modified after the standard stainless steel squeezer of Manheim and Sayles (1974). The piston was positioned on top of the squeezer, which was then flushed with nitrogen through the outlet for >2 min. Pressures of up to 76 MPa were applied in the squeezer, calculated based on the measured hydraulic press pressure and the ratio of the piston areas of the hydraulic press and the squeezer. Interstitial water was passed through a prewashed Whatman number 1 filter fitted above a titanium screen, filtered through a 0.45-μm Gelman polysulfone disposable filter, and subsequently extruded into a precleaned (10% HCl) 50-mL plastic syringe attached to the bottom of the squeezer assembly. After collection of interstitial water, the syringe was removed to dispense aliquots for shipboard and shore-based analyses.

A modification of the above procedure was implemented to prevent loss of ephemeral constituents because of the backlog of interstitial water samples awaiting dispensing from the 50-mL syringes. In addition to

the 50-mL syringe, IW samples were also collected in a 10-mL glass syringe attached to the squeezer assembly and the 50-mL syringe via a three-way plastic valve. Interstitial water emerging from the disposable filter at the bottom of the squeezer assembly was directed into one or the other syringe as necessary for appropriate dispensing of aliquots. Use of the 10-mL syringe also avoided air bubbles and minimized contamination of this fraction of the interstitial water by dissolved O_2.

Interstitial Water Analyses

Most IW samples were analyzed for routine shipboard measurements according to standard procedures (Gieskes et al., 1991). Salinity was measured as total dissolved solids using a Goldberg optical handheld refractometer. The pH was determined by ion-selective electrode. Alkalinity was determined by Gran titration with a Metrohm autotitrator.

A new procedure was implemented during Leg 201 to analyze for dissolved inorganic carbon, employing a Coulometrics 5011 CO_2 coulometer. An aliquot of 1.0 mL of interstitial water was pipetted into the reaction tube, followed by addition of 3.0 mL of 2-N HCl after attaching the reaction tube to the coulometer apparatus. The liberated CO_2 was titrated, and the end point was determined by a photodetector. Measured concentrations were corrected for the value of the acid blank. Analytical uncertainty, based on repeated measurements of a sample of surface seawater, was ±1%.

Concentrations of chloride and sulfate were determined by manual dilution and manual injection into a Dionex DX-120 ion chromatograph. Chloride concentrations were also determined at some sites by titration with $AgNO_3$. Quantification was based on comparison with International Association of the Physical Sciences of the Ocean (IAPSO) standard seawater.

Dissolved silica, phosphate, and ammonium concentrations were determined by spectrophotometric methods using a Shimadzu UV Mini 1240 spectrophotometer. For phosphate analyses at Sites 1227–1229, the standard protocol was slightly modified. Previous analyses of dissolved phosphate in interstitial waters of shallow Peru Margin sediments at Site 684 and also Sites 680 and 681 were strongly affected by color interference because of high concentrations of hydrogen sulfide (Shipboard Scientific Party, 1988). At the Peru Margin Sites 1227, 1228, and 1229, we aimed to improve upon the standard ODP technique for dissolved phosphate analysis in H_2S-rich IW samples. One approach was to remove sulfide from the sample by acidification and degassing. Samples that had been titrated for alkalinity were used, as they are acidified and degassed. Furthermore, they are in a pH range appropriate for colorimetric determination of phosphate by the phosphomolybdate blue method.

Selected trace metal concentrations were obtained using the Jobin-Yvon Ultrace inductively coupled plasma–atomic emission spectrometer (ICP-AES). Concentrations of boron, barium, iron, lithium, manganese, and strontium were determined following the procedures outlined by Murray et al. (2000). Given the anticipated range of redox environments at Leg 201 sites and the fact that many microbially mediated reactions depend on metal catalysts, IW samples were also examined for a suite of redox-sensitive transition metals—copper, molybdenum, nickel, vanadium, and zinc. For these analyses, the shipboard "master" ICP-AES standard was modified so that concentrations of iron,

manganese, lithium, boron, and strontium remained the same but with concentrations of copper, molybdenum, nickel, vanadium, and zinc at 200, 200, 200, 200, and 500 mM, respectively. Analytical standards for all elements were then prepared by analyzing mixtures of this master standard and seawater.

Dissolved sulfide ($\Sigma H_2S = H_2S + HS^-$) was determined on 1-mL interstitial water samples injected into a pre-tared vial containing 0.5 mL of 20% zinc acetate solution (20 g ZnAc/100 mL solution). Dissolved sulfide was determined by the methylene blue method of Cline (1969) using a Shimadzu UV Mini 1240 spectrophotometer and a Milton Roy Mr. Sipper sample introduction system. Iodometrically calibrated zinc sulfide suspensions in zinc acetate solution were used to calibrate the diamine reagent.

Nitrate and nitrite concentrations were determined spectrophotometrically on 1-mL samples according to the methods of Strickland and Parsons (1972) using a Shimadzu UV Mini 1240 spectrophotometer with a Milton Roy Mr. Sipper sample introduction system.

Volatile fatty acids (i.e., acetate and formate) were analyzed by ion exchange chromatography on a Dionex ion chromatograph equipped with an anion exchange column (Dionex AS-15). Solutions of sodium hydroxide and sulfuric acid were utilized as eluent and suppressant, respectively. A 1.0-mL sample of filtered interstitial water was slowly applied to a sequence of ion exchange cartridges to remove interfering ions (cartridge A: Dionex OnGuard II H packed with a Ag-form cationic resin to remove chloride followed by cartridge B: Dionex OnGuard II H packed with a proton-form cationic resin to remove excess Ag eluting from previous cartridge) and after a period of at least 5 min eluted with 1.0 mL H_2O. Prior to use, cartridges were conditioned by rigorous flushing with deionized water (at least 20 mL). The detection limit for acetate was constrained by interferences with variable amounts of lactate and typically ranged from 0.2 to 0.5 µM. The detection limit for formate was 0.1 µM.

Gas Analyses

Hydrogen concentrations were determined on incubated sediment samples following published procedures that assume the headspace hydrogen is in equilibrium with the dissolved pore fluid hydrogen (Lovley and Goodwin, 1987; Hoehler et al., 1998). Four replicate incubations were conducted on each sample. For each incubation, a 5-cm³ bulk sediment sample was collected from a freshly exposed end of a core section using a sterilized plastic syringe with its Luer tip cut off. The sediment sample was extruded into a 20-mL headspace vial and immediately capped with a rubber septum that was sealed with an aluminum crimp cap. The sealed vials were flushed with low-hydrogen nitrogen using two hypodermic needles inserted through the septum. One needle was connected to the nitrogen and one allowed for gas release. These septa and vials were previously shown not to leak significant hydrogen over the timescale of the incubations. Headspace hydrogen concentrations were analyzed daily until approximately steady-state concentrations were reached. Hydrogen concentrations were determined by gas chromatography on a Trace Analytical reduction gas analyzer. Quantification was by comparison to a standard curve generated from a single primary gas standard and mixed to different concentrations immediately prior to analysis. To correct for drift, the primary gas standard was re-

peatedly analyzed. Reported concentrations are based on the temperature-dependent solubility of hydrogen and the mean of replicates.

Concentrations of methane were monitored at intervals of 2 to 17 samples per core. The standard gas analysis program for safety and pollution prevention purposes (Kvenvolden and McDonald, 1986) was complemented by additional headspace analyses following a slightly different approach (Iversen and Jørgensen, 1985; Hoehler et al., 2000) with the intent to better constrain the concentrations of dissolved gases. Compared to the rapid safety-oriented protocol, the latter, more time-consuming alternative led to higher yields of methane (e.g., see **"Biogeochemistry,"** p. 14, in the "Site 1225" chapter).

Upon core retrieval, a 3-mL sediment sample was collected with a cut-off plastic syringe from a freshly exposed end of a core section and was extruded into a 20-mL glass serum vial. For this purpose, the plunger was held at the sediment surface while inserting the barrel to avoid trapping air bubbles. After withdrawing the syringe, the plunger was advanced slightly to extrude a small amount of sediment. This excess was shaved off with a flat spatula flush with the end of the syringe barrel to provide an accurate determination of the sediment volume within the syringe. Samples required for safety and pollution prevention purposes were immediately sealed with a septum and metal crimp cap and heated to 60°C for 20 min. The headspace was subsequently analyzed by gas chromatography. For samples designated for refined headspace analysis, the sediment was extruded into a 20-mL vial containing 5 mL of 1-M NaOH. The vial was immediately capped with a silicone/Teflon septum. After vigorous manual shaking for 2 min, the vials were shaken automatically for an additional hour and subsequently left to stand for at least 23 hr at room temperature prior to gas chromatographic analysis. Additionally, when gas pockets were observed, headspace samples were complemented by vacutainer samples, which were collected directly from gas voids formed in the core liner by penetrating the liner using a syringe connected to a penetration tool.

Gas chromatographic analyses of headspace samples resulting from both protocols were performed in an identical manner. A 5-mL volume of headspace gas was extracted from the vial using a standard gas syringe. This volume was compressed in the syringe to a volume of 3 mL. The created overpressure was released by briefly opening the valve of the gas-tight syringe. Constituents of the headspace and vacutainer gas samples were analyzed using a Hewlett Packard 6890 Plus gas chromatograph (GC) equipped with an 8-ft × 1/8-in stainless steel column packed with HaySep S (100–120 mesh) and a flame ionization detector (FID). Concentrations of methane, ethane, ethene, propane, and propene were obtained. The carrier gas was helium, and the GC oven was programmed from 100°C (5-min hold) to 140°C (4.5-min hold) at a rate of 50°C/min. Data were collected using a Hewlett-Packard 3365 ChemStation data processing program. Gas samples collected with vacutainers were routinely analyzed on the natural gas analyzer (NGA). The NGA system consists of a Hewlett-Packard 6890 Plus GC equipped with three different columns and two detectors. Hydrocarbons from methane to hexane were analyzed using a 60-m × 0.32-mm DB-1 capillary column connected to a FID. The GC oven was heated isothermally at 50°C for 15 min.

The concentration of methane in interstitial water was derived from the headspace concentration by the following equation:

$$CH_4 = \chi_M \cdot P_{atm} \cdot V_H \cdot R^{-1} \cdot T^{-1} \cdot \phi^{-1} \cdot V_S^{-1}, \tag{1}$$

where,

V_H = volume of the sample vial headspace,
V_S = volume of the whole sediment sample,
χ_M = molar fraction of methane in the headspace gas (obtained from GC analysis),
P_{atm} = pressure in the vial headspace (assumed to be the measured atmospheric pressure when the vials were sealed),
R = the universal gas constant,
T = temperature of the vial headspace in degrees Kelvin, and
ϕ = sediment porosity (determined either from moisture and density measurements on adjacent samples or from porosity estimates derived from gamma ray attenuation [GRA] data representative of the sampled interval).

Quantities of methane that remain undetected because of dissolution in the aqueous phase are minimal (e.g., Duan et al., 1992) and are not accounted for. The internal volumes of 15 representative headspace vials were carefully measured beforehand and were determined to average 18.42 ± 0.13 mL. This volume was taken as constant in calculations of gas concentrations.

During Leg 201, we discovered that at most sites the concentrations obtained from the safety-related headspace protocol were significantly lower than those obtained from comparable samples analyzed by the prolonged extraction method using sediment slurries in NaOH solution. We suggest that the prolonged extraction solution led to the detection of a methane fraction that is not dissolved in interstitial water. For Sites 1229–1231, where particularly long extraction times had been applied and led to unusually high-yield increases, we consider the data obtained from the safety protocol as the best approximation for the fraction of dissolved methane. Future research will verify the nature of the additional pool of methane tapped by prolonged extraction in alkaline solution.

Sediments

Sediment samples were not routinely analyzed during Leg 201 because of the emphasis on interstitial water and gas analyses and because all of the sites drilled during this leg were sampled during previous legs. However, some analyses were obtained on sediment samples according to the standard methodology employed during previous legs. Inorganic carbon (IC) concentration was determined using a Coulometrics 5011 CO_2 coulometer. About 10 to 15 mg of freeze-dried, ground sediment was weighed and reacted with 2-N HCl. The liberated CO_2 was titrated, and the end point was determined by a photodetector. Calcium carbonate, expressed as weight percent, was calculated from the IC content, assuming that all evolved CO_2 was derived from dissolution of $CaCO_3$, by the following equation:

$$CaCO_3 \text{ (wt\%)} = 8.33 \times IC \text{ (wt\%)}. \tag{2}$$

No correction was made for the presence of other carbonate minerals.

Total carbon (TC), nitrogen, and sulfur concentrations were determined using a Carlo Erba 1500 CNS elemental analyzer. About 10 mg of freeze-dried, ground sediment was weighed and combusted at 1000°C

in a stream of oxygen. Nitrogen oxides were reduced to nitrogen, and the mixture of carbon dioxide, nitrogen, and sulfur dioxide was separated by GC and detected by thermal conductivity detector (TCD). Total organic carbon (TOC) concentration was calculated as the difference between TC and IC concentrations.

The organic matter in selected sediment samples was characterized by pyrolysis using a Delsi Nermag Rock-Eval II system. This method is based on a whole-rock pyrolysis technique designed to characterize the type and maturity of organic matter and to estimate the petroleum potential of the sediments (Espitalié et al., 1986). The Rock-Eval system incorporates a temperature program that initially expels volatile hydrocarbons (S_1) as the sample is heated at 300°C for 3 min and then, as the temperature increases from 300° to 600°C at 25°C/min, releases the hydrocarbons (S_2) resulting from thermal cracking of kerogen. S_1 and S_2 hydrocarbons are measured and reported in milligrams per gram of dry sediment. The temperature at which the kerogen yields the maximum amount of hydrocarbons during the S_2 program provides T_{max}, a parameter used to assess the maturity of the organic matter. Between 300° and 390°C of the pyrolysis program, carbon dioxide (S_3) is released from the organic matter, trapped, measured by TCD, and reported in milligrams per gram of dry sediment. Rock-Eval II parameters are used to characterize organic matter by calculation of hydrogen index (HI), oxygen index (OI), and S_2/S_3:

$$HI = (S_2/TOC) \times 100 \text{ and} \tag{3}$$

$$OI = (S_3/TOC) \times 100. \tag{4}$$

Rock-Eval data are generally unreliable for samples containing <0.5 wt% TOC.

MICROBIOLOGY

Introduction and Background

ODP's recent progress in exploring the deep subseafloor biosphere has revealed that prokaryotes are consistently present in core samples recovered from the deep oceanic subsurface (Parkes et al., 1994; Wellsbury et al., 1997). The subseafloor biosphere has been estimated to constitute one-third of the biomass on Earth (Whitman et al., 1998). However, the structure, diversity, and function of subsurface microbial communities remain poorly understood. Total cell numbers alone do not provide information about prokaryotic physiologies that are critical to understanding deep biosphere biogeochemical processes. It is important to know (1) what types of prokaryotes are present and in what abundance and (2) which of these prokaroytes are truly active (i.e., not dormant) and are participating in deep sedimentary geochemical processes. We used a range of approaches to quantify prokaryote abundance, diversity, and activity, including (1) total counts; (2) adenosine triphosphate (ATP); (3) cultivation methods, particularly the most probable number (MPN) technique; (4) nucleic acid–based techniques, particularly fluorescence in situ hybridization (FISH); and (5) radiotracer and stable isotope tracer experiments on specific microbial processes. In order to ensure that we were indeed analyzing the indigenous prokary-

otes and their activities, tests for contamination were conducted during the entire coring process for microbiological samples.

Core Handling and Sampling

Drilling

Microbiological sampling depends on careful and appropriate sample handling technique. Precise operational definitions for special microbiology handling terminology is given in Table T1. Because the samples were retrieved from very stable sedimentary environments, the prokaryotes are expected to be sensitive to chemical and physical change, in particular to changes in oxygen, temperature, and (for the deep-sea sites) pressure. Consequently, all samples for microbiology and process studies were transferred from the drilling platform to the hold refrigerator (set to <10°C) as quickly as possible and were kept as whole-core sections until processed (to date, there is no system for retrieving and maintaining samples under in situ pressure). In order to avoid intermittent warming of retrieved cores, ODP's usual core handling procedure was modified. Once a core was retrieved, it was immediately transferred to the catwalk for labeling and cutting before the next core barrel was deployed. When piston coring at 3800 m water depth, this prolonged the drilling operation by 33% per core (from 63 to 84 min) but was considered important to prevent damage to heat-sensitive microorganisms. Efforts were also made to obtain APC cores even when this led to an increase in core recovery times, as APC cores were generally much less disturbed than XCB cores.

While drilling cores for microbiology, the potential for contamination with bacteria from the surface is highly critical. Contamination tests were continuously conducted using solutes (perfluorocarbon tracer [PFT]) or bacterial-sized particles (fluorescent microspheres) to check for the potential intrusion of drill water from the periphery toward the center of cores and thus to confirm the suitability of the core material for microbiological research. We used the chemical and particle tracer techniques described in ODP *Technical Note* 28 (Smith et al., 2000a). Furthermore, the freshly collected cores were visually examined for possible cracks and other signs of disturbance by observation through the transparent core liner. Core sections observed to be disturbed before or after subsampling were not analyzed further. Such disturbance phenomena are critical to the integrity of the core material and therefore also to its usefulness for microbiological studies.

Sampling on the Catwalk

A limited number of microbiological and related biogeochemical samples were collected on the catwalk as soon as the core was retrieved. After the core was cleaned and the IR camera scan completed, the core was marked into 1.5-m sections for cutting and visually inspected for signs of disturbance, such as gas voids, cracks, and drilling disturbance. The appropriate sections, usually from the middle, were taken for microbiological analyses. The top end of the selected sections were cut and capped (without acetone). The top 15 cm of this section (or the bottom 15 cm of the previous section) was often used as an interstitial water biogeochemistry sample. The lower end was cut, and a temperature image was immediately taken by a calibrated IR-sensitive video camera (see "Infrared Thermal Imaging," p. 42, in "Physical Properties") to estimate the maximum temperature reached in the core center before it was transferred to the cold room. Samples for total prokaryotic

cell counts and perfluorocarbon contamination checks were immediately collected using 5-cm³ sterile syringes from the lower, freshly cut end, whereas samples for methane and porosity were taken from the adjacent core section end. This catwalk syringe sampling enabled collection of these samples at a much greater frequency than was possible for the whole-round cores (WRCs). The lower core end was then sealed with an end cap (without acetone). The microbiological section and an adjacent section were quickly transported to the cold room to limit temperature increase (see **"Infrared Scanner,"** p. 24, in "Physical Properties," in the "Site 1225" chapter).

Whole-Round Core Sampling in the Cold Room

It is important to emphasize that the different analyses, experiments, and cultivation attempts that fall under the rubric "microbiological methods" have widely different requirements concerning handling and storage. Keeping samples cool, processing times short, and minimizing contamination were the key criteria for determining how the core sections were processed. To minimize changes in the microbial population, all handling took place in a cold room. The lower refrigerated core room on the hold deck of the ship served as a cold room at <10°C and was equipped with a work bench and working space for two to four persons. It was important that all materials, including core cutters, glass vials, and so on, were kept cold so that no unintentional warming of the samples took place. In addition, as the core liner is not sterile and the outer surface of the core is contaminated during drilling (Smith et al., 2000a, 2000b), subsampling must exclude the sediment next to the core liner. Where appropriate, handling and subsampling were performed under anoxic conditions.

Normally, two 1.5-m core sections at a time were brought down to the cold room in case the standard section or a part of this section was found to be disturbed on subsampling. In such cases, part or all of the subsequent section was also subsampled. Table **T2** and Figure **F6** show the various categories of samples and how they were handled. The subsectioning equipment included the standard ODP core cutter coupled with a clean wire or blade and a nitrogen-flushed cutting rig that was modified from an earlier published version (Fig. **F7**) (Parkes et al., 1995). The cutting rig system enabled a 1.5-m section, after cleaning the outer surface with ethanol, to be sequentially cut into a number of WRC sections using a sterile blade. Some of these WRC sections were immediately capped with clean end caps and stored at 4°C for shorebased analysis, whereas others were immediately subsampled into sterile 5-cm³ or larger syringes (with the Luer end removed).

To minimize contamination and to increase handling efficiency, several modifications of the core cutting procedure were introduced for microbiology subsamples intended for cultivation, starting from Site 1226. These include the following:

1. Replacing sterile cutting blades with a sterile cutting wire to minimize the surface area that can draw contamination from the outer or inner core liner surface into the center portion of the core;
2. Taking slurry samples using a large syringe that is centered on a core section instead of using several smaller syringes that, if not properly centered, more easily pick up contamination from the outer core layers (the many smaller syringes that had been used

T2. Sampling codes and packing types, p. 82.

F6. Diagram of WRC sectioning for MBIO, p. 72.

F7. N₂-gassed cutting rig for WRCs, p. 73.

for the initial slurry subsampling on Cores 201-1225A-2H and 12H may have contributed to contamination); and

3. Obtaining an uncontaminated sediment surface by breaking the core after precutting the core liner (however, in a Site 1225 test, depending on its texture and lamination a core tended to break at irregular points and angles or even at more positions, thus enhancing the air exposure of the samples).

After Site 1225, the nitrogen-flushed cutting rig was used principally for samples requiring anoxic sampling conditions (e.g., activity measurements).

Anoxic subsampling with cut-off syringes was conducted under a flow of filter-sterilized nitrogen in a gassing "bucket" designed at Bristol University (Fig. F8). The bucket system prevents the nitrogen flow from creating turbulence and thus introducing contamination or oxygen. Syringe subcores were taken from the central uncontaminated part of the WRC and then sealed under nitrogen with a sterile stopper. To preserve the integrity of the sample during subcoring and to prevent sediment near the core liner from being sampled, sterile acrylic pegs were inserted into the holes left after each subcore was removed. Subcores were stored at 10°C under nitrogen atmosphere in gas-tight bags until further processing. In compacted sediments, it was occasionally necessary to drive the syringe into the WRC with a syringe adapter and hammer. Syringe subcores were used for various analyses, including radiotracer studies, production of sediment slurries for bacterial enrichments, MPN counts, FISH, bead contamination tests, and measurements of hydrogen concentration.

WRCs to be immediately preserved were sectioned with a standard ODP cutter and sterile wire from the same core. The samples for deoxyribonucleic acid (DNA) and lipid biomarker analysis were frozen in a –80°C freezer. Samples for iron, manganese, and sulfur solid-phase speciation and isotopes were placed in aluminum gas-tight bags, vacuum sealed, and frozen at –20°C. WRCs for further shore-based microbiological experimentation were stored in a nitrogen gas–flushed aluminum bag, often together with a welled Merck Anaerocult strip, and stored at +4°C. Clean disposable gloves were worn during all handling procedures. Any remaining portions of the sections used for microbiology subsampling were returned to the core laboratory for reintroduction into the standard core handling process. In order to obtain uncontaminated material for slurry preparation and cultivation, cores were broken after precutting the core liner with the ODP cutter. Bending the outer ends upward allowed released particles to drop into a bin. This technique provided untouched (although not always smooth) surfaces that were sampled by a 60-mL syringe. Only deeper sediment contents of the syringe, which did not contain oxygen, were transferred to nitrogen-flushed sterile slurry vessels containing artificial seawater. An overview of the cutting and subsampling scheme for the microbiology section is given in Figure F6 and in Table T2.

Total Cell Counts and Contamination Tests

The most immediate method to visualize and quantify the deep biosphere are total prokaryotic cell counts using the nucleic acid stain acridine orange. These counts have been made on a wide range of ODP sediment cores, including cores from the Peru margin and the equatorial Pacific (Parkes et al., 1994). In general, these counts have demonstrated

F8. Bucket for clean anoxic subsampling of WRCs, p. 74.

an exponential decrease of prokaryotic cells with depth. Prokaryotic cells were consistently detected, even in the deepest sediments. The method detects sediment layers of increased cell density that often coincide with particular geochemical conditions that are conducive to prokaryote growth (Parkes et al., 2000). The acridine orange direct count (AODC) enumeration method was used at all sites during this leg. Contamination during drilling and handling was evaluated by tests using micrometer-sized fluorescent beads and PFT. These tests have shown that core samples can be obtained without introducing prokaryotic cell contamination, which is essential for almost all microbiological analyses that follow core retrieval (Smith et al., 2000a, 2000b).

Adenosine Triphosphate Analysis

WRCs were cut in the cold room and stored at –80°C for shore-based analysis of ATP concentrations using the luciferin-luciferase assay. Adenosine-5′-triphosphate is used as a common currency of energy for all organisms on Earth. ATP is generated by energy-yielding reactions and is subsequently consumed in energy-requiring reactions in the cell. Because ATP molecules degrade rapidly upon cell death, ATP concentrations can be used as an indicator of total living biomass (Levin et al., 1964). This approach has been used in various marine environments (Holm-Hanson and Booth, 1966), including sediments (Karl and LaRock, 1975; Stoeck and Duineveld, 2000). ATP will be extracted from sediments and quantified using the luciferin-luciferase assay. These data will be compared to total cell counts in order to estimate the fraction of the observed community that is viable.

Cultivation Techniques

Using classic cultivation techniques such as the MPN cultivation method, various physiological types of prokaryotes have been enriched from deep sediments and their abundances determined (e.g., Parkes et al., 2000). The MPN method allows quantification of the number of viable prokaryotes according to a statistical evaluation of the number of tubes of different tenfold dilutions in which growth has been detected (Garthright, 2001). The prokaryotic types that have been cultured from sediment ODP obtained using the MPN method include aerobic ammonifiers, nitrate reducers, fermentative anaerobic heterotrophs, sulfate reducers, methanogens, acetogens, and anaerobic hexadecane oxidizers (Cragg et al., 1990, 1996; Bale et al., 1997; Barnes et al., 1998; Parkes et al., 2000; Wellsbury et al., 2000). MPN population counts range from 0 to 10^5 cells/cm^3 and generally decrease with increasing depth. By MPN enumeration, however, generally far fewer than 0.6% of the total cell numbers in deep sediments are detected, and these viable counts thus yield only limited quantitative information about the microbiology of the deep subsurface. In surface sediments, higher MPN counts have been obtained by the use of complex low-substrate media prepared from sediment extracts and containing fine particles (Vester and Ingvorsen, 1998). Such an approach was used during Leg 201 for the first time with deep sediments.

Cultivation is the only way to obtain microorganisms and study their physiology in order to estimate their impact on biogeochemical cycles in deep sediments. For this reason, we enriched (with the aim to isolate and characterize) various types of microorganisms using a wide range of media and culture conditions that covered a wide range of en-

vironmental conditions and metabolic requirements. Without going into detail about the media, which are listed in "Enrichments Near In Situ Temperatures," p. 29, in "Methods for Enrichment and MPN" in "Procedures and Protocols," the following groups of prokaryotes were targeted:

1. Psychrophiles and mesophiles. Because the deep subsurface sediments drilled during Leg 201 are generally cold, many incubations were kept at low temperatures of 4°–15°C in order to obtain cold-adapted (psychrophilic) prokaryotes that are characteristic of permanently cold sediments (Knoblauch et al., 1999a, 1999b; Knoblauch and Jørgensen, 1999).

2. Thermophiles. As microbial surveys of cold near-surface sediments have in several cases detected thermophilic microorganisms (Isaksen and Jørgensen, 1994; Inagaki et al., 2001) that presumably represent dispersed microorganisms from other environments or remnant populations of former high-temperature environmental regimes, thermophiles, extreme thermophiles, and hyperthermophiles were also enriched during Leg 201.

3. Anaerobic prokaryotes. Because anaerobic processes (sulfate reduction, metal reduction, fermentation, acetogenesis, and methanogenesis) are assumed to be the most relevant microbial processes in deeply buried sediments, media were almost exclusively geared toward enrichment of anaerobic prokaryotes (Balch et al., 1879; Widdel and Bak, 1992; Lovley and Phillips, 1986, 1988; Thamdrup et al., 2000).

4. Oligotrophic prokaryotes. Whereas some bacteria may be isolated from marine sediments on media rich in acetate, lactate, and so on, others may not be able to cope with high concentrations of low molecular weight substrates in synthetic media. Microorganisms in nature have available complex organic substrates in small concentrations. Therefore, media that contain natural sterilized organic sediment extract or complex mixtures of recalcitrant substrates were included in the survey.

5. Chemolithotrophic bacteria. Organic carbon availability is generally a dominant factor in shaping prokaryote community composition and density. However, many microorganisms have a chemolithotrophic energy metabolism, which means that they utilize inorganic electron donors. Potential electron donors include ammonium, hydrogen sulfide, elemental sulfur, hydrogen, iron(II), manganese(II), or methane. Electron acceptors may be oxygen, nitrate, iron(III), manganese(IV), sulfate, or carbon dioxide. The media used during Leg 201 included combinations of such inorganic electron donors and acceptors.

Microbial Molecular Analysis

Culture-independent molecular ecological surveys are becoming an indispensable and powerful approach to investigating naturally occurring microbial diversity. Molecular community analysis of deep subsurface microbial ecosystems also offers new ways to understand the relationship between microbial community composition, microbial activities, and the biogeochemical characteristics of the sedimentary microbial biosphere (Sahm et al., 1999; Madson, 2000; Marchesi et al., 2001). Multiple molecular analytical techniques were applied to the

deeply buried sediments drilled during Leg 201. These techniques are briefly described in the following subsections.

Nucleic Acid-Based Techniques

16S rRNA Gene

Molecular phylogenetic analyses are frequently based on the 16S ribosomal ribonucleic acid (rRNA) sequence. The 16S rRNA is an essential component of each ribosome, the multienzyme complex that translates messenger RNA into proteins, and therefore is a universal component of every living cell. Because of strict functional constraints, the 16S rRNA evolves very slowly and shows clearly recognizable homologies (similarity due to shared evolutionary ancestry) for all living organisms. In other words, the 16S gene is a short but central page from the book of life (~1500 letters) that has survived continued copying and editing for 3.5 billion years. The evolutionary division of life into the three domains of Bacteria, Archaea, and Eukarya is based on ribosomal RNA (Woese et al., 1990). In microbiology, 16S rRNA sequence analysis allowed for the first time a natural classification of microorganisms (including Ludwig and Schleifer, 1999). The analysis of 16S rRNA genes from mixed microbial communities in natural environments has, in combination with biomarker studies (see **"Molecular Biomarkers,"** p. 22), opened a new way to determine microbial community structure without cultivation. By such techniques, numerous entirely new and so-far uncultivated phylogenetic lineages of prokaryotes have been discovered (Barns et al., 1996; Hugenholtz et al., 1998). In various microbial ecosystems, rRNA surveys have demonstrated that microbial diversity is much greater than previously assumed based on cultivation and isolation methods. During the past decade, extensive surveys of extreme environments such as geothermal hot springs, deep-sea sediments, or hydrothermal vent fields (Takai and Horikoshi, 1999; Li et al., 1999; Inagaki et al., 2001; Takai et al., 2001; Inagaki et al., in press; Teske et al., 2002) using culture-independent molecular ecological techniques have extended our knowledge of the phylogenetic diversity in naturally occurring microbial communities.

Metabolic Key Genes

Many prokaryotes have unique metabolic and biochemical properties that are not found elsewhere in the living world. For example, anaerobic respiration with sulfate as an electron acceptor (sulfate reduction), carbon dioxide reduction to methane (methanogenesis), and acetate synthesis from carbon dioxide and hydrogen (acetogenesis) are exclusively prokaryotic processes. The specific enzymes that catalyze these processes are coded by key genes that are unique for these metabolic pathways. Thus, the presence of a key gene in a prokaryote is indicative of the corresponding key enzyme and the metabolic capacity of this organism. Because of functional constraints (the amino acid sequence has to remain conserved to ensure proper enzyme function), many of these key enzymes and their genes are highly conserved in their protein and nucleic acid sequence. A comparison of different versions of the same key gene from different prokaryotes reveals the following:

1. The evolutionary relationships of the gene and, if the prokaryotes have carried this gene continuously throughout their own evolutionary history and have not swapped it with other

    prokaryotes (lateral gene transfer), the evolutionary relation-
ships of the prokaryotes that carry this gene;

2. The shared metabolic and biogeochemical potential of prokary-
otes that carry this gene; and

3. In environmental surveys, new versions of a key gene obtained
from mixed prokaryotic populations in environmental samples
can be compared to the database of cultured known prokaroytes
and their key genes. In this way, the composition of a mixed
prokaryotic community from the environment can be analyzed
under two aspects simultaneously: identity (who is where) and
function (what are they doing).

    In addition to the well-documented 16S rRNA gene (~10,000
sequences in the databases and rapidly growing) (Maidak et al., 2001),
databases and assays for several phylogenetically informative and func-
tionally conserved metabolic key genes have been developed. Some key
genes that will be studied postcruise in samples from Leg 201 and are
specifically relevant for anaerobic subsurface prokaryotic populations
and their activities are dissimilatory sulfite reductase (dsrAB) and
adenosine-5′-phosphosulfate (APS) reductase for bacterial sulfate
reduction (Wagner et al., 1998; Klein et al., 2001; Perez-Jimenez et al.,
2001), coenzyme-M methyl reductase for methanogenesis (Springer et
al., 1995; Lueders et al., 2001), formyl tetrahydrofolate synthase for
acetogenesis, benzoyl-coA reductase, and group I/II dehalogenases for
degradation of complex organic compounds. This list can be easily
extended. The diversity and occurrence patterns of these key genes will
be correlated with biogeochemical measurements of the microbial pro-
cesses and with microbial counts using general stains and fluorescent in
situ hybridization (FISH) probes (see next section, FISH).

Fluorescence In Situ Hybridization

    A powerful technique to quantify prokaryotic cells in environmental
samples is FISH (Amann et al., 1990, 1995). In this approach, fluores-
cently labeled oligonucleotides are used to stain individual prokaryotic
cells according to their phylogenetic affiliation. The probes hybridize
with a universal phylogenetic marker molecule, the 16S ribosomal ribo-
nucleic acid (16S rRNA), a polyribonucleotide of ~1500 bases that is an
integral component of the ribosome, and therefore of every living cell
(see "16S rRNA Gene," p. 20). The 16S rRNA contains phylogenetically
informative sequence regions that range from universally conserved to
genus and species specific (Ludwig and Schleifer, 1999) and present a
large variety of target sites for FISH techniques of defined specificity. Be-
cause high rRNA content is indicative of actively metabolizing bacteria,
FISH can provide quantitative information about active prokaryotes in
an environmental sample. Using a fluorescence microscope, cells can be
visualized and counted after fixing sample material and performing the
hybridization. FISH has been successfully applied to quantify sulfate-
reducing bacteria and other phylogenetic groups of prokaryotes in near-
surface marine sediments (Llobet-Brossa et al., 1998; Boetius et al.,
2000; Ravenschlag et al., 2000, 2001). An important characteristic of
the technique is that a sufficient content of cellular ribosomes is a pre-
requisite for its successful application in sediments (Amann et al.,
1995). To the date of Leg 201, the deepest positive FISH result is from
<0.02 mbsf (Ravenschlag et al., 2001). Thus, the usefulness of FISH to
quantify low-abundance and low-activity prokaryotes in deep sedi-
ments had to be evaluated during this cruise. Newer protocols for sedi-

ments have been published and were used for shipboard analyses (Pernthaler et al., 2001).

A novel approach, FISH-SIMS, combines FISH with secondary ion mass spectrometry (SIMS) and allows the analysis of stable carbon isotopic compositions of individual cells or cell clusters in environmental samples that are identified using nonspecific fluorescence stains or FISH probes (Orphan et al., 2001). This approach will be tested in shore-based research with deep subsurface samples.

Molecular Biomarkers

Living bacterial and archael populations may be identified through structural analysis of prokaryotic polar lipids. Such molecular biomarker evidence can provide additional evidence as to the identity and abundance of various prokaryotic groups. Isotopic analysis (i.e., ^{13}C) of intact polar lipids can provide information on metabolic pathways, in particular methylotrophy. These frozen (–80°C) samples will be analyzed on shore.

Measuring Microbial Rates and Activities

Background

A range of radioisotope experiments were initiated on board the *JOIDES Resolution* during Leg 201. Because radioisotope studies had not previously been carried out on board the *JOIDES Resolution,* we include descriptions of the rationale, procedures, and safety protocols for radioisotope use in this chapter as a reference for future researchers. A radioisotope van equipped specifically for and dedicated to radioisotope experiments was purchased and outfitted by ODP/Texas A&M University (TAMU) prior to departure from San Diego. This van was installed above the Core Tech shop on the port side of the ship, aft of the rig floor. All radioisotope work was carried out in the restricted area in the isotope van. Every scientist who worked in the radioisotope facility (four scientists during Leg 201) was experienced in performing these radiotracer experiments and was required to provide documentation of such from his or her home institution. Only low-energy beta emitters were used during the cruise. Extensive care was taken to avoid any radioactive contamination that could be a potential problem for other research, particularly for the sensitive analyses of natural radioisotopes.

After subsampling according to the methods described in "Core Handling and Sampling," p. 15, in "Introduction and Background," the subsamples dedicated to radioisotope studies were hand carried in a cool box and placed in the appropriate incubator in the van. Sample processing was conducted in a plastic tray on a laboratory bench covered with plastic-backed absorbent paper in the back 10°C room. All solutions were stored in tightly capped containers, and routine postwork contamination wipe tests were performed and logged. All usage of radioactivity was logged, and all contaminated laboratory products were stored in the van. Unused radioactive solutions and contaminated laboratory products remained in the van for transfer to TAMU for final disposal.

Rationale for Radioisotope Experiments

The use of radiotracers is critical to the analysis of prokaryotic activities in the deep subsurface. Such prokaryotic processes as sulfate reduction, methanogenesis, acetogenesis, and methane oxidation take place in deep sediments at extremely low rates, sub-nanomole per cubic cen-

timeter per day or even sub-picomole per cubic centimeter per day (Wellsbury et al., 1997). Such rates are a hundredfold to a millionfold lower than process rates found in surface sediments of the continental shelf and upper slope (Jørgensen, 1982; Ferdelman et al., 1999; Fossing et al., 2000). Interstitial water gradients of sulfate, bicarbonate, or methane may be used in diffusion-diagenesis models to calculate the in situ rates of these processes. However, such models generally cannot take product recycling into account, and therefore they provide net transformation rates rather than gross rates. The difference between net and gross process rates cannot, for the most part, be estimated, but it may be large. As an alternative to modeling, the gross process rates may be determined experimentally in freshly retrieved ODP cores by incubating sediment samples in which the prokaryotes are still in their original physiological state.

Because of the high concentrations of substrates and products such as sulfate, bicarbonate, methane, and so on, it is not possible to detect the small concentration changes during incubations within a realistic time period. Long incubations (exceeding months to years) would be required, leading to strongly altered chemical conditions and prokaryote populations in the sediment samples. Therefore, the determined rates would no longer reflect in situ conditions. By the use of radiotracers, however, rate determinations in incubated sediment samples may become >10,000-fold more sensitive than when using chemical measurements alone (see **"Sensitivity of Process Rate Determinations,"** p. 23). Only by radiotracer techniques is it possible to conduct direct experimental measurements of the most important microbial processes in the deep subsurface, and even then, such methods are operating close to their detection limits when studying million-year-old sediments. Consequently, the amounts of radioactivity applied and incubation times used must be higher than those normally used in studies of near-surface sediments.

It is critical to all experimental process measurements that the sediment remains as intact as possible. Otherwise, data become unreliable. Successful process studies require the following:

1. Fast handling of cores on deck to avoid warming of cold sediments (in cold deep-sea sediments, bacteria may be sensitive to warming and could be killed at >10°–15°C; in warmer sediments this problem is not critical);
2. Subsampling by clean and anoxic techniques from whole-round cores (i.e., the normal ODP procedure of splitting the entire core section cannot be used on microbiological sections); and
3. Starting radiotracer experiments as soon as possible after coring because the chemistry and microbiology gradually change once the sediment has been brought up on deck. Experiments that start after the cruise are still very useful (e.g., for studies of factors regulating process rates), but the absolute rates become less trustworthy with time.

Sensitivity of Process Rate Determinations

The following example demonstrates why the use of radioactive isotopes as tracers in experimental process studies may enhance the detectability by many orders of magnitude. The example illustrates a measurement of sulfate reduction in the middle of the sulfate zone of a sediment core. We assume that the interstitial water sulfate concentration is about one-third that of seawater (i.e., 10 mM). By normal ion

chromatography, this concentration may be determined with an accuracy of ±1%. In order to detect sulfate reduction in an incubated sediment sample by chemical analysis alone, the sulfate concentration would thus need to change by at least 1% of 10 mM (i.e., by 0.1 mM or 10^{-4} M). If the reduction rate is, for example, 1 pmol/cm³/day = ~10^{-9} M/day, then the experiment must run for at least 10^5 days, which is 300 yr.

If, instead, radioactive sulfate is added to the sediment in trace amounts, the sulfate reducing bacteria will reduce this labeled sulfate at the same relative rate as they reduce the nonradioactive sulfate (i.e., the same fraction of radiolabeled and interstitial water sulfate will be reduced per unit time). With the use of radiotracer, the reduction of a much smaller fraction of the sulfate can be detected. This is not because the determination of sulfate radioactivity is substantially more accurate but because the radioactive sulfate is converted into radioactive sulfide that can be detected instead. After the experiment has been terminated, the sulfide is converted to hydrogen sulfide gas by acidification of the sediment, and this gas can be very efficiently separated from the sediment and from the radioactive sulfate. As the hydrogen sulfide starts out with a radioactivity of zero, it is possible to detect the reduction of <10^{-6} of the radioactive sulfate. A 10^{-6} fraction of 10 mM sulfate is 10^{-8} M sulfate (i.e., 10,000-fold lower than the minimum detectable fraction by chemical analysis). This would reduce the minimum duration of the experiment to 10 days, which is obviously more realistic for the length of an ODP cruise. This calculation demonstrates only the minimum experimental time required to detect sulfate reduction at a rate of 10^{-9} M/day. To obtain reasonable quantitative data for the process, the incubation time would need to be somewhat longer (e.g., 1 month), which is still practical. Similar calculations may be performed for ^{14}C-labeled acetate, bicarbonate, and methane. In addition, the $^{35}SO_4^{2-}$ tracer will also be used in part of the MPN experiments for sensitive detection of active bacteria (cf. Vester and Ingvorsen, 1998) (see **"Radiotracer MPN Experiments,"** p. 31, in "MPN Analyses near In Situ Temperature" in "Procedures and Protocols").

^{18}O Stable Isotope Tracer Studies of Phosphate and Sulfate Turnover

Stable isotopes (e.g., ^{13}C, ^{15}N, and ^{34}S) are important "natural" tracers of microbiological processes and are also useful in labeled-tracer studies, such as, the ^{13}C-labeled substrates used in FISH-SIMS experiments described in a previous subsection. Although widely used in biochemical research but only rarely applied in biogeochemical/microbiological studies, oxygen isotopes are also powerful tracers of enzymatic/metabolic reactions. Varner and Kok (1967) first proposed the use of oxygen isotopes in water as a means for detection of enzymatic activity in extraterrestrial soil samples to be collected during the Mars *Viking* missions. The basis for using oxygen isotopes in water is that biologically active oxy-anions such as sulfate, nitrate, phosphate, or acetate may undergo rapid oxygen isotope exchange with water at low temperature, but only in reactions that are catalyzed by enzymes. Thus, the presence of enzyme catalytic activity, detected by the transfer of ^{18}O from labeled oxy-anion substrates to water, implies the presence of life. Using this approach with ^{18}O-labeled phosphate, Varner and Kok (1967) report a detection limit of 0.05% change, which during a 24-hr incubation period might be achieved by 10^4 active prokaryotic cells per gram sediment. A modified version of this approach involving $^{18}O/^{16}O$ ratios of

phosphate and sulfate rather than of water was employed for Leg 201 sediment samples to assess the utility of stable oxygen isotope tracers in detecting metabolic activity in deep-sea sediments characterized by very low rates of microbial growth. This primarily shore-based research was initiated during Leg 201 to optimize the survival and growth of microbes in long-term ^{18}O-label incubation experiments.

One advantage of using oxygen isotope ratios of phosphate and sulfate as reaction tracers is the ability to carry out incubation experiments over relatively long periods of time. Radioisotope tracers such as ^{35}S are useful over weeks to a few months (half-life of ^{35}S decay = ~3 months), whereas incubations that utilize changes in phosphate oxygen isotope ratios as a reaction tracer can be carried out over many months to years. This is because ^{18}O is a stable isotope and P–O bonds are highly resistant to chemical cleavage at low temperature, resulting in extremely low rates of oxygen isotope exchange between phosphate and water, on the order of 10^5 yr at 25°C (Lécuyer et al., 1999). Phosphate solutions used as laboratory standards and stored at room temperature show no change in phosphate oxygen isotope composition ($^{18}O_P$) over several years. Further, abiotic/nonenzymatic reactions involving phosphate, such as mineral precipitation/dissolution, produce little (~1‰ for precipitation of apatite) or no fractionation of oxygen in phosphate.

Procedures and Protocols

Total Prokaryotic Cell Counts

Potentially contaminated sediment was removed with a sterile scalpel. A 1-cm^3 minicore was then taken with a sterile 5-mL plastic syringe. The syringe was sealed with a sterile Suba-Seal stopper. In a clean area of the laboratory, the 1-cm^3 plug was extruded into a sterile serum vial containing 9 mL of 2% (v/v) filter sterilized (0.2 µm) formaldehyde in 3.5% NaCl. The vial was crimped and shaken vigorously to disperse the sediment particles. Where cell counts were performed on sediment slurries, then a 2-mL volume of slurry was added to a sterile serum vial containing 9 mL of 2% (v/v) filtered sterilized (0.2 µM) formaldehyde in 3.5% NaCl.

Total prokaryotic cell numbers and numbers of dividing or divided cells were determined using acridine orange as a fluorochrome dye with epifluorescence microscopy (Fry, 1988). Fixed samples were mixed thoroughly, and a 5- to 50-µL subsample was added to 10 mL of 2% (v/v) filter-sterilized (0.1 µm) formaldehyde in 3.5% NaCl. Where sediments contained significant amounts of carbonate, then the 2% formaldehyde was made up in 3.5% NaCl and 2% acetic acid. Acetic acid dissolves a substantial amount of carbonate, allowing larger samples to be processed, and thus resulting in greater accuracy and lower detection limits. Acridine orange (50 µL of a 1-g/L filter-sterilized [0.1 µm] stock solution) was added, and the sample was incubated for 3 min. Stained cells and sediment were removed on a 0.2-µm black polycarbonate membrane (Osmonics, USA). Excess dye was flushed from the membrane by rinsing with a further 10-mL aliquot of 2% (v/v) filter sterilized formaldehyde in 3.5% NaCl, and the membrane was mounted for microscopic analysis in a minimum of paraffin oil under a coverslip.

Mounted membranes were viewed under incident illumination with a Zeiss Axiophot microscope fitted with a 100-W mercury vapor lamp, a wide-band interference filter set for blue excitation, a 100× (numerical aperture = 1.3) Plan Neofluar objective lens, and 10× oculars. Pro-

karyote-shaped fluorescing objects were enumerated, with the numbers of cells on particles doubled in the final calculation to account for masking by sediment grains.

The percentage of cells involved in division has been suggested as an indication of growth, although the assessment of dividing cells has never had a standardized approach in the literature. Dividing cells were defined operationally as those having clear invagination. A divided cell is operationally defined as a visually separated pair of cells of identical morphology. The percentage of cells involved in division is then calculated as follows:

$$\text{Percentage of cells involved in division} =$$
$$[\text{number of dividing cells} + 2(\text{number of divided cell pairs})]$$
$$\times\ 100/\text{total number of prokaryotic cells.}$$

The detection limit for prokaryotic cells is usually 1×10^5 cells/cm^3 (Cragg, 1994); however, the use of acetic acid with carbonate sediments reduced this to 4.5×10^4 cells/cm^3.

Live and Dead Stains

As commonly applied to subseafloor sediments, nucleic acid stains such as acridine orange only provide information on the presence or absence of cells in the sediment matrix. Such use does not demonstrate if these cells are alive and active, dormant, senescent, or even dead. A number of stains have recently been used to determine proportions of living and dead cells, predominantly in laboratory cultures. One stain that appears to have the potential for use with environmental samples is CFDA/SE (5[6]-carboxyfluorescein diacetate/succinimidyl ester; Molecular Probes, Oregon, USA). Samples were obtained from cores for shore-based analysis. The procedure requires a 48-hr incubation in phosphate-buffered mineral salt solution and observation under UV light (Fuller, et al., 2000).

Perfluorocarbon Tracer Contamination Tests

PFT was continuously fed into the seawater drill fluid at a tracer concentration of 1 mg/L seawater drill fluid. Concentrations of PFT were measured in all sections used for microbiological studies. A 5-cm^3 subcore from the adjacent section was routinely taken, as described by Smith et al. (2000a). In many cases, two 5-mL subcores were taken and placed in the same headspace vial to increase sensitivity. Further, a 5-mL sample was tested from the "master slurry" prepared in the cold room for microbial incubation experiments. Air samples were occasionally taken to monitor the ambient concentration of PFT in the cold room air or on the catwalk. The concentrations of PFT at the outer periphery of the drill cores were measured to verify delivery of the PFT. Additionally, during APC drilling at each site, the concentration of PFT was measured in radial transects from the edge of the core to the middle in an "X" pattern, providing a two-dimensional view of contamination from four separate edge points to the common center. Finally, during XCB drilling, chunks of intact core (biscuits) surrounded by slurries of sediment and drilling fluid were collected, measured in length, and digitally photographed. PFT concentrations in the slurry, at the edge of the intact core on fracture surfaces, and in the middle of the chunk were measured, thus providing data on the minimal size and quality of intact

core pieces that could be confidently sampled for microbiological investigations.

The conditions used on the GC were somewhat different than those previously used by Smith et al. (2000a). We used a HP-PLOT/AL203 "S" deactivated column with film thickness = 50 μM, length = 15 m, phase ratio = 12, and column ID = 0.25 mm. The inlet temperature was 180°C with 10 psi, the detector temperature was 250°C, and the column temperature was 100°C for 3.5 min and then ramped up 50°C/min until it reached 200°C. The PFT peak was at a retention time of 5.1 min. We used a 1-mL injection. Larger injections were found to result in loss of material.

The routine that gave the best results was to first bake the sample headspace vial and the syringe at 80°C, then inject clean nitrogen gas onto the column to make sure that no PFT peak resulted from residual PFT in the syringe or in the GC. After a clean run was achieved, the sample was injected using the same baked syringe. At the time of the injection, the syringe was also still hot so PFT would not condense out before injection. Also, for best results, background air samples need to be taken regularly from the same location that is used for capping headspace vials (ideally on the catwalk when no core is present). Finally, cleaning PFT out of used syringes is critical. We found it was best to use a large Hamilton syringe (10 mL) that could be flushed several times with wash methanol to remove the PFT. The syringe had to be baked for a long time to remove the methanol in order to avoid having an interfering GC peak. It was also found that cores with high levels of sulfide resulted in GC traces with small air peaks, presumably from the sulfide scrubbing out oxygen in the headspace vial. Therefore, for cores rich in sulfide, the air peak cannot be used to normalize various GC runs. The PFT detection limit reported for Leg 201 sites was not set as a lower limit of the ability to detect PFT by the GC, but as a lower limit of ability to confidently assess the presence of PFT in real samples given the uncertainty inherent in subtracting background levels of PFT and the reliability of the integration of small GC peaks.

Fluorescent Microparticle Tracer

A suspension of submicron-sized fluorescent microspheres was introduced into the drill fluid at all stations at selected depths that were also used for microbiological sampling. A plastic bag with a suspension of beads, positioned within the core catcher, released the beads inside the core barrel as it hit the sediment, thus providing maximum effectiveness of the beads as tracers of potential bacterial contamination. The procedure for assessing this particle contamination was adapted from that used during Leg 190 (Smith et al., 2000a, 2000b). The sediment sample (5 mL of sediment or 10 mL of 25% sediment slurry) was mixed with an equal volume of saturated sodium chloride solution. The solution was centrifuged (Marathon 10K; 5 min; $2800 \times g$), and the supernatant was filtered onto black polycarbonate filters (0.2-μm pore size). Fluorescent microspheres were counted under UV light, and data are reported as number of microspheres per gram of sediment.

When comparing the results of both contamination tests, the presence of beads and PFT concentration inside 5-cm^3 subcores, one should consider some important aspects. First, in contrast to the beads, PFT can travel through very small pore spaces and is found in the laboratory air and on the hands of anyone who has handled a core liner. Therefore, although its presence at high concentrations in a sediment sample

(>0.1 ng PFT/g sediment) may suggest contamination, it is not necessarily an indication that microorganisms from the drilling fluid have in fact contaminated the sample. On the other hand, the absence of PFT from a sample indicates that contamination by drill water has not occurred.

Second, whereas the number of beads (5×10^{11} beads/20-mL bag) that are deployed is equivalent to the number of bacteria in ~1000 L of seawater (assuming 5×10^8 bacteria/L), their deployment does not produce a uniform dispersion along the core. Although PFT can always be found in sediment samples taken from the edge of cores, the same is not true for the beads. At this point, without knowing the factors that control the final concentration and distribution of beads along the core barrel, one should consider the beads as a qualitative rather than a quantitative measure of contamination. The presence of beads is a strong indication that contamination by prokaryote-sized particles from the drilling water has occurred; the absence of beads alone does not mean that a sample is uncontaminated.

Cultivation of Microorganisms

Here we describe the subsampling from WRCs and the media, incubation conditions, and research rationales for the shipboard microbiologists who were using media for cultivation and quantification of subsurface prokaryotes. The different kinds of media were inoculated from a sediment slurry or directly from WRC material, both kept cold and anoxic. For quantitative enrichments using the MPN technique, parallel assays were inoculated from a dilution series (Fig. F9). For MPN evaluation and enrichments in general, the assays will continue to be incubated in different shore-based laboratories at different temperatures after the cruise, with the goal to quantify particular prokaryotic physiological types and to isolate pure cultures.

Preparation of Slurries

Slurries were prepared in 250-mL Buchner flasks closed with stoppers that allowed sterile nitrogen flushing by means of a gas filter and a stainless steel tube. The side arms could be closed with sterile stopcocks. A salt solution (150 mL, containing 23.5 g NaCl and 10.8 g $MgCl_2 \cdot 6H_2O$ per liter) and a magnetic stirring bar were added and autoclaved at 121°C for 20 min, then the solution was cooled under nitrogen. A slurry (25% v/v) was prepared by adding the sediment contents of $10 \times$ 5-mL or 2×25-mL syringes under a nitrogen counterflow and sterile conditions. The slurry was homogenized by repeated shaking and vortexing at 0°C for 30 min. Subsamples of this master slurry were distributed to all research groups conducting total cell counts, contamination checks, cultivation (five groups), FISH analyses, ^{13}C and ^{18}O experiments, and measurement of hydrogen production.

Methods for Enrichment and MPN

To enrich prokaryotes, the different media, which are described in detail in "Enrichments near In Situ Temperatures," p. 29, were inoculated with subsamples from the slurry or with intact sediment. To obtain slurry subsamples, sterile syringes were first flushed with nitrogen and then filled with the slurry via the Buchner flask side arm. As soon as possible, the media were inoculated, either in an anaerobic chamber

F9. Inoculation scheme for MPN, p. 75.
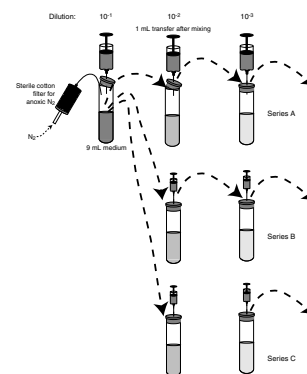
or, in cases when Hungate or Balch tubes were used, directly on a laboratory bench (Balch et al., 1979; Widdel and Bak, 1992). For MPN counts, the subsamples were used to make a dilution series in tenfold dilution steps (Fig. F9). To each tube containing 9 mL of medium, 1 mL of inoculum from the previous dilution step was added under an nitrogen atmosphere. From each dilution tube, three (or up to six) tubes of an identical medium were inoculated in parallel.

The tubes were incubated on the ship and shipped back to home laboratories for further incubation at the specified temperatures for periods of several months to >1 yr. The long incubation periods are necessary to allow slow-growing prokaryotes time to develop a detectable population size in the culture tubes. For example, the first MPN counts of cold-adapted sulfate-reducing bacteria from Arctic surface sediments required 2 yr before full development (Knoblauch et al., 1999a). Subsamples will be taken postcruise from the highest dilutions showing positive growth and used for inoculation of new sterile dilution series. The highest dilutions are used for further transfer to maximize the probability of transferring and ultimately isolating dominant representatives of the microbial populations.

Enrichments near In Situ Temperatures

The in situ temperatures in the sediments drilled at Leg 201 sites ranged mostly from 1° to 10°C in the upper 100 m at the deep-sea sites and 12°–25°C at the continental shelf sites and in the lower part of some deep-sea sites (see "Physical Properties" sections in each site chapter). Accordingly, psychrophilic (cold-adapted, with temperature optimum <15°C) prokaryotes are most relevant for the ongoing biogeochemical processes in much of the deep sea, and mesophilic (temperature optimum between 20° and 45°C) prokaryotes are most relevant on the shelf.

This section describes the enrichment and MPN methods that were applied for fermenting prokaryotes, sulfate-reducing bacteria, and methanogens during Leg 201. Most of the following media were based on artificial seawater (marine salts medium [MM]) (see Table T3). After autoclaving and cooling under nitrogen, bicarbonate buffer, a vitamin mixture, and $FeCl_2$ plus Na_2S were added to this MM. Upon addition, the latter two compounds form black FeS precipitate at the bottom of the vial. The FeS functions as a reducing agent and microenvironment for prokaryotes. Sediment prokaryotes are not accustomed to living in a pure liquid environment and often attach to particles. In contrast to most classic media, those made from MM are thus turbid from the beginning and require a microscopic or molecular biological analysis to detect growth. Different carbon sources were added to the MM as specified in Table T4.

Monomer medium (Mono) (Table T4) contained 36 monomers, among them the 20 most common amino acids and many compounds that are intermediates in the anaerobic prokaryotic degradation of organic matter and are used by fermenting, sulfate-reducing, or methanogenic prokaryotes. In contrast to most classic media, the concentration of the substrates is low, as it is known that prokaroytes from low-substrate environments might be killed by high substrate concentrations.

Polymer medium (Poly) (Table T4) contained nonsoluble substrates that under anaerobic conditions require sequential cooperation of different prokaryotes for degradation. Chitin is present in many marine organisms. Xylane and cellulose are common polysaccharides. Peptone

T3. MM salts, p. 83.

T4. Media for psychrophiles and mesophiles, p. 84.

contains poly- and oligopeptides. It is expected that fermenters, sulfate-reducing bacteria, and methanogens will grow in this medium.

The medium with aromatic compounds and long-chain fatty acids (Aro) (Table **T4**) contained substrates that are usually only slowly degraded. Those substrates are typical for low-substrate environments, where easily degradable low molecular weight substrates have been depleted.

The lactate medium (Lac) (Table **T4**) used is a classic substrate for sulfate-reducing bacteria. It might be partially degraded to acetate by incompletely oxidizing sulfate reducers (Widdel and Bak, 1992) or fermented to propionate and acetate. Acetate can then be used by completely oxidizing sulfate reducers or methanogenic archea.

Sulfate-free medium (no-SO$_4$) (Table **T4**) was used for sulfate-poor sediment layers in order to compare with sulfate-containing medium. This comparison should indicate how sulfate limitation influences the prokaryotic communities. Sulfate-free medium was prepared with MM salts to which Na$_2$SO$_4$, Na$_2$S, and FeCl$_2$ had not been added. In this medium, titanium(III)citrate (Zehnder and Wuhrmann, 1976) was used as the reducing agent.

Sediment extract medium (Sed) (Table **T4**) was used to offer a complex mixture of substrates containing many natural substrates. It does not reflect the natural situation, since the extracted sediment was rather young and was treated with heat. However, it has been found that such media may support the growth of more types of prokaroytes than those composed of defined compounds. The extraction solution had the same composition as the MM salts, except that it did not yet contain NaHCO$_3$, vitamins, Na$_2$S, and FeCl$_2$. 4-(2-Hydroxyethyl)piperazine-1-ethansulfonic acid (HEPES) was added as a buffer. Sediment from the 5- to 20-cm subsurface layer of North Sea tidal flats was mixed with the same weight of extraction solution and stirred overnight at room temperature. The mixture was then heated to 80°C for 30 min. After cooling and sedimentation of larger particles, the supernatant was filtered through a cellulose filter. The extract was autoclaved and cooled under nitrogen before vitamins, FeCl$_2$, and Na$_2$S were added to the same concentration as to the MM salts.

MPN Analyses near In Situ Temperature

MPN counts of psychrophilic and mesophilic microorganisms were performed using deep-well titer plates (8 wells × 12 wells; Beckmann 27007) at temperatures of 4° or 15°C (Fig. **F10**). Wells were filled with 900 µL of medium under nitrogen. Then, 100 µL of master slurry was added, and triplicate tenfold dilution series were made down to 10^{-6}. For each triplicate dilution series, a row remained uninoculated as a control. Plates were closed by sterile capmats (Beckmann 267005) and stored in anoxic bags under nitrogen with oxygen scrubber trays (Anaerocult, Merck). The media turbidity (because of iron sulfide precipitation) and the limited growth (because of low substrate concentrations) require the wells to be analyzed by microscopy, fluorescence microscopy, molecular biology, or with radiotracers (see **"Radiotracer MPN Experiments,"** p. 31). The incubation time at 4°or 15°C will be up to 2 to 6 months.

MPN Series with Background Bacteria

Under anoxic conditions, many substrates are degraded syntrophically by cooperation of different groups of bacteria. Fermenters require the activity of hydrogen-consuming sulfate reducers or methanogens.

F10. MPN counts with a microtiter plate, p. 76.
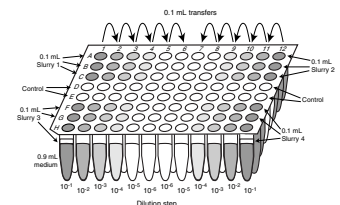
In order to promote syntrophic growth, sulfate-reducing bacteria were added to some MPN series. To Sed and Poly mediums, *Desulfomicrobium norvegicum* was added as background bacterium (~10^6 bacteria/mL medium). This bacterium has a restricted substrate spectrum. It can function as an hydrogen scavenger for the syntrophic degradation of substrates, thereby stimulating the degradation and the growth of the prokaryotes involved. It is also quite robust, consumes oxygen rapidly (which protects other oxygen-sensitive prokaryotes), and tolerates marine salt concentrations and temperatures.

Radiotracer MPN Experiments

Radiotracer MPN series (Vester and Ingvorsen, 1998) were not designed to determine activity rates but aim to detect active cells with similar high sensitivity as can be obtained by fluorescence microscopy or molecular biological techniques. By the radiotracer MPN technique, growth of the prokaryotes may not be required or may be marginal, yet the technique allows the detection of metabolically active cells. MPN series were inoculated in the deep-well microtiter plates (Fig. F10) with medium to which radiolabeled ^{35}S-sulfate (100 Bq/well) had been added. Radiolabeled sulfide formed during sulfate reduction, including FeS, S°, and FeS_2, will be detected at high sensitivity by later cold distillation of hydrogen sulfide (as modified from Fossing and Jørgensen, 1989).

Gradient Cultures

In order to study the reaction of the prokaryotic communities in undisturbed sediment samples to low concentrations of incoming substrates, gradient cultures were inoculated on whole pieces of sediment (Fig. F11). A mixture of monomers (4 mM each; 0.5 mL) was placed on the bottom of a glass tube and fixed with 0.5 mL agar (4% in MM at 60°C). When the agar was solidified, another 2.5 mL of agar plus 4 mL MM was added as spacer. Finally, 2 mL of a sediment subcore in 5 mL MM was placed on top, then the tube was gassed with nitrogen, closed by a rubber stopper, and cooled on ice, before incubating at the proper temperature.

Enrichments at 25°, 50°, and 80°C

Thermophiles are generally prokaryotes that grow optimally at >55°C (T_{opt}) and have an upper temperature limit for growth (T_{max}) >60°C. Most of these prokaryotes do not grow at <40°C. Thus, incubation temperatures of 50° and 60°C were used to cover different populations of thermophiles. Extreme thermophiles have a T_{opt} > 60°C and a T_{max} ≥ 70°C, whereas hyperthermophiles have a T_{opt} > 80°C and usually cannot grow at 60°C. Many cannot grow even at <75°C (Wiegel, 1992). Thus, an incubation temperature of 80°C was used for the hyperthermophiles.

Several kinds of media for enrichment and cultivation of heterotrophic, chemolithoautotrophic, and chemolithorganotrophic prokaryotes were prepared on board. Cultivation media were incubated at three different temperatures: 25° (mesophiles), 50° (thermophiles), and 80°C (hyperthermophiles). Although the drilling sites do not include hydrothermal sediments, recent molecular ecological research has demonstrated that genes of anaerobic thermophiles or hyperthermophiles and extreme halophiles can be detected in shallow sediment layers (Isaksen and Jørgensen, 1994; Inagaki et al., 2001). These extremophilic microorganisms are considered to be present as dormant or relict

F11. Gradient culture tube preparation, p. 77.
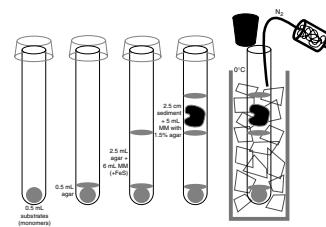
communities. The ecological and biogeochemical significance of successfully enriched and cultured isolates will be evaluated in the context of their physiology and metabolic pathways.

Media incubated at 25°, 50°, and 80°C targeted the following physiological types of prokaryotes (numbers correspond to medium numbers in Table T5):

201-1: Anaerobic, heterotrophic sulfur reducers,
201-2: Anaerobic, heterotrophic iron(III) reducers,
201-3: Anaerobic, heterotrophic nitrate reducers,
201-4: Anaerobic, heterotrophic sulfate reducers,
201-5: Anaerobic, autotrophic hydrogen-oxidizing sulfate reducers,
201-6: Anaerobic, autotrophic sulfide-, thiosulfate-, or sulfur-oxidizing iron(III) or nitrate reducers,
201-7: Microaerobic, autotrophic sulfide-, thiosulfate-, or sulfur-oxidizing iron(III) or nitrate reducers,
201-8: Methanogens,
201-9: Anaerobic, autotrophic ammonium-oxidizing iron(III) or nitrate reducers,
201-10: Microaerobic, autotrophic ammonium-oxidizing iron(III) or nitrate reducers, and
201-11: Extremely halophilic archaea, genus *Haloarcula*.

These enrichment media for shipboard cultivations were prepared on board and were based on MJ artificial seawater salts solution (Table T6) to which substrates were added according to the requirements of the physiological type of prokaryotes targeted. All media and incubations were anaerobic, unless otherwise stated. A 0.5- to 1.0-mL sample of master slurry was anoxically inoculated into 5 mL of media and incubated. The growth of cells was observed by microscopy. Successful enrichments were kept at 4°C until further transfers to the shore-based laboratory (JAMSTEC).

Enrichments at 60°C

For the following enumerations and enrichments of anaerobic thermophiles, all incubations were done at a temperature of 60°C and a pH of ~8.0 and 9.0 (for exact pH at 60°C [pH$^{60°C}$], see media recipes in Table T7). Some enrichments were conducted at a more alkaline pH because of a special interest in the biodiversity of alkalithermophiles. All shipboard incubations were done using the basic marine sea salt media (MSSM) (see Table T8), supplemented with the corresponding carbon sources, electron donors, and electron acceptors. Incubations that showed no growth after several weeks were heat treated (1 min at 100°C) to activate possible spores (some do not germinate during incubations at 60°C) and then were again incubated for 3 weeks for a final postcruise evaluation. The following groups were enriched at 60°C:

1. Heterotrophic fermenters (ferm) (Table T7). Incubations were done in the presence of hexoses or pentoses plus yeast extract to enumerate and isolate various obligately and facultatively anaerobic heterotrophic thermophiles. Thiosulfate was added as an additional electron acceptor to enhance the recovery of specific groups (especially when using pentoses as a carbon source), such as *Thermoanaerobacterium* species. These usually reduce thiosulfate to sulfur, which is accumulated intracellularly in sulfur gran-

ules and are easily recognizable by light microscopy. Substrates were

    a. Glucose, fructose, and mannose (+ thiosulfate if no growth occurs),
    b. Xylose and ribose for pentose utilizers, and
    c. Xylose and pentose plus thiosulfate.

Tests of metabolic activity and growth can include a decrease in pH, an increase in cell numbers, and, in further dilutions or subcultures, turbidity.

2. Autotrophic methanogens and acetogens (H_2/HCO_3^-) (Table **T7**). These may be enumerated and isolated on MSSM containing hydrogen gas and bicarbonate. Spore-forming acetogens are expected to be found, although it is also conceivable to find methanogens. Decreases in hydrogen pressure and an increase in cell numbers (microscopy) and, in further dilutions, turbidity will be used to indicate positive metabolic activity and growth. On board ship, differentiation of methanogens and acetogens were done by fluorescence microscopy utilizing the F_{420} cofactor autofluorescence of methanogens. In case of positive growth, the headspace of 100% hydrogen was replenished by pressurizing through a sterile filter.

3. Autotrophic iron reducers (H_2/HCO_3^-/Fe[III]) (Table **T7**). It is hypothesized that the capability to use iron(III) as an electron acceptor is much more widespread among anaerobic microorganisms than is presently recognized. The present conditions mainly favor the obligately chemolithoautotrophic iron reducers and the facultative ones with high hydrogen oxidizing capabilities. Very little is known about marine iron reducers, and no thermophilic marine iron reducer has been validly described to date. A decrease in hydrogen pressure, formation of magnetite as visualized with a magnet, and, in further dilutions, turbidity will be used to indicate positive metabolic activity and growth.

4. Autotrophic manganese reducers (H_2/HCO_3^-/Mn[IV]) (Table **T7**). Although most thermophilic iron(III)-reducing bacteria that have been characterized thus far can use manganese(IV) as an electron acceptor, it is anticipated that at the sites where higher manganese concentrations have been found, manganese(IV)-reducing thermophiles can be isolated that possibly are not iron(III) reducers. The capability of reducing manganese(IV) to manganese(II) is widespread among the gram-negative mesophilic iron reducers. Positive metabolic activity and growth will be indicated by a color change from brown (MnO_2) to white ($MnCO_3$), an increase in cell density, and, in further dilutions, turbidity. Quantification of manganese(II) will be done postcruise.

5. Lipolytic microorganisms (C-18 lipo) (Table **T7**). Triglycerates or diglycerates (derived from phospho- and glycolipids by losing the polar phosphate or sugar group) are components of many eukaryotic organisms and thus are expected to be present in marine sediments. Presently, very little is known about the distribution and consumption of these compounds in deep marine sediments. Positive metabolic activity will be indicated by a decrease in a C_{18}-triglycerate and, in further dilutions, by turbidity. Quantification of either glycerol or fatty acids, depending on the type of microorganisms, will take place postcruise.

6. Sulfate reducers (SRB) (Table T7). The presence of moderately thermophilic sulfate reducers (mainly *Desulfotomaculum* species) in marine sediments is well established. It was previously shown for a different location that all thermophilic sulfate reducers were present as spores (Isaksen and Jørgensen, 1994), and thus it is possible that the enumerations yield basically an even distribution with depth. Two different media were used with either (a) acetate and lactate or (b) benzoate as energy and carbon source. Positive metabolic activity and growth will judged by color change to black, due to iron sulfide formation and increase in cell numbers (microscopy), and, in further dilutions, turbidity.

7. Chlorate reducers (Chlor) (Table T7). The chlorate and perchlorate utilizers have been studied only recently (Coates et al., 1999). No thermophilic chlorate reducer has been described so far, but they are expected to exist. Enrichments at 4°C were also prepared. An increase in cells and, in further dilutions, turbidity will be used to indicate positive growth metabolic activity. Quantification of chlorate and intermediates will be done post-cruise.

Manganese(IV)- and Iron(III)-Reducing Bacteria

Acetate-oxidizing iron(III)- and manganese(IV)-reducing bacteria were enumerated by the MPN technique with acetate as the sole organic carbon source and either FeOOH or MnO_2 as an electron acceptor as described by Thamdrup et al. (2000). The anaerobic, sulfate-free, bicarbonate-buffered marine mineral medium with vitamins and trace elements according to Widdel and Bak (1992) was supplemented with 5-mM acetate as electron donor and 50-mM concentration of either FeOOH or MnO_2 as electron acceptor. FeOOH or MnO_2 were synthesized according to Lovley and Phillips (1986, 1988). The MPN tubes for enrichment of manganese(IV)- and iron(III)-reducing bacteria were prepared before the cruise (Fe[III] red and Mn[IV] red in Table T9) and were inoculated anaerobically in tenfold dilution steps directly after sampling on board. Samples were taken from sites and depths where interstitial water gradients of manganese or iron indicated activity of manganese(IV)- or iron(III)-reducing bacteria. After the cruise, the MPN tubes are incubated at 10°C, close to in situ temperatures, for at least 1 yr. Isolation of strains and their characterization will be done from tubes with positive growth. Positive tubes will be recognized from the change in color of the precipitates from reddish brown to black (iron) and from dark brown to white (manganese) or by measuring the amount of iron(II) or manganese(II) in the medium.

T9. Media definitions, p. 90.

Nitrifying and Methylotrophic Bacteria

Aerobic chemolithoautotrophic ammonium- or nitrite-oxidizing bacteria as well as aerobic methylotrophic prokaryotes utilizing chloride compounds have not been studied previously in deep sediments. Because of lateral seawater flow through basement rock, oxygenated seawater could penetrate into overlying deep subsurface sediment. As a consequence, ammonium could be oxidized via nitrite to nitrate by aerobic nitrifying bacteria, and methane could be consumed by aerobic methylotrophic prokaryotes. These processes are suggested by ammonium and methane profiles (see "Biogeochemistry," p. 14, in the "Site 1225" chapter and "Biogeochemistry," p. 13, in the "Site 1226" chapter), which show lower ammonium and methane concentrations in the bottom sediment than at medium depths. MPN counts for nitrifying

bacteria were performed in liquid medium, whereas methylotrophic prokaryotes were enriched on agar plates. After inoculation, the MPNs and agar plates are incubated at 10°C for several months. For details, see Table T4.

Rock Sampling

Basement Basalt and Breccia

Igneous rock samples were washed in 250-mL Pyrex bottles containing 50 mL of nitrogen-flushed marine salts solution (23.5 g NaCl and 10.8 g $MgCl_2 \cdot 6H_2O$ per liter). This washing step removed most of the adhering sediment particles and surface contamination. After the first washing step, the rock sample was transferred into a second wash bottle containing 50 mL of fresh nitrogen-flushed marine salts solution and was washed again by shaking and rinsing. After this step, the rock sample was collected with sterile forceps and carefully cleaned by scraping off small remaining pockets of sediment from the surface using fresh syringe needles. The loosened particles were then rinsed off with previously nitrogen-flushed marine salts solution from a syringe. Afterward, the rock was crushed into several pieces to be used for different investigations. Crushing was done either by wrapping the rock in sterile aluminum foil and breaking it into pieces with several forceful hammer strokes or by crushing the rock inside a rock crusher. This crusher is an autoclavable metal block with a well that can hold a small rock piece. A solid piston is placed into the well on the rock sample and crushes the rock with several hammer strokes aimed at the flat top of the piston.

Several pieces of the rock samples were placed into 3-M HCl for 1 min to sterilize the rock surface, rinsed with sterile marine solution, and subsequently crushed as described. These pieces were only used to inoculate media.

The pieces were stored in sterile plastic bags for thin sectioning and petrographic analysis, put into phosphate buffered saline (PBS)/50% ethanol for ion microprobe analysis, fixed for AODC), frozen at –80°C for DNA analysis, fixed in PBS/4% formaldehyde for 4′,6-diaminidino-2-phenylindole (DAPI) staining, FISH, and thin sectioning, and used for inoculation of different media. The compositions of the media are described in "Enrichments near In Situ Temperatures," p. 29, in "Methods for Enrichment and MPN." In addition, to enrich for hydrogen-oxidizing endolithic prokaryotes, an autotrophic basalt medium (A-bas) was prepared (Table T4).

The A-bas was dispensed in 5-mL amounts into Hungate tubes. Half of the tubes already contained 50 µL of 1-mol/L $Fe(OH)_3$ and 50 µL of 1-mol/L MnO_2; the other half did not contain metal oxides (Thamdrup et al., 2000). The tubes were sterilized for 20 min in an autoclave at 121°C and were gassed with nitrogen while cooling on ice. Afterward, 0.15 mL $NaHCO_3$ (1-M sterile stock) and 0.5 mL $Fe(NH_4)(SO_4)_2 \cdot 6H_2O$ (5-mM sterile stock) were added to each tube. The pH of the medium was 7.4. The tubes were inoculated with a number of basalt chips from weathered basalt (Table T10). Finally, the tubes were flushed with CO_2 and 10 mL of hydrogen was added with a syringe. The tubes were incubated close to the in situ temperature for several months.

Dolomite

There is increasing evidence that dolomite precipitation is a microbially mediated process in which sulfate-reducing bacteria take part (Warthmann et al., 2000). Earlier studies have shown that some phos-

pholipid fatty acids are indicative for sulfate-reducing bacteria (Parkes, 1987). Dolomite samples for phospholipid biomarker analysis were taken under clean conditions during the cold room microbiological sampling. A segment of 5–10 cm length was cut directly from the whole-round core. This segment should contain enough soft material around the hard nodule to be appropriate for a biomarker analysis. After subsampling the segment for FISH, the segment was wrapped in aluminum foil and frozen in a plastic sample bag at –20°C within 30 min. All samples were shipped frozen to the shore-based laboratory (in Zurich). Phospholipids will be extracted with organic solvents from the dolomite nodule and from the soft sediment around it. In this procedure, a solid-phase extraction is performed with dichloromethane, acetone, and methanol before saponification by mild alkaline methanolysis. The three fractions will be analyzed by GC/FID.

About 20 dolomite samples from different cores and depths were subsampled for FISH analysis. Samples were taken from the soft sediment around the hard dolomite nodules with a sterile 5-cm^3 syringe, fixed in formaldehyde/PBS solution, washed, and stored in ethanol at –20°C.

Molecular Analysis

Several kinds of molecular ecological analyses will be performed as postcruise investigations. The universally used approach to obtain the DNA sequences of genes of interest is polymerase chain reaction (PCR), an enzymatic reaction that produces exponentially increasing copy numbers of a target gene sequence. These multiple copies (several hundred thousand) are the prerequisite for further analysis. Molecular techniques using PCR allow rapid, sensitive, and extensive surveys of present (or past) subsurface prokaryotic communities (Marchesi et al., 1998, 2001). A plethora of molecular approaches are based, in one way or another, on PCR. Here, we list techniques that will form the basis for molecular postcruise work for Leg 201:

1. Terminal restriction fragment length polymorphism allows identification of PCR products based on length variations after restriction endonuclease digest and is used as a fingerprinting technique for nucleic acids of mixed prokaryote communities (Liu et al., 1997; Inagaki et al., 2001).
2. Denaturing gradient gel electrophoresis and temperature gradient gel electrophoresis are gel electrophoretic methods that separate mixed PCR products in denaturing polyacrylamide gradients based on melting domain structure of the DNA double strand (Muyzer and Smalla, 1998). Bands appearing on the gel may be extracted and sequenced for a phylogenetic identification of members of the prokaryote community.
3. Quantitative PCR, a modification of classical PCR, is essentially a fluorogenic assay used to quantity the number of target genes and cells in a given environmental sample (Heid et al., 1996; Suzuki et al., 2000; Takai and Horikoshi, 2000; Stults et al., 2001).
4. cDNA-PCR of reverse-transcribed RNA is a technique by which the 16S rRNA molecule or the unstable messenger RNA copy of a gene is transcribed into its corresponding DNA copy (cDNA) before qualitative and quantitative PCR and further processing (Wilson et al., 1999).

5. Gene sequencing provides the primary information for all phylogenetic analysis and identification. 16S rDNA sequence libraries for prokaryote diversity will be established and compared downhole and between sites. Functional genes to be analyzed include key genes for dissimilatory sulfate reduction (dissimilatory sulfite reductase and APS reductase), methanogenesis (co-enzyme-M methyl reductase), acetogenesis (formyl tetrahydro-folate synthase), and complex organic compound degradation (benzoyl-CoA reductase and group I/II dehalogenase).

Sampling and Storage Considerations

High-quality, nondegraded DNA and RNA of the native prokaryotic communities in deep subsurface sediments are required as starting material for PCR and for all the molecular approaches listed here (Rochelle et al., 1992, 1994). Instant deep-freezing of the sample material and storage at –80°C is essential to preserve the DNA and RNA of the native microbial community. Thawing, especially repeated freeze-thaw cycles, increases the risk of hydrolysis of high molecular weight DNA and RNA and must be avoided. The equipment and time demands of molecular community analysis, at least with the current state of technology, require that this work be done postcruise. Shipboard work was therefore limited to collecting and preserving 5-cm^3 WRC samples for all parties that are interested in molecular community analysis. Recovery of living cells from deep-frozen material may be possible on a nonquantitative basis from either –80°C or liquid nitrogen; however, –20°C is not cold enough for this purpose.

Protocols

As outlined in the introduction, 16S rRNA-based FISH is an important direct method to identify and count individual prokaryotic cells, based on their phylogenetic affiliation, in mixed prokaryotic communities, and environmental samples (Amann et al., 1995). In principle, a FISH profile of a prokaryotic community results in a phylogenetic and physiological profile of this prokaryotic community, as the correlation between the 16S rRNA phylogenetic framework and the physiological characteristics of particular bacterial and archaeal branches of the 16S rRNA tree is well characterized. General FISH probes for the two domains of prokaryotes, bacteria and archaea, are complemented by probes for specific bacterial and archaeal groups (e.g., probes for delta-proteobacterial sulfate-reducing bacteria, for the dominant marine cluster of sulfate-reducing bacteria, for dominant marine heterotrophs including the Planctomycetales and Cytophagales, and for methane-oxidizing archaea of the ANME-1 and ANME-2 lineages).

The protocol for FISH (Pernthaler et al., 2001) begins with a fixation step of sediment for shipboard or postcruise FISH analysis (Table T11). The cell walls of the microorganisms have to be permeabilized to the extent that oligonucleotide probes can pass through the cell walls, and at the same time the cellular ribosomal RNA content has to be preserved. This is done by fixing cells in buffered formaldehyde solution, followed by washing steps, and, at last, addition of ethanol. At this stage, the procedure can be stopped and the cells can be kept at –20°C until there is sufficient time for hybridization and microscopic examination.

The protocol for the continuation of the FISH procedure is outlined in Table T12. The first five steps describe how the samples are collected on a membrane filter and how they can be manipulated easily for hy-

bridization and microscopy. One must adjust the sample concentration and volume empirically in order to prevent overload of the filter with sediment. An even monolayer of sediment particles and cells on the filter is desirable.

Sample Preparation for FISH-SIMS

Samples were taken for shore-based geobiological analysis that will use SIMS. The purpose of this method is to analyze the stable isotopic composition of individual microbial cells (^{13}C, ^{15}N, and ^{34}S), which gives important information on their biochemistry and assimilation pathways for different elements. The ion beam of the spectroscopic analysis focuses on cells or cell clusters that are immobilized on a glass slide or filter and that are identified with nonspecific fluorescence stains (DAPI/AODC) or with a phylogenetic stain (FISH). For example, combined FISH-SIMS has traced the ^{13}C signature of methane assimilation and oxidation in methane-oxidizing prokaryotic consortia (Orphan et al., 2001). FISH-SIMS requires an ion microprobe facility, all of which are currently shore based. Therefore, shipboard work was limited to harvesting sediment samples for FISH and preserving material using different fixation and preservation protocols (Table **T13**).

In order to identify prokaryotic community members that are substrate limited but nevertheless active, sediment samples were preincubated with ^{13}C-labeled substrates (glucose, acetate, and methane) before preservation and shore-based FISH-SIMS analysis. The medium chosen was a general saline solution, except for the addition of Wolfe's trace metals for methanogens. ^{13}C-labeled tracer experiments were executed at 20 different depths (see the protocol in Table **T13**).

Rate and Biogeochemical Process Measurements

In general, the procedures for rate measurements with radiotracers involved preincubation at in situ temperature in the radioisotope van until equilibrium was reestablished. Only then was radiotracer injected into the samples and the experiments continued at in situ temperature in the isotope van for up to a month or more (if necessary, cooled samples still incubating were packed according to international regulations and shipped back to the appropriate institute by air freight). At the end of the incubation period, samples were fixed in a manner that kills the prokaryotes and preserves the radiolabeled substrate and product. Fixation ensures sample integrity and minimizes the risk of radioactive contamination during shipping and processing. At the end of the leg, these fixed samples were packed and shipped according to international regulations to postcruise investigators for further processing.

Sulfate Reduction

The measurement of sulfate reduction during Leg 201 is described in Table **T14.** The purpose was to experimentally determine the rates of bacterial sulfate reduction in subsamples of sediment taken from whole-round cores using the radiotracer $^{35}SO_4^{2-}$. The use of ^{35}S enables measurements over days to weeks with minimal disturbance of the redox equilibrium and bacterial milieu. Because of the use of radiotracer, the reduction of less than one-millionth of the sulfate can be detected, as explained in **"Sensitivity of Process Rate Determinations,"** p. 23, in "Measuring Microbial Rates and Activities" in "Introduction and Background." This typically corresponds to <1 pmol of sulfate per cubic

T13. Sample preparation for FISH-SIMS, p. 94.

T14. Sulfate reduction procedure, p. 95.

centimeter per day (equal to a <1 nM sulfate per day), depending on incubation time and interstitial water sulfate concentration.

Methanogenesis and Acetate Turnover (^{14}C Tracer)

Measurements of methanogenesis from bicarbonate or acetate were carried out by the use of ^{14}C-labeled substrates, applying procedures similar to those for sulfate reduction (cf. Wellsbury et al., 2000). The procedure used during Leg 201 is outlined in Table **T15.**

Anaerobic Oxidation of Methane (^{14}C Tracer)

Whole-round cores from selected intervals were cleanly and anoxically sectioned, sealed in nitrogen-purged gas-tight bags with an Anaerocult A (Merck) oxygen scrubber, and stored at 4°C for shipment to postcruise investigators. The samples will be used for experimental studies of anaerobic oxidation in these sediments using $^{14}CH_4$ as the substrate. The experiments will be carried out similar to those for methanogenesis (see Table **T15**) and incubated at in situ temperature. The conversion of the tracer substrate into carbon dioxide or biomass will be monitored.

Thymidine Incorporation (^{3}H Tracer)

Incubations using tritiated (methyl-^{3}H)thymidine were initiated to measure prokaryotic DNA formation and, hence, prokaryotic growth rates. Procedures were identical to the above ^{14}C radioisotope (Table **T15**) experiments except that 25 µL (650 kBq) of undiluted (methyl-^{3}H)thymidine (3.1 MBq/mmol; Amersham, UK) was injected and incubation times were much shorter (0.5–48 hr). These experiments will be complete postcruise.

Leucine Incorporation (^{3}H Tracer)

Tritiated leucine was used to measure protein production rates of prokaryotes in the sediments. Cellular protein is well correlated with total cell carbon and can therefore be used to calculate biomass production rates. Subsamples will be examined postcruise using microautoradiography to determine the fraction of the total population that incorporated the leucine. These data will be used to infer the percentage of the total cells observed that are metabolically active. The procedure used for these experiments during Leg 201 is outlined in Table **T16.**

Hydrogen Turnover (^{3}H Tracer)

Hydrogen is a key intermediate in anaerobic sedimentary prokaryotic communities. It is a product of fermentation and is utilized by sulfate reducers, methanogens, and other prokaryotes. As hydrogen is believed to be turned over rapidly, sedimentary interstitial water gradients cannot be used to infer reaction rates. Two types of incubation experiments were conducted to determine the rate of microbial hydrogen utilization. One set of experiments utilized $^3H_2$ (see Table **T17**), and the other set utilized the introduction of elevated hydrogen concentrations to incubated sediments. The experiments that utilize $^3H_2$ will be completed postcruise.

In the experiments that utilized elevated hydrogen concentrations, hydrogen was added to the headspace of a 20-mL vial that contained ~3 cm³ of a bulk sediment plug sampled with a syringe with the Luer end removed. The headspace of the vial was purged with high-purity nitrogen before the introduction of the hydrogen. The hydrogen concentration in the headspace at the start of the incubation was either 15 or 30

T15. Methanogenesis and acetate turnover procedure, p. 96.

T16. Leucine tracer procedure, p. 97.

T17. Tritrated hydrogen turnover procedure, p. 98.

ppm. Samples were incubated at near in situ temperatures, and hydrogen concentration was monitored daily. Based on the change with time of the measured concentration (taking into account the approach to a new equilibrium concentration), hydrogen utilization rates were calculated. Sediment samples that were autoclaved in vials purged with nitrogen were used as controls.

Equipment and Safety Protocol for Radioisotopes

Only personnel trained in radioisotope work were allowed in the radioisotope van, and all personnel in the van were required to wear disposable shoe covers, a lab coat, and safety glasses at all times. Disposable gloves were worn when handling open radioactive materials. After each experiment session, handling trays and laboratory equipment (e.g., syringes and spatulas) were monitored with a handheld surface contamination monitor (Berthold). If any contamination was present, the plastic-backed absorbent shelf paper was replaced and trays and equipment were decontaminated. A radioisotope stock log was maintained to monitor and record isotope usage. The total amounts of radioisotopes applied for radiotracer experiments during Leg 201 are presented in Table **T18.** At the end of the leg, samples were shipped by airfreight to appropriate institutes for further processing. All samples were packed in break-proof containers, double bagged, and packed in a sturdy International Air Transport Association (IATA)-approved container (packed and shipped as "UN2910–Radioactive material, excepted package–limited quantity of material"). Thorough (30 point) wipe tests were performed after 1 week, 3 weeks, and at the end of the expedition.

In preparation for Leg 201, a radioisotope van, manufactured according to University-National Oceanic Laboratory System (UNOLS)-approved design, was purchased and outfitted by ODP-TAMU. The van was installed on top of the Core Tech shop, on the starboard side of the *JOIDES Resolution* just aft of the driller's shack. The facility is a 20-ft-long steel van, equipped with two entry/exit doors (end and side) and a plumbed exterior sink. The rear one-third of the van was equipped with a cooling system that can maintain 10°C internal temperature for low-temperature sample handling. The low-temperature room includes a vent hood, counter-top working area, cabinet and drawer storage, and a nitrogen tank for sample preparation. The larger part of the van is air conditioned and houses three upright, floor-to-ceiling, adjustable temperature incubators, as well as an under-counter refrigerator and freezer. A sink (with a small isolated drained fluid capture tank) and additional cabinet and drawer storage are also installed. The van also contains a liquid scintillation counter for sample, standard, and contamination monitoring. After installation, the facility was plumbed and attached to the shipboard electrical system, phone and alarm system, and computer network. The facility is monitored with multistation contamination wipe tests on a regular basis, as well as daily personal wipe tests and routine sampling of the captured water tank. The facility remains locked at all times except when occupied by approved personnel, and access is limited to only those scientists certified by their home institution in handling radioisotopes and to members of the ODP technical staff approved by the Texas A&M Office of Radiation Safety. Protocols for spill control and decontamination procedures are outlined in Table **T19.**

T18. Radioisotopes used during Leg 201, p. 99.

T19. Spill control and decontamination procedure, p. 100.

Phosphate: $H_2^{18}O$-Label Incubations

Two depths at each of the low-activity sites (1225 and 1231), high-activity sites (1228, 1229, and 1230), and intermediate-activity site (1227) were targeted for ^{18}O-label incubation studies. Incubations were carried out at near in situ temperatures of 4°–7°C for Sites 1225 and 1231 and at 20°–25°C for Peru margin sites. Each incubation slurry was sampled immediately after inoculation to determine starting values for water and dissolved phosphate ($^{18}O_P$), dissolved phosphate concentrations, and prokaryotic cell counts. These values will be compared with those from later extractions.

To avoid potential contamination by the use of heavily ^{18}O-labeled compounds (50–99 atom% ^{18}O) typical of biochemical approaches, incubation media were prepared using very low level ^{18}O-labeled water (10‰–99‰ ^{18}O), sulfate, and unlabeled phosphate in various combinations. A 0.1- to 1-mL subsample of the master slurry was used as inoculum in anaerobic incubations with 10 mL of ^{18}O-labeled media.

Three types of shipboard incubation conditions were used with phosphate:

1. Medium 201-X: artificial seawater plus phosphate (ASW-P) medium made with ^{18}O-labeled DDH_2O (99‰) and unlabeled phosphate (as KH_2PO_4; 100 µmol/10 mL);
2. Medium 201-Y: ASW-P plus glucose (0.05% w/v); and
3. Sterilized controls with 201-X and 201-Y for a total of four incubation bottles (25-mL serum bottles) per interval sampled.

Relatively high phosphate concentrations were required to detect the low level of ^{18}O label in the water at the high water:phosphate ratio (10^5:10^2) used here. Additional shore-based ^{18}O-label incubation studies will be carried out using preserved slurry and sediment samples (collected cleanly and stored anoxically at 4°C) with more heavily labeled $P^{18}O_4^{3-}$ so that the label transfer into the water can be detected. Also, more heavily labeled $H_2^{18}O$ to permit smaller concentrations of phosphate (20–100 µM) will also be employed.

PHYSICAL PROPERTIES

A suite of physical property measurements were made to support the main scientific objectives of Leg 201. Physical characterization of the subsurface environment, particularly including density, porosity, and matrix composition, is necessary for specification of the hydrodynamic environment that is expected to strongly affect the microbial community. In addition, physical properties can be used to define geochemical and, hence, population and community boundaries. In many cases, we used nonstandard downcore spacings and instrument precision to better physically define known zones of special biochemical or geochemical interest.

Selected cores from Sites 1225, 1226, 1230, and 1231 were thermally imaged on the catwalk prior to sectioning. All other physical property measurements were conducted after the cores had equilibrated to near ambient room temperature (i.e., 22°–24°C), a settling period of typically 2–4 hr, except for cores sampled for microbiology in the cold room. Physical properties measured on the MST and thermal conductivity measurements were normally made on whole-round core sections dur-

ing the same time interval. Discrete moisture and density (MAD) parameters, *P*-wave velocities, and electrical resistivity were subsequently measured on each split-core section. A summary of each of the physical property measurement procedures for Leg 201 is outlined below; more detailed descriptions are provided in Blum (1997).

Tables of physical properties in ASCII are provided on the "Log and Core Data" CD-ROM included with this publication. These data tables include GRA density, magnetic susceptibility, natural gamma radiation (NGR), *P*-wave velocity, MAD, thermal conductivity, Hamilton frame velocity (PWS), resistivity, and paleomagnetism.

Infrared Thermal Imaging

Infrared thermal imaging was introduced during this leg for technique development prior to expected critical use during Leg 204. IR imaging was shown to successfully identify thermal anomalies in sediment cores attributed to the location of gas hydrate (cold anomalies) and voids (warm anomalies). The primary benefits of using IR (in preference to estimating temperature differences by touch) include more precise identification of thermal anomalies and the possible estimation of hydrate volume from processed images. It is quicker, simpler, and more compact than the system of thermistors used during Leg 164 (Paull, Matsumoto, Wallace, et al., 1996). Small-scale hydrate nodules and disseminated gas hydrate were the primary forms identified, suggesting the camera can detect small quantities. Volumetric analysis will require further study.

Another proposed use for the camera is for the lithologic characterization of ambient-temperature cores because of slight variations in their thermal emission properties attributable to sediment composition or water content. Data were collected during Leg 201 to examine this possibility. Processing and analysis will be completed postcruise.

A third use for the camera during Leg 201 was to monitor the rate of warming of cores to determine the maximum radial temperature distribution reached before of microbiological sampling in the cold room. The method and results for this monitoring effort are described in **"Infrared Scanner,"** p. 24, in "Physical Properties" in the "Site 1225" chapter.

Methodology

A ThermaCam SC 2000 camera (FLIR Systems) was used. This camera images temperatures from –40° to +1500°C. For onboard application, it was set to record a range of temperatures from –40° to +120°C (range 1).

By experimentation, we determined that a 10-cm field of view on the core was obtained with the camera lens located 34 cm above the highest point on the core. In order to minimize the effect of external IR radiation reflecting from the core liner, the camera and the space between the lens and the core was enclosed within a cardboard sheath covered on the outside with crumpled aluminum foil (Fig. **F12**) in order to disperse ambient IR energy.

To record data for each core, the mounted camera was placed on top of the core liner and the camera was focused on the edges of the core using computer controls. During focusing, camera span and level parameters were auto-adjusted to optimize visual contrast of the expected downcore temperature variation on the computer screen. Immediately after recovery, the core liner was cleaned and the camera was manually

F12. IR thermal imaging camera, p. 78.

rolled along the core from top to bottom. The ThermaCam Researcher 2001 software, running on a dedicated laptop computer, acquired images from the camera at a rate of 5 frames/s. During trials conducted on the transit to the first site, we found that a ~45-s acquisition time for a 10-m core produced images with minimal blurring and with considerable sequential overlap. While the images were being recorded by the computer, the computer screen would freeze at the first image frame, preventing real-time viewing of the core liner temperatures. At Site 1230, we discovered that the camera itself provides real-time images of the core, and a detachable external screen was therefore used to view the core as it was scanned. The screen span and level parameters were set to optimize visual contrast on the external screen of the expected downcore temperature variation (since the camera and computer spans and levels could be different). Initially, this was 0°–20°C. After hydrates were identified at ~16°C, compared with a background level of >20°C, the span and level were set to show a range of 15°–25°C.

Depth Integration

To facilitate depth integration of the IR data with other physical property measurements, a depth scale was constructed using a 10-m × 4-cm aluminum unistrut. A 5-cm spaced numbered scale was painted onto the unistrut using Rustoleum Specialty High Heat oil-based enamel (black #7778). This combination initially produced sufficient thermal contrast for subsequent discrimination of the scale markers. However, the scale was only clearly visible in still images. Images recorded while the camera was moving were too blurred to identify the scale. Holes drilled in the unistrut at 5-cm intervals also proved to be of limited use. Thermal contrast of the holes was very clear, particularly during the day or when a hand was run under the unistrut while the camera was being rolled down the core. However, blurring remained a significant problem. Additionally, producing a single depth-matched downhole record of temperature variation based on the scale required extensive image processing, as only one image could be viewed at time. Several attempts at developing an automated technique proved unsuccessful. The process was further complicated by the varying rate of scan between different camera operators and mechanical problems with the manually operated trolley. At Site 1230, we decided to assign the curated depth of the top of the core to the top of the first image. Then the curated recovered depth was divided by the number of images taken for the core. This interval was sequentially added to the images to assign depths in a core to each image.

Image Processing

In order to develop depth-matched downcore temperature profiles, the following process was established through experimentation over the course of Leg 201. At this writing, only Site 1230 data have been thoroughly examined.

1. ThermaCam Researcher software was embedded as an object into a Microsoft Excel spreadsheet. The sequence file containing each image from the core scan was selected and opened in Researcher.

2. An analysis area was selected by drawing a box on the first image of the sequence file. The analysis box was placed to avoid areas of significant reflection or other obvious interference.
3. The sequence file was played from beginning to end to ensure appropriate box placement on each image. The sequence file was then reset to the beginning.
4. In Excel, a macro was written to run the sequence file and extract the maximum, minimum, and average temperature from the analysis box in each image, as well as the time at which each image was taken.
5. The recovered core length was divided by the total number of images in the sequence file. This interval was sequentially added to the curated top depth of the core, thereby assigning a depth to each temperature reading.

Following this process, core data files were combined to provide downhole temperature profiles. Where recovery was >100% in any core, the overlapping depth interval from the upper core was removed from the composite record.

MST Measurements

The MST comprises four physical property sensors on an automated track that sequentially measure volume magnetic susceptibility, wet bulk density, compressional wave velocity, and natural gamma ray radiation on whole-round intact core sections. Measurements are nondestructive of core fabric and are used principally to facilitate shipboard core-to-core correlation, to construct composite stratigraphic sections, and to correlate with downhole tools. Each device has an intrinsic spatial resolution determined by its design specifications (see discussion of each measurement below). Data quality depends on core condition and instrument precision. Optimal MST measurements require a completely filled liner with minimal drilling disturbance. Precision is generally a function of measurement time, especially with respect to magnetic susceptibility, wet bulk density, and natural gamma radiation detection. The final sensor-specific spatial resolution chosen for each site balances the spatial footprint and accuracy with core flow requirements and was particularly critical during rapid core recovery at the shallow-water sites along the Peru margin. In all cases, the scientific objectives of Leg 201 placed primary importance on a high-resolution and precise determination of wet bulk density; therefore, the count times and spatial resolution on this instrument were maximized at the expense of other measurements.

Magnetic Susceptibility

Whole-core volume magnetic susceptibility was measured with the MST using a Bartington MS2 meter coupled to a MS2C sensor coil with a diameter of 8.8 cm operating at 565 Hz. The measurement resolution of the MS2C sensor is 4 cm. The instrument has two precision settings, a minimum statistically significant count time of 1 s and a 10-s count time. During Leg 201, MST magnetic susceptibility was routinely measured at a spacing of 5.0 cm, recording the average of two 1-s (low resolution) data acquisitions for each sample location, unless otherwise stated. The instrument automatically zeros and records a free-air value for magnetic susceptibility at the start and end of each section run. In-

strument drift during a section run is then accommodated by subtraction of a linear interpolation between the first and last free-air readings. Drift-corrected magnetic susceptibility data were archived as raw instrument units (SI) and were not corrected for changes in sediment volume.

Wet Bulk Density

Determination of wet bulk density is carried out by the GRA densitometer. This system is based on the principle that the attenuation, mainly by Compton scattering, of a collimated beam of gamma rays produced by a ^{137}Cs source passing through a known volume of sediment is related to material bulk density (Evans, 1965). Calibration of the GRA system was completed using known graduated seawater/aluminum density standards. The measurement resolution of the GRA sensor is ~5 mm, with sample spacing generally set at 5.0 cm for Leg 201 cores unless otherwise stated. The minimum integration time for a statistically significant GRA measurement is 1 s. During most legs, a count time of 2 s is used; however, during Leg 201, GRA measurements were acquired over longer periods, from 5- to 10-s integration time in order to reduce scatter and improve precision. A freshwater control was run with each section to measure instrument drift. GRA bulk density data are of highest quality when determined on APC cores because the liner is generally completely filled with sediment. In XCB cores, GRA measurements are unreliable for the determination of true bulk density on their own because of the breakdown of in situ density by the mixing of drilling slurry and core biscuits.

Compressional Wave Velocity

Compressional wave velocity was measured by two methods shipboard. Transverse *P*-wave velocity was measured on the MST track with the *P*-wave logger (PWL) for all cores at a routine sample interval of 10 cm. The PWL transmits a 500-kHz compressional wave (*P*-wave) pulse through the core at a specified repetition rate (50/s). The transmitting and receiving ultrasonic transducers are aligned so wave propagation is perpendicular to the core axis. Ultrasonic transducer separation is measured by two displacement transducers. The recorded velocity is the average of the user-defined number of acquisitions per location (10). Calibration of the displacement transducers and measurement of electronic delay in the PWL circuitry were conducted using a series of acrylic blocks of known thickness and *P*-wave traveltime. Repeated measurement of *P*-wave velocity through a core liner filled with distilled water was used to check calibration validity.

Natural Gamma Radiation

Natural gamma ray emissions of sediments are a function of the random and discrete decay of radioactive isotopes, predominantly those of uranium, thorium, and potassium, and are measured through scintillation detectors arranged at 90° to each other and perpendicular to the core axis. The installation and operating principles of the NGR system used on the *JOIDES Resolution* are discussed by Hoppie et al. (1994). Data from 256 energy channels were collected and archived. For presentation purposes, the counts were summed over the range of 200–3000 keV to be comparable with data collected during previous legs. This integration range also allows direct comparison with downhole logging

data, which were collected over a similar integration range (Hoppie et al., 1994). Over the 200- to 3000-keV integration range, background counts, measured using a core liner filled with distilled water, averaged 30 during a 1-hr measurement period. Before taking measurements, each of the four NGR amplifiers were adjusted so the thorium peak was at the highest resolution possible when the other three amplifiers were disabled. The multichannel analyzer was then calibrated by assigning certain channels to the characteristic energies of ^{40}K and the main peak of ^{232}Th (Blum, 1997). The measurement width of the NGR is ~15 cm, with a statistically significant count time of at least 5 s, depending on lithology. Because of the long time required for NGR measurements, sample spacing and count time for NGR measurements varied depending on the age and lithology of the sediment recovered. No corrections were made to NGR data obtained from XCB cores to account for sediment incompletely filling the core liner.

Thermal Conductivity

Thermal conductivity measurements of one per core were made using the TK04 (Teka Bolin) system described by Blum (1997). During Leg 201, we employed the single-needle probe (Von Herzen and Maxwell, 1959), heated continuously in full-space configuration. At the beginning of each measurement temperatures in the samples were monitored automatically, without applying a heater current, until the background thermal drift was <0.04°C/min. Once the samples were equilibrated, the heater circuit was closed and the temperature rise in the probe was recorded. The needle probe contains a heater wire and calibrated thermistor. The probe is assumed to be a perfect conductor because of its high conductance relative to the core sediments. With this assumption, the temperature of the superconductive probe has a linear relationship with the natural logarithm of the time after the initiation of the heat:

$$T(t) = (q/4k)\ln(t) + C, \qquad (5)$$

where,

T = temperature,
q = heat input per unit length per unit time,
k = thermal conductivity,
t = time after the initiation of the heat, and
C = a constant.

The thermal conductivity (k) was determined using equation 5 by fitting the temperatures measured during the first 150 s of each heating experiment (for details see Kristiansen, 1982, and Blum, 1997).

The reported thermal conductivity value for each sample is the average of three repeated measurements. Data are reported in watts per meter degree Kelvin, with measurement errors of 5%–10%.

Moisture and Density Analysis

Moisture and density parameters were determined from wet mass, dry mass, and dry volume measurements of split core sediments after Blum (1997). Push-core samples of ~10 cm³ were placed in 10-mL beakers. Care was taken to sample undisturbed parts of the core and to

avoid drilling slurry. Immediately after the samples were collected, wet sediment mass (M_{wet}) was measured. Dry mass and volume were measured after samples were heated in an oven at 105° ± 5°C for 24 hr and allowed to cool in a desiccator. Sample mass was determined to a precision of 0.01 g using two Scientech 202 electronic balances and a computer averaging system to compensate for the ship's motion. Sample volumes were determined using a helium-displacement Quantachrome penta-pycnometer with a precision of 0.02 cm³. Volume measurements were repeated three times, until the last two measurements exhibited <0.01% standard deviation. A reference volume was included within each sample set and rotated sequentially among the cells to check for instrument drift and systematic error. Standard sampling frequency was one per section. However, in many cases during Leg 201 we carried out high-resolution sampling through specific zones of interest. One of the MAD samples was always taken adjacent to any sample for dissolved methane and permeability.

Moisture content, grain density, bulk density, and porosity were calculated from the measured wet mass, dry mass, and dry volume as described by Blum (1997). Corrections were made for the mass and volume of evaporated seawater using a seawater density of 1.024 g/cm³ and a salt density of 2.20 g/cm³.

Compressional Wave Velocity

P-wave velocities were also measured at selected locations on split cores, usually near a MAD sample, by the ODP standard insertion probe system comprising two transducer pairs that measure velocities along axial (PWS2) and transverse (PWS1) directions. The insertion probe system determines *P*-wave velocity based on the traveltime of a 500-kHz wave between a pair of piezoelectric crystals separated by a fixed distance. System accuracy was checked prior to testing the first section of each hole by measuring the velocity in distilled water at a specific temperature.

Routine sampling frequency and location for *P*-wave measurements was coincident with the discrete MAD samples. Note that the velocity data stored in the Janus database are uncorrected for in situ temperature and pressure. These corrections can be made using the relationships outlined in Wyllie et al. (1956), Wilson (1960), and Mackenzie (1981).

Velocity anisotropy (as a percent) was calculated using axial (V_{Pa}) and transverse (V_{Pt}) *P*-wave velocities. Anisotropy is determined from the difference between the average horizontal and vertical velocity using

$$\text{anisotropy} = 200 \times (V_{Pt} - V_{Pa})/(V_{Pt} + V_{Pa}). \quad (6)$$

Formation Factor

Formation factor (*F*) was determined from electrical resistivity measurements taken adjacent to discrete MAD samples on split-core sediments. Four in-line electrodes, 2 cm long and spaced ~1 cm apart mounted on a plastic block, were inserted into the split-core sediments. The two outer electrodes produce an alternating current (5–10 kHz) in the sediment. The resulting potential difference is measured by the two inner electrodes (Wenner array). In samples saturated with saline interstitial water, polarization effects are minimal in this frequency range and the measured resistivity is largely independent of frequency.

At each sampling location two measurements of sediment resistance were made, one oriented axially ($R_{core,\ axial}$) and the other transverse ($R_{core,\ trans}$) to the core axis, as with discrete P-wave velocity data collection. Measurement of resistance for room-temperature seawater (R_{wtr}) was made regularly so that formation factors,

$$F_{axial} = R_{core,\ axial}/R_{wtr} \text{ and} \qquad (7)$$

$$F_{trans} = R_{core,\ trans}/R_{wtr}, \qquad (8)$$

in each direction could be calculated. Temperature measurements for the sediment and seawater were not made, as both were equilibrated to ambient laboratory temperature.

This simple method for determination of formation factor does not take into account surface conductivity effects of the sediment matrix. However, this is not of concern in high-porosity sediments where the conductive pathways depend dominantly on intergranular porosity and pore connectivity, even where the sediment matrix contains significant clays. Previous drilling at the sites cored during Leg 201 indicate that porosities should exceed 50% everywhere from seafloor to total depth.

Using the axial and transverse formation factors from equations 7 and 8, anisotropy can be computed as

$$\text{anisotropy} = 200 \times (F_{axial} - F_{trans})/(F_{axial} + F_{trans}). \qquad (9)$$

Paleomagnetism

During Leg 201, no scientist sailed as a paleomagnetic specialist. However, based on results from previous legs, paleomagnetic measurements were made at sites where better resolution could be provided by updated shipboard laboratory facilities. The data are expected to facilitate both the identification of iron redox intervals and the correlation of cores. Preliminary interpretation of paleomagnetic data was undertaken during the cruise when possible.

Instrumentation and Measurement Procedures

Measurements of remanent magnetization were made using an automated pass-through cryogenic magnetometer with direct-current superconducting quantum interference devices (DC SQUIDs) (2-G Enterprises Model 760-R). The magnetometer is equipped with an in-line alternating-field (AF) demagnetizer (2-G Enterprises Model 2G600) capable of producing peak fields of 80 mT with a 200-Hz frequency. The magnetometer and AF demagnetizer are interfaced to a PC-compatible computer and are controlled by the 2-G Long Core software program by National Instruments. Based on tests conducted during Leg 200, the background noise level of the magnetometer in the shipboard environment is $\sim 2 \times 10^{-9}$ Am^2 and the minimum measurable remanent intensities for split cores will be greater than $\sim 2 \times 10^{-5}$ A/m (Shipboard Scientific Party, 2003).

The natural remanent magnetization was measured in increments ranging from 2 to 10 cm (depending on the specific interest in a particular section) along selected archive-half sections before and after AF demagnetization. AF demagnetizations were applied at multiple demagne-

tization steps on the initial two sections of a hole in incremental steps of 5 mT up to 20 mT in order to remove drilling overprints.

Core Orientation

During APC coring, orientation was achieved using the Tensor multishot tool. Orientation of cores is of particular importance in paleomagnetic studies of paleoequatorial regions, where the paleomagnetic inclination is close to zero. ODP core orientation designates the positive x-axis direction as the horizontal direction (geomagnetic north in a global coordinate reference frame) from the center of the core to the median line between a pair of lines inscribed lengthwise on the working half of each core liner (Fig. F13).

Discrete Samples

An automatic portable spinner magnetometer (Niitsuma and Koyama, 1994) was used to measure remanent magnetization of the discrete samples collected during Leg 201. The samples were collected from working halves of core sections in 2-cm × 2-cm × 2-cm plastic cubes. The sampling frequency was generally one sample per core from one hole at each site.

The noise level of this magnetometer is roughly equivalent to that of the cryogenic magnetometer for the 8-cm³ discrete samples when 10 repeat spinner magnetometer measurements are averaged (Shipboard Scientific Party, 2003). This magnetometer is equipped with an AF demagnetizer, an anhysteretic remanent magnetizer, and a magnetic susceptibility anisotropy meter.

DOWNHOLE TOOLS

During Leg 201, a suite of downhole tools were employed to better characterize the environment hosting the subsurface microbial populations. Temperature is a key parameter because it affects the rates of microbial activities, and different groups of microorganisms are known to be active over different temperature ranges. Pore pressure is also important because if the pressure gradient differs from hydrostatic then fluid flow may affect the supply of dissolved substrates to the microbial populations. Finally, the concentrations of dissolved gases and methane hydrates at in situ conditions must be known to determine rates of certain microbial processes, particularly the formation and consumption of methane. In situ sediment thermal measurements were made during Leg 201 using the Adara APC temperature tool and the Davis-Villinger temperature probe (DVTP) (Davis et al., 1997). Formation pore pressures were measured using a DVTP modified to include a pressure port and sensor that was previously used during Leg 190. Samples of sediment, water, and gas at in situ pressure were collected with the pressure coring sampler (PCS) (Pettigrew, 1992). The instruments and procedures are summarized below. Additional information regarding the PCS is presented in Dickens et al. (this volume).

Adara APC Temperature Tool

The Adara temperature tool fits directly into the cutting shoe on the APC and can therefore be used to measure sediment temperatures dur-

F13. Paleomagnetic coordinate conventions, p. 79.
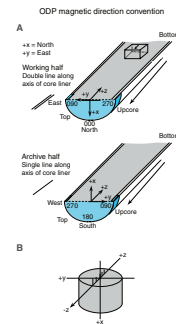
ing regular piston coring. The tool consists of electronic components, including battery packs, a data logger, and a platinum resistance-temperature device calibrated over a temperature range of 0°–30°C. A photograph of the components can be found in Fisher and Becker (1993). The thermal time constant of the cutting shoe assembly into which the Adara tool is inserted is ~2–3 min. The only modification to normal APC procedures required to obtain temperature measurements is to hold the corer in place for ~10 min after cutting the core. During this time, the Adara tool equilibrates toward the in situ temperature of the sediments. The Adara tool logs data on a microprocessor contained in the instrument. Following deployment, the data are downloaded for processing. The tool can be preprogrammed to record temperatures at a range of sampling rates. Sampling with 10-s intervals was used during Leg 201. A typical APC measurement consists of a mudline temperature record lasting 10 min. This is followed by a pulse of frictional heating when the piston is fired, a period of thermal decay that is monitored for 10 min, and a frictional pulse upon removal of the corer. Before reduction and drift corrections, nominal accuracy of Adara temperature data is estimated at 0.1°C. A second stop of 10 min at the mudline is made before raising the core to the surface.

Davis-Villinger Temperature Probe

The temperature measurement aspects of the DVTP are described in detail by Davis et al. (1997). The probe is conical and has two thermistors, one 1 cm from the tip of the probe and the other 12 cm above the tip. A third thermistor, referred to as the internal thermistor, is in the electronics package. Thermistor sensitivity is 1 mK in an operating range of –5° to 20°C, and the total operating range is –5° to 100°C. The thermistors were calibrated at the factory and on the laboratory bench before installation in the probe. In addition to the thermistors, the probe contains an accelerometer sensitive to 0.98 m/s^2. Both peak and mean acceleration are recorded by the logger. The accelerometer data are used to track disturbances to the instrument package during the equilibration interval. Temperature data were recorded at 10-s intervals. In a DVTP deployment, mudline temperatures (within the drill pipe) are measured for 10 min before descent into the hole for a 10-min equilibration interval in the bottom. The time constants for the sensors are ~1 min for the probe tip thermistor and ~2 min for the thermistor at 12 cm from the tip. Unless stated otherwise, data from the probe tip thermistor were used for estimation of in situ temperatures. Upon retrieval, a second stop of 10 min is made at the mudline.

Thermal Data Reduction

Similar data reduction procedures were used for the two temperature tools. The transient thermal decay curves for sediment thermal probes are known to be a function of the geometry of the probes and the thermal properties of the probe and the sediments (Bullard, 1954; Horai and Von Herzen, 1985). Analysis of data requires fitting the measurements to analytical or synthetic decay curves calculated based on tool geometry, sampling interval, and tool and sediment thermal properties. For the DVTP tool, thermal decay data are analyzed by comparison to computed type curves using the software program CONEFIT, developed by Davis et al. (1997). However, it is generally not possible to obtain a perfect match between the synthetic curves and the data because (1) the

probe does not reach thermal equilibrium during the penetration period; (2) contrary to ideal theory, the frictional pulse upon insertion is not instantaneous; and (3) temperature data are sampled at discrete intervals, so that the exact time of penetration is uncertain. Thus, both the effective penetration time and equilibrium temperature must be estimated by applying a fitting procedure, which involves shifting the synthetic curves in time to obtain a match with the recorded data. The data collected more than 20–50 s beyond penetration usually provide a reliable estimate of equilibrium temperature. Thermal conductivities measured shipboard were used for estimation of in situ temperatures and for calculation of heat flow. Laboratory thermal conductivity measurements were not corrected for in situ conditions because the correction would be small at the shallow depths drilled during Leg 201.

Davis-Villinger Temperature-Pressure Probe

Measurement of formation pressure was achieved using a modified DVTP. The probe has a tip that incorporates both a single thermistor in an oil-filled needle and ports to allow hydraulic transmission of formation fluid pressures to a precision Paroscientific pressure gauge inside. A standard data logger was modified to accept the pressure signal instead of the second thermistor signal in the normal DVTP described above. Thermistor sensitivity of the modified tool is reduced to 0.02 K in an operating range of –5° to 20°C. Deployment of the tool consists of lowering by wireline to the mudline, where there is a 10-min pause. Subsequently, the tool is lowered to the base of the hole and latched in at the bottom of the drill string, with the end of the tool extending 1.1 m below the drill bit. The extended probe is pushed into the sediment below the bottom of the hole, and pressure is recorded for 30 min or as long as deemed operationally safe. In later deployments a 2- to 5-min stop at the base of the hole was made after the in situ measurement to provide a reference for hydrostatic pressure. If smooth pressure decay curves are recorded after penetration, then extrapolations to in situ pore pressures are possible. This pressure response is qualitatively similar to but slower than the thermal response. The model for the characteristic response of pressure to the displacement and sediment deformation associated with penetration is more complex than the model used to estimate in situ temperatures from the decay of the frictional heating pulse. Construction of a complete analytical or numerical model of the pressure response had not been completed by the time of Leg 201, so shipboard extrapolations to estimated formation pressures must be considered preliminary until thoroughly processed postcruise.

APC-Methane Tool

The APC-Methane tool under development is designed to continuously record temperature, pressure, and conductivity at the face of the APC piston assembly during core ascent. Its purpose is to provide a continuous record of sediment gas temperatures, internal pressure, and timing of gas headspace formation during core recovery.

Pressure Coring Sampler

Large quantities of gas can escape sediment cores when a drop in pressure or increase in temperature during recovery lowers methane saturation (Paull et al., 2000; Wallace et al., 2000). Based on previous drill-

ing during Legs 112 and 138, significant gas loss was expected to occur at two or more of the proposed sites (Table T20). Visible gas escape structures appeared in cores between 58 and 62 mbsf and below 30 mbsf at Sites 681 and 685, respectively. High headspace methane concentrations (>1000 µL/L), which may signify gas concentrations approaching or exceeding saturation at depth, also were present at these two sites and at Site 684.

The PCS is a downhole tool designed to recover a 1-m-long, 1385-cm³ cylindrical sediment core—including gas and interstitial water—at in situ pressure (Pettigrew, 1992). When its valves seal properly, controlled release of pressure from the PCS through a manifold (below) permits collection of gases that would otherwise escape during the wireline trip. At the time of Leg 201, the PCS provided the only proven means to determine in situ gas abundance in deep-sea sediments where gas concentrations at depth exceed saturation on the ship (Dickens et al., 1997). However, the PCS had only been successfully used to capture and analyze in situ gases during Leg 164 (Paull, Matsumoto, Wallace, et al., 1996; Dickens et al., 1997). Consequently, the PCS was deployed 17 times during Leg 201 to achieve two objectives: (1) to quantify gas abundance at Site 1230 along the Peru margin and (2) to ensure that the tool was fully operational for upcoming legs targeting gas-rich sediments. The basic operations and results of these deployments are presented in Dickens et al. (this volume).

Water Sampling Temperature Probe

Samples of bottom water were collected at each of the Peru margin sites (1227–1231) using the Water Sampling Temperature Probe (WSTP). The WSTP is a passive sampler that is deployed in the bottom-hole assembly (BHA). Before deployment, the fluid path is filled with deionized water and an overflow chamber is filled with air. A timer is set to open the valve at a fixed time, exposing the sampling line and chamber to ambient pressure. The time also closes the chamber after a prearranged time interval has passed. In operation, the WSTP is mounted inside a core barrel and lowered down the drill pipe by wireline. Before beginning to drill, the tool is lowered to 10 m above the seafloor with the probe tip extending 1.1 m ahead of the bit. The tool is then held in position with the pumps off for a total of 15 min to measure the bottom-water temperature. Approximately halfway into this interval, the timer-operated valve is opened. During Leg 201, the interval that the valve was left open varied from 3 to 5 min. When the valve is open, bottom water is drawn under negative relative pressure through the filter and into the sample chamber, displacing the deionized water. Upon retrieval, the water sample recovered from the sample chamber is analyzed and the amount of sample dilution by deionized water is assessed by comparing the chemistry to IAPSO standard seawater.

Fugro Percussion Corer

As part of ODP's engineering development program, operations time was allocated to deployment of a third-party pressure coring tool. The Fugro Percussion Corer (FPC) uses a water hammer driven by drilling fluid circulation to push a core barrel into the sediment ~1 m ahead of the bit. After coring, the 58-mm-diameter core is retracted into an autoclave and sealed by a flapper valve to return a core under pressure. Six

deployments were in our initial operation plan, spread over three sites. Ultimately, seven deployments of the FPC were completed at Sites 1227, 1228, and 1229.

DOWNHOLE LOGGING

Downhole logs are used to determine physical, compositional, and structural properties of the formation surrounding the borehole. The data are rapidly collected, continuous with depth, and measured in situ; they can be interpreted in terms of the stratigraphy, lithology, mineralogy, and geochemical composition of the penetrated formation. Where core recovery is incomplete or disturbed, log data is crucial for characterizing the borehole section. Where core recovery is good, log and core data complement one another and may be interpreted jointly. Logs are sensitive to formation properties on a scale intermediate between laboratory measurements on core samples and geophysical surveys. Logging during Leg 201 helped characterize physical properties to define constraints on the downhole microbial communities. It was also useful in delineating the possible hydrologic conduits and the flow regime that can affect the deep biosphere.
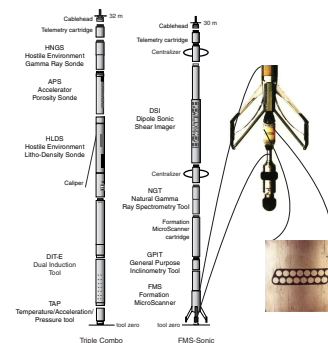
Operations

Logs are recorded with a variety of Schlumberger logging tools combined into several tool strings that are run down the hole after coring operations are complete. Two wireline tool strings were used during Leg 201: the triple combination (triple combo) tool string (resistivity, density, and porosity) and the Formation MicroScanner (FMS)-sonic tool string (resistivity image of the borehole wall and sonic velocities) (Fig. **F14;** Table **T21**).

Each tool string contains a telemetry cartridge for communicating through the wireline with the minimum configuration MAXIS (MCM) unit on the drill ship and a natural gamma radiation tool, which provides a common reference for correlation and depth shifting between multiple logging runs. Logging runs are typically conducted at 250–275 m/hr.

In preparation for logging, the boreholes were flushed of debris by circulating a pill of viscous drilling fluid (sepiolite mud mixed with seawater; weight = ~8.8 lb/gal or 1.11 kg/dm³) through the drill pipe to the bottom of the hole. The BHA was pulled up to a depth of between 60 and 100 mbsf then run down to the bottom of the hole again to ream borehole irregularities. The hole was subsequently filled with a sepiolite mud pill, and the pipe was raised to 60–100 mbsf and kept there to prevent hole collapse during logging. The tool strings were then lowered downhole by a seven-conductor wireline cable during sequential runs. A wireline heave motion compensator (WHC) was employed to minimize the effect of ship's heave on the tool position in the borehole. During each logging run, incoming data were recorded and monitored in real time on the MCM logging computer. The tool strings were then pulled up at constant speed to provide continuous measurement as a function of depth of several properties simultaneously.

F14. Tool strings used during Leg 201, p. 80.

T21. Wireline tool strings, p. 102.

Tool Measurement Principles

The properties measured by the tools and the methods used by the tools to measure them are briefly described below. The operating principles, applications, and approximate vertical resolution of the tools are summarized in Table **T21.** Some of the principal data channels of the tools, their physical significance, and units of measure are listed in Table **T22.** More detailed information on individual tools and their geological applications may be found in Ellis (1987), Goldberg (1997), Lovell et al. (1998), Rider (1996), Schlumberger (1989, 1998), and Serra (1984, 1986).

Natural Radioactivity

Two wireline spectral gamma ray tools were used to measure and classify natural radioactivity in the formation: the Natural Gamma Ray Spectrometry Tool (NGT), and the Hostile Environment Gamma Ray Sonde (HNGS). The NGT uses a sodium iodide scintillation detector and five-window spectroscopy to determine concentrations of potassium (in weight percent), thorium (in parts per million), and uranium (in parts per million), the three elements whose isotopes dominate the natural radiation spectrum. The HNGS is similar to the NGT, but it uses two bismuth germanate scintillation detectors for significantly improved tool precision. Spectral analysis in the HNGS filters out gamma ray energies below 500 keV, eliminating sensitivity to bentonite or potassium chloride in the drilling mud and improving measurement accuracy. Although the NGT response is sensitive to borehole diameter and the weight and concentration of bentonite or potassium chloride present in the drilling mud, these effects are routinely corrected for during processing at Lamont-Doherty Earth Observatory (LDEO).

Density

Formation density was determined from the number of electrons in the formation, which is measured with the Hostile Environment Litho-Density Sonde (HLDS). The sonde contains a radioactive cesium (^{137}Cs) gamma ray source (622 keV) and far and near gamma ray detectors mounted on a shielded skid, which is pressed against the borehole wall by a hydraulically activated eccentralizing arm. Gamma rays emitted by the source undergo Compton scattering, which involves the transfer of energy from gamma rays to the electrons in the formation via elastic collision. The number of scattered gamma rays that reach the detectors is directly related to the number of electrons in the formation, which is in turn related to bulk density. Porosity may also be derived from this bulk density if the matrix density is known.

The HLDS also measures photoelectric absorption as the photoelectric effect factor (PEF). Photoelectric absorption occurs when gamma rays reach <150 keV after being repeatedly scattered by electrons in the formation. As PEF depends on the atomic number of the elements in the formation, it also varies according to the chemical composition of the minerals present and is essentially independent of porosity. For example, the PEF of pure calcite = 5.08 b/e$^-$, illite = 3.03 b/e$^-$, quartz = 1.81 b/e$^-$, and kaolinite = 1.49 b/e$^-$. PEF values can be used in combination with NGT curves to identify different types of clay minerals. Coupling between the tool and borehole wall is essential for good HLDS logs; poor contact results in underestimation of density values.

Porosity

Formation porosity was measured with the Accelerator Porosity Sonde. The sonde incorporates a minitron neutron generator, which produces fast (14.4 MeV) neutrons, and five neutron detectors (four epithermal and one thermal), positioned at different spacings. The tool is pressed against the borehole wall by an eccentralizing bowspring. Emitted neutrons are slowed down by collisions inside the formation. The amount of energy lost per collision depends on the relative mass of the nucleus with which the neutron collides. The highest energy loss occurs when a neutron strikes a hydrogen nucleus, which has practically the same mass (neutrons simply bounce off heavier elements without losing much energy). The neutron detectors record the number of neutrons arriving at various distances from the source. The lower the porosity and, accordingly, the lower the hydrogen content, the farther the neutron will be able to travel and vice versa. However, as hydrogen bound in minerals such as clays or in hydrocarbons also contributes to the measurement, the raw porosity value is commonly an overestimate.

Upon reaching thermal energies (0.025 eV) after multiple collisions, the neutrons are captured by the nuclei of chlorine, silicon, boron, and other elements, resulting in a gamma ray emission. The capacity of the formation to capture these neutrons is the neutron capture cross section (Σ_f), which is a function of the porosity and is also measured by the Accelerator Porosity Sonde.

Electrical Resistivity

The Phasor Dual Induction-Spherically Focused Resistivity (DIT-E) tool was used to measure electrical resistivity. The DIT-E provides three measures of electrical resistivity, each with a different depth of investigation into the formation: a deep-reading induction (IDPH), a medium-reading induction (IMPH), and a spherically focused log (SFLU). The two induction devices transmit high-frequency alternating currents through transmitter coils, creating time-varying magnetic fields that induce currents in the formation. These induced currents form loops around the borehole, creating a magnetic field that induces new currents in the receiver coils, producing a voltage. These induced currents are proportional to the conductivity of the formation, as is the voltage. The measured conductivities are then converted to resistivity. The SFLU is a shallow-penetration galvanic device that measures the current necessary to maintain a constant voltage drop across a fixed interval of the formation. It is a direct measurement of resistivity, with a higher resolution than the induction devices but more sensitive to borehole conditions. Sand grains and hydrocarbons are electrical insulators, whereas ionic solutions and clays are good conductors. Electrical resistivity can therefore be used to evaluate fluid salinity, water saturation, porosity, and the characteristics of the pore structure.

In addition, the DIT-E measures the spontaneous potential (SP) of the formation. SP can originate from a variety of causes: electrochemical, electrothermal, electrokinetic streaming potentials, and membrane potentials, due to differences in the mobility of ions in the pore and drilling fluids. SP may be useful to infer fluid flow zones and formation permeability.

Temperature, Acceleration, and Pressure

Downhole temperature, acceleration, and pressure were measured with the LDEO Temperature/Acceleration/Pressure (TAP) tool. Attached to the bottom of the triple combo tool string, the TAP is run in an autonomous mode, with data stored in built-in memory. Two thermistors with distinct responses are mounted near the bottom of the tool to detect borehole fluid temperatures. A thin, fast-response thermistor is able to detect small abrupt changes in temperature. A thicker slow-response thermistor is used to estimate temperature gradients and thermal regimes more accurately. The pressure transducer is included to activate the tool at a specified depth. A three-axis accelerometer measures tool movement downhole, providing data for analyzing the effects of heave on a deployed tool string.

The temperature record must be interpreted with caution, as the amount of time elapsed between the end of drilling and the logging operation is generally not sufficient to allow the borehole to recover thermally from the influence of drilling fluid circulation. The data recorded under such circumstances may differ significantly from the actual formation temperature. Nevertheless, from the spatial temperature gradient it is possible to identify abrupt temperature changes that may represent localized fluid flow into the borehole, indicative of fluid pathways and fracturing and/or breaks in the temperature gradient that may correspond to contrasts in permeability at lithologic boundaries.

Acoustic Velocity

The Dipole Sonic Shear Imager measures the transit times between sonic transmitters and an array of eight receivers. It averages replicate measurements at each depth, providing a direct measurement of sound velocity through sediments that is relatively free from the effects of formation damage and enlarged borehole (Schlumberger, 1989). Along with the monopole transmitters found on most sonic tools, it also has two crossed dipole transmitters, which allow the measurement of shear and Stoneley wave velocities in addition to the compressional wave velocity, even in the slow formations typically encountered during ODP cruises. Stoneley waveforms can be indicators of fractured and/or permeable intervals

Formation MicroScanner

The FMS provides high-resolution electrical resistivity–based images of borehole walls. The tool has four orthogonal arms (pads), each containing 16 microelectrodes, or buttons, which are pressed against the borehole wall during the recording (Fig. F14). The electrodes are arranged in two diagonally offset rows of eight electrodes each and are spaced ~2.5 mm apart. A focused current is emitted from the four pads into the formation, with a return electrode near the top of the tool. Array buttons on each of the pads measure the current intensity variations. Processing transforms these measurements, which reflect the microresistivity variations of the formation, into continuous, spatially oriented, high-resolution images that mimic geologic structures behind the borehole walls. Further processing can provide measurements of dip and direction (azimuth) of planar features in the formation. Features such as bedding, fracturing, slump folding, and bioturbation can be resolved.

The maximum extension of the caliper arms is 15.0 in. In holes with a diameter >15 in, the pad contact will be inconsistent and the FMS images can be blurred. Irregular borehole walls will also adversely affect the images, as contact with the wall is poor.

Accelerometry and Magnetic Field Measurement

Three-component acceleration and magnetic field measurements were made with the General Purpose Inclinometer Tool. The primary purpose of this tool, which incorporates a three-component accelerometer and a three-component magnetometer, is to determine the acceleration and orientation of the FMS-sonic tool string during logging. Thus, the FMS images can be corrected for irregular tool motion, and the dip and direction (azimuth) of features in the FMS image can be determined.

Log Data Quality

The principal influence on log data quality is the condition of the borehole wall. If the borehole diameter is variable over short intervals, resulting from washouts during drilling, clay swelling, or borehole wall collapse, the logs from those tools that require good contact with the borehole wall (i.e., FMS, density, and porosity tools) may be degraded. Deep investigation measurements such as resistivity and sonic velocity, which do not require contact with the borehole wall, are generally less sensitive to borehole conditions. Very narrow (bridged) sections will also cause irregular log results. The quality of the borehole is improved by minimizing the circulation of drilling fluid, flushing the borehole to remove debris, and logging as soon as possible after drilling and conditioning are completed.

Log Depth Scales

The depth of the logging measurements is determined from the length of the logging cable payed out at the winch on the ship. The seafloor is identified on the natural gamma log by the abrupt reduction in gamma ray count at the water/sediment boundary (mudline). The coring depth (driller's depth) is determined from the known length of the BHA and pipe stands; the mudline is usually recovered in the first core from the hole.

Discrepancies between the driller's depth and the wireline log depth occur because of core expansion, incomplete core recovery, incomplete heave compensation, and drill pipe stretch in the case of drill pipe depth and incomplete heave compensation, cable stretch (~1 m/km), and cable slip in the case of log depth. Tidal changes in sea level will also have an effect. To minimize the wireline tool motion caused by ship heave, a hydraulic WHC adjusts for rig motion during wireline logging operations. The small but significant differences between drill pipe depth and logging depth should be taken into account when using the logs for correlation with core and log measurements. Core measurements such as susceptibility and density can be correlated to the equivalent downhole logs using the "Sagan" program, which allows shifting of the core depths onto the log depth scale. Precise core-log depth matching is difficult in zones where core recovery is low because of the inherent ambiguity of placing the recovered section within the cored interval.

Logs from different wireline tool strings will have slight depth mismatches. Distinctive features recorded by the natural gamma tool, run on every log tool string, provide correlation and relative depth offsets among the logging runs.

Data Recording and Processing

Data for each logging run were recorded, stored digitally, and monitored in real time using the Schlumberger MCM. On completion of logging in each hole, data were transferred to the downhole measurements laboratory for preliminary interpretation. Basic processing provides scientists with a comprehensive quality-controlled downhole log data set that can be used for comparison and integration with other data collected. This processing is carried out onshore at LDEO after the data are transmitted by satellite from the ship. Processing includes depth adjustments to remove depth offsets between data from different logging runs, corrections specific to certain tools and logs, documentation for the logs with an assessment of log quality, and conversion of the data to a widely accessible format (ASCII for the conventional logs and GIF for the FMS images). Schlumberger GeoQuest's GeoFrame software package is used for most of the processing. Further postcruise processing of FMS data was performed at LDEO.

Processed acoustic, caliper, density, gamma ray, magnetic, neutron porosity, resistivity, and temperature data in ASCII format are available directly from the LDEO-Borehole Research Group (BRG) internet web site at **www.ldeo.columbia.edu/BRG/ODP/DATABASE.** Access to logging data is restricted to Leg 201 participants for 12 months following the completion of the leg, and a password is required to access data during this period. Thereafter, access to this log data is openly available. A summary of logging highlights is also posted on the LDEO-BRG web site at the end of each leg.

REFERENCES

Amann, R.I., Krumholz, L., and Stahl, D.A., 1990. Fluorescent-oligonucleotide probing of whole cells for determinative, phylogenetic, and environmental studies in microbiology. *J. Bacteriol.,* 172:762–770.

Amann, R.I., Ludwig, W., and Schleifer, K.-H., 1995. Phylogenetic identification and in situ detection of individual microbial cells without cultivation. *Microbiological Rev.,* 59:143–169.

Balch, W.E., Fox, G.E., Magrum, L.J., Woese, C.R., and Wolfe, R.S., 1979. Methanogens: reevaluation of a unique biological group. *Microbiol Rev.,* 43:260–296.

Bale, S.J., Goodman, K., Rochelle, P.A., Marchesi, J.R., Fry, J.C., Weightman, A.J., and Parkes, R.J., 1997. *Desulfovibrio profundus* sp. nov., a novel barophilic sulfate-reducing bacterium from deep sediment layers in the Japan Sea. *Int. J. Syst. Bacteriol.,* 47:515–521.

Balsam, W.L., and Damuth, J.E., 2000. Further investigations of shipboard vs. shore-based spectral data: implications for interpreting Leg 164 sediment composition. *In* Paull, C.K., Matsumoto, R., Wallace, P., and Dillon, W.P. (Eds.), *Proc. ODP, Sci. Results,* 164: College Station, TX (Ocean Drilling Program), 313–324.

Balsam, W.L., Damuth, J.E., and Schneider, R.R., 1997. Comparison of shipboard vs. shore-based spectral data from Amazon-Fan cores: implications for interpreting sediment composition. *In* Flood, R.D., Piper, D.J.W., Klaus, A., and Peterson, L.C. (Eds.), *Proc. ODP, Sci. Results,* 155: College Station, TX (Ocean Drilling Program), 193–215.

Balsam, W.L., Deaton, B.C., and Damuth, J.E., 1998. The effects of water content on diffuse reflectance measurements of deep-sea core samples: an example from ODP Leg 164 sediments. *Mar. Geol.,* 149:177–189.

Barnes, S.P., Bradbrook, S.D., Cragg, B.A., Marchesi, J.R., Weightman, A.J., Fry, J.C., and Parkes, R.J., 1998. Isolation of sulfate-reducing bacteria from deep sediment layers of the Pacific Ocean. *Geomicrobiol. J.,* 15:67–83.

Barns, S.M., Delwiche, C.F., Palmer, J.D., and Pace, N.R., 1996. Perspectives on archaeal diversity, thermophily and monophyly from environmental rRNA sequences. *Proc. Natl. Acad. Sci. USA,* 93:9188–9193.

Berggren, W.A., Hilgen, F.S. Langereis, C.G., Kent, D.V., Obradovich, J.C., Raffi, I., Rayun, M.E., and Shakleton, N.J., 1995a. Late Neogene chronology: new perspectives in high-resolution stratigraphy. *GSAB,* 107:1272–1287.

Berggren, W.A., Kent, D.V., Swisher, C.C., and Aubry, M.P., 1995b. A revised Cenozoic geochronology and chronostratigraphy. *In* Berggren, Kent, Aubry, and Hardenbol, J., (Eds.), *Geochronology, Time Scales and Global Stratigraphic Correlation.* Spec. Pub. SEPM 59:129–212.

Blum, P., 1997. Physical properties handbook: a guide to the shipboard measurement of physical properties of deep-sea cores. *ODP Tech. Note,* 26 [Online]. Available from World Wide Web: <http://www-odp.tamu.edu/publications/tnotes/tn26/INDEX.HTM>. [Cited 2002-01-23]

Boetius, A., Ravenschlag, K., Schubert, C.J., Rickert, D., Widdel, F., Gieseke, A., Amann, R., Jorgensen, B.B., Witte, U., and Pfannkuche, O., 2000. Microscopic identification of a microbial consortium apparently mediating anaerobic methane oxidation above marine gas hydrate. *Nature,* 407:623–626.

Bullard, E.C., 1954. The flow of heat through the floor of the Atlantic Ocean. *Proc. R. Soc. London A,* 222:408–429.

Cline, J.D., 1969. Sectrophotometric determination of hydrogen sulfide in natural waters. *Limnol. Oceanogr.,* 14:454–458.

Coates, J.D., Michaelidou, U.A., Bruce, A., O'Connor, S.M., Crespi, J.N., and Achenbach, L.A., 1999. Ubiquity and diversity of dissimilatory (per)chlorate-reducing bacteria. *Appl. Environ. Microbiol.,* 65:5234–524.

Cragg, B.A., 1994. Bacterial profiles in deep sediment layers from the Lau Basin (Site 834). *In* Hawkins, J., Parson, L., Allan, J., et al., *Proc. ODP, Sci. Results,* 135: College Station, TX (Ocean Drilling Program), 147–150.

Cragg, B.A., Parkes, R.J., Fry, J.C., Herbert, R.A., Wimpenny, J.W.T., and Getliff, J.M., 1990. Bacterial biomass and activity profiles within deep sediment layers. *In* Suess, E., von Huene, R., et al., *Proc. ODP, Sci. Results,* 112: College Station, TX (Ocean Drilling Program), 607–619.

Cragg, B.A., Parkes, R.J., Fry, J.C., Weightman, A.J., Rochelle, P.A., and Maxwell, J.R., 1996. Bacterial populations and processes in sediments containing gas hydrates (ODP Leg 146: Cascadia Margin). *Earth Planet. Sci. Lett.,* 139:497–507.

Davis, E.E., Villinger, H., MacDonald, R.D., Meldrum, R.D., and Grigel, J., 1997. A robust rapid-response probe for measuring bottom-hole temperatures in deep-ocean boreholes. *Mar. Geophys. Res.,* 19:267–281.

Dickens, G.R., Paull, C.K., Wallace, P., and the ODP Leg 164 Scientific Party, 1997. Direct measurement of in situ methane quantities in a large gas-hydrate reservoir. *Nature,* 385:427–428.

Duan, Z., Møller, N., Greenberg, J., and Weare, J.H., 1992. The prediction of methane solubility in natural waters to high ionic strengths from 0° to 250°C and from 0 to 1600 bar. *Geochim. Cosmochim. Acta,* 56:1451–1460.

Ellis, D.V., 1987. *Well Logging for Earth Scientists:* New York (Elsevier).

Espitalié, J., Deroo, G., and Marquis, F., 1986. La pyrolyse Rock-Eval et ses applications, Partie III. R*ev. Inst. Fr. Pet.,* 41:73–89.

Evans, H.B., 1965. GRAPE—a device for continuous determination of material density and porosity. *Trans. SPWLA 6th Ann. Logging Symp., Dallas,* 2:B1–B25.

Ferdelman, T.G., Fossing, H., Neumann, K., and Schulz, H.D., 1999. Sulfate reduction in surface sediments of the southeast Atlantic continental margin between 15°38′S and 27°57′S (Angola and Namibia). *Limnol. Oceanogr.,* 44:650–661.

Fisher, A.T., and Becker, K., 1993. A guide to ODP tools for downhole measurements. *ODP Tech. Note,* 10 [Online]. Available from World Wide Web: <http://www-odp.tamu.edu/publications/tnotes/tn10/INDEX.HTM>. [Cited 2002-01-23]

Fossing, H., Ferdelman, T.G., and Berg, P., 2000. Sulfate reduction and methane oxidation in continental margin sediments influenced by irrigation (South-East Atlantic off Namibia). *Geochim. Cosmochim. Acta,* 64:897–910.

Fossing, H., and Jørgensen, B.B., 1989. Measurement of bacterial sulfate reduction in sediments: evaluation of a single-step chromium reduction method. *Biogeochemistry,* 8:205–222.

Freier, D., Mothershed, Ch.P., and Wiegel, J., 1988. *Clostridium thermocellum* characterization of JW20. *Appl. Environ. Microbiology,* 54:104–111.

Fry, J.C., 1988. Determination of biomass. *In* Austin, B. (Ed.), *Methods in Aquatic Bacteriology:* Chichester (Wiley), 27–72.

Fuller, M.E., Streger, S.H., Rothmel, R.K., Meilloux, B.J., Hall, J.A., Onstott, T.C., Fredrickson, J.K., Balkwill, D.L., and De Flaun, M.F., 2000. Development of a vital fluorescent staining method for monitoring bacterial transport in subsurface environments. *Appl. Env. Microbiol.,* 66:4486–4496.

Garthright, W.E., 2001. Most probable number from serial dilutions. *In Bacteriological Analytical Manual Online* (App. 2), U.S. Food and Drug Administration. Available from World Wide Web: http://www.cfsan.fda.gov. [Cited 18-09-2002]

Gieskes, J.M., Gamo, T., and Brumsack, H., 1991. Chemical methods for interstitial water analysis aboard *JOIDES Resolution. ODP Tech. Note,* 15 [Online]. Available from World Wide Web: <http://www-odp.tamu.edu/publications/tnotes/tn15/INDEX.HTM>. [Cited 2002-01-23]

Goldberg, D., 1997. The role of downhole measurements in marine geology and geophysics. *Rev. Geophys.,* 35:315–342.

Heid, C.A., Stevens, J., Livak, K.J., and Williams, P.M., 1996. Real time quantitative PCR. *Genome Res.,* 6:986–994.

Hoehler, T.M., Alperin, M.J., Albert, D.B., and Martens, C.S., 1998. Thermodynamic control on hydrogen concentrations in anoxic sediments. *Geochim. Cosmochim. Acta,* 62:1745–1756.

Hoehler, T.M., Borowski, W.S., Alperin, M.J., Rodriguez, N.M., and Paull, C.K., 2000. Model, stable isotope, and radiotracer characterization of anaerobic methane oxidation in gas hydrate–bearing sediments of the Blake Ridge. *In* Paull, C.K., Matsumoto, R., Wallace, P.J., and Dillon, W.P. (Eds.), *Proc. ODP, Sci. Results,* 164: College Station, TX (Ocean Drilling Program), 79–85.

Holm-Hansen, O., and Booth, C.R., 1966. The measurement of adenosine triphosphate in the ocean and its ecological significance. *Limnol. Oceanogr.,* 11:510–519.

Hoppie, B.W., Blum, P., and the Shipboard Scientific Party, 1994. Natural gamma-ray measurements on ODP cores: introduction to procedures with examples from Leg 150. *In* Mountain, G.S., Miller, K.G., Blum, P., et al., *Proc. ODP, Init. Repts.,* 150: College Station, TX (Ocean Drilling Program), 51–59.

Horai, K., and Von Herzen, R.P., 1985. Measurement of heat flow on Leg 86 of the Deep Sea Drilling Project. *In* Heath, G.R., Burckle, L.H., et al., *Init. Repts. DSDP,* 86: Washington (U.S. Govt. Printing Office), 759–777.

Hugenholtz, P., Pitulle, C., Hershberger, K.L., and Pace, N.R., 1998. Novel division level bacterial diversity in a Yellowstone hot spring. *J. Bacteriol.,* 180:366–376.

Inagaki, F., Sakihama, Y., Takai, K., Komatsu, T., Inoue, A., and Horikoshi, K., in press. Transition in microbial community structure and presence of unusual microorganisms in a deep-sea rock. *Geomicrobiol. J.,* 19.

Inagaki, F., Takai, K., Komatsu, T., Kanamatsu, T., Fujioka, K., and Horikoshi, K., 2001. Archaeology of Archaea: geomicrobiological record of Pleistocene thermal events concealed in a deep-sea subseafloor environment. *Extremophiles,* 5:385–392.

Isaksen, M.F., and Jørgensen, B.B., 1994. Thermophilic sulfate reducing bacteria in cold marine sediment. *FEMS Microbiol. Ecol.,* 14:1–8.

Iversen, N., and Jørgensen, B.B., 1985. Anaerobic methane oxidation rates at the sulfate–methane transition in marine sediments from Kattegat and Skagerrak (Denmark). *Limnol. Oceanogr.,* 30:944–955.

Jørgensen, B.B., 1978. A comparison of methods for the quantification of bacterial sulfate reduction in coastal marine sediments. I. Measurement with radiotracer techniques. *Geomicrobiol. J.,* 1:11–28.

————, 1982. Mineralization of organic matter in the seabed—the role of sulphate reduction. *Nature,* 296:643–645.

Karl, D.M., and LaRock, P.A., 1975. Adenosine triphosphate measurements in soil and marine sediments. *J. Fish. Res. Board Can.,* 32:599–607.

Klein, M., Friedrich, M., Roger, A.J., Hugenholtz, P., Fishbain, S., Abicht, H., Blackall, L.L., Stahl, D.A., and Wagner, M., 2001. Multiple lateral transfers of dissimilatory sulfite reductase genes between major lineages of sulfate-reducing prokaryotes. *J. Bacteriol.,* 183:6028–6035.

Knoblauch, C., and Jørgensen, B.B., 1999. Effect of temperature on sulfate reduction, growth rate, and growth yield in five psychrophilic sulfate-reducing bacteria from Arctic sediments. *Environ. Microbiol.,* 1:457–467.

Knoblauch, C., Jørgensen, B.B., and Harder, J., 1999a. Community size and metabolic rates of psychrophilic sulfate-reducing bacteria in Arctic marine sediments. *Appl. Environ. Microbiol.,* 65:4230–4233.

Knoblauch, C., Sahm, K., and Jørgensen, B.B., 1999b. Psychrophilic sulphate reducing bacteria isolated from permanently cold arctic marine sediments: description of *Desulfofrigus oceanense* gen. nov., sp. nov., *Desulfofrigus fragile* sp. nov., *Desulfofaba gelida* gen. nov., sp. nov., *Desulfotalea psychrophila* gen. nov., sp. nov., and *Desulfotalea arctica* sp. nov. *Int. J. Syst. Bacteriol.,* 49:1631–1643.

Kristiansen, J.I., 1982. The transient cylindrical probe method for determination of thermal parameters of earth materials [Ph.D. dissert.]. Åarhus Univ.

Kvenvolden, K.A., and McDonald, T.J., 1986. Organic geochemistry on the *JOIDES Resolution*—an assay. *ODP Tech. Note,* 6.

Lécuyer, C., Grandjean, P., and Sheppard, S.M.F., 1999. Oxygen isotope exchange between dissolved phosphate and water at temperatures ≤135°C: inorganic vs. biological fractionation. *Geochim. Cosmochim. Acta,* 63:855–862.

Levin, G.V., Clendenning, J.R., Chappelle, E.W., Heim, A.H., and Rocek, E., 1964. A rapid method for detection of microorganisms by ATP assay. *Bioscience,* 14:37–38.

Li, L., Kato, C., and Horikoshi, K., 1999. Bacterial diversity in deep-sea sediments from different depths. *Biodivers. Conserv.,* 8:659–677.

Liu, W.-T., Marsh, T.L., Cheng, H., and Forney, L.J., 1997. Characterization of microbial diversity by determining terminal restriction fragment length polymorphisms of genes encoding 16S rRNA. *Appl. Environ. Microbiol.,* 63:4516–4522.

Llobet-Brossa, E., Rossello-Mora, R., and Amann, R., 1998. Microbial community composition of Wadden Sea sediments as revealed by fluorescence in situ hybridization. *Appl. Environ. Microbiol.,* 64:2691–2696.

Lovell, M.A., Harvey, P.K., Brewer, T.S., Williams, C., Jackson, P.D., and Williamson, G., 1998. Application of FMS images in the Ocean Drilling Program: an overview. *In* Cramp, A., MacLeod, C.J., Lee, S.V., and Jones, E.J.W. (Eds.), *Geological Evolution of Ocean Basins: Results from the Ocean Drilling Program.* Spec. Publ.—Geol. Soc. London, 131:287–303.

Lovley, D.R., and Goodwin, S., 1988. Hydrogen concentrations as an indicator of terminal elect-on-accepting reactions in aquatic sediments. *Geochim. Cosmochim. Acta,* 52:2993–3003.

Lovley, D.R., and Phillips, E.J.P., 1986. Organic matter mineralization with reduction of ferric iron in anaerobic sediments. *Appl. Environ. Microbiol.,* 51:683–689.

————, 1988. Novel mode of microbial energy metabolism: organic carbon oxidation coupled to dissimilatory reduction of iron or manganese. *Appl. Environ. Microbiol.,* 54:1472–1480.

Ludwig, W., and Schleifer, K.-H., 1999. Phylogeny of bacteria beyond the 16S rRNA standard. *ASM News,* 65:752–757.

Lueders, T., Chin, K.-J., Conrad, R., and Friedrich, M., 2001. Molecular analyses of methyl-coenzyme M reductase α-subunit (mcrA) genes in rice field soil and enrichment cultures reveal the methanogenic phenotype of a novel archacal lineage. *Environ. Microbiol.,* 3:194–204.

Mackenzie, K.V., 1981. Nine-term equation for sound speed in the oceans. *J. Acoust. Soc. Am.,* 70:807–812.

Madson, E.L., 2000. Nucleic-acid characterization of the identity and activity of subsurface microorganisms. *Hydrogeol. J.,* 8:112–125.

Maidak, B.L., Cole, J.R., Lilburn, T.G., Parker, C.T., Jr., Saxmen, P.R., Farris, R.J., Garrity, G.M., Olsen, G.J., Schmidt, T.M., and Tiedje, J.M., 2001. The RDP-II (Ribosomal Database Project). *Nucleic Acids Res.,* 29:173–174.

Manheim, F.T., and Sayles, F.L., 1974. Composition and origin of interstitial waters of marine sediments, based on deep sea drill cores. *In* Goldberg, E.D. (Ed.), *The Sea* (Vol. 5): *Marine Chemistry: The Sedimentary Cycle:* New York (Wiley), 527–568.

Marchesi, J.R., Sato, T., Weightman, A.J., Martin, T.A., Fry, J.C., Hiom, S.J., and Wade, W.G., 1998. Design and evaluation of useful bacterium-specific PCR primers that amplify genes coding for bacterial 16S rRNA. *Appl. Environ. Microbiol.,* 64:795–799.

Marchesi, J.R., Weightman, A.J., Cragg, B.A., Parkes, R.J., and Fry, J.C., 2001. Methanogen and bacterial diversity and distribution in deep gas hydrate sediments from the Cascadia Margin as revealed by 16S rRNA molecular analysis. *FEMS Microbiol. Ecol.,* 34:221–228.

Mazzullo, J.M., Meyer, A., and Kidd, R.B., 1988. New sediment classification scheme for the Ocean Drilling Program. *In* Mazzullo, J., and Graham, A.G. (Eds.), Handbook for Shipboard Sedimentologists. *ODP Tech. Note,* 8:45–67.

Murray, R.W., Miller, D.J., and Kryc, K.A., 2000. Analysis of major and trace elements in rocks, sediments, and interstitial waters by inductively coupled plasma—atomic emission spectrometry (ICP-AES). *ODP Tech. Note,* 29 [Online]. Available from

World Wide Web: <http://www-odp.tamu.edu/publications/tnotes/tn29/INDEX.HTM>. [Cited 2002-01-23]

Muyzer, G., and Smalla, K., 1998. Application of dematuring gradient gel electrophoersis (DGGE) and temperature gradient electrophoresis (TGGE) in microbial ecology. *Antonie van Leeuwenhoek,* 73:127–141.

Niitsuma, N., and Koyama, M., 1994. Paleomagnetic processor: a fully automatic portable spinner magnetometer combined with an AF demagnetizer and magnetic susceptibility anisotropy meter. *Shizuoka Univ. Geosci. Rep.,* 21:11–19.

Orphan, V.J., Howes, C.H., Hinrichs, K.-U., McKeegan, K.D., and DeLong, E.F., 2001. Methane-consuming archaea revealed by directly coupled isotopic and phylogenetic analysis. *Science,* 293:484–487.

Parkes, R.J., 1987. Analysis of microbial communities within sediments using biomarkers. In *Ecology of Microbial Communities* (SGM Symposium, Series 41): Cambridge (Cambridge Univ. Press), 147–177.

Parkes, R.J., Cragg, B.A., Bale, S.J., Getliff, J.M., Goodman, K., Rochelle, P.A., Fry, J.C., Weightman, A.J., and Harvey, S.M., 1994. A deep bacterial biosphere in Pacific Ocean sediments. *Nature,* 371:410–413.

Parkes, R.J., Cragg, B.A., Bale, S.J., Goodman, K., Rochelle, P.A., and Fry, J.C., 1995. A combined ecological and physiological approach to studying sulfate reduction within deep marine sediment layers. *J. Microbio. Meth.,* 23:235–249.

Parkes, R.J., Cragg, B.A., and Wellsbury, P., 2000. Recent studies on bacterial populations and processes in marine sediments: a review. *Hydrogeol. Rev.,* 8:11–28.

Paull, C.K., Lorenson, T.D., Dickens, G., Borowski, W.S., Ussler, W., III, and Kvenvolden, K.A., 2000. Comparisons of in situ and gas core measurements in ODP Leg 164 bore holes. *In* Holder, G.D., and Bishnoi, P.R. (Eds.), *Gas Hydrates; Challenges for the Future:* New York (NY Acad. Sci.), 23–31.

Paull, C.K., Matsumoto, R., Wallace, P.J., et al., 1996. *Proc. ODP, Init. Repts.,* 164: College Station, TX (Ocean Drilling Program).

Pérez-Jiménez, J.R., Young, L.Y., and Kerkhof, L.J., 2001. Molecular characterization of sulfate-reducing bacteria in anaerobic hydrocarbon-degrading consortia and pure cultures using the dissimilatory sulfite reductase (dsr AB) genes. *FEMS Microbiol. Ecol.,* 35:145–150.

Pernthaler, J., Gloeckner, F.-O., Schoenhuber, W., and Amann, R., 2001. Fluorescence in situ hybridization (FISH) with rRNA-targeted oligonucleotide probes. *Meth. Enzymol.,* 30:207–226.

Pettigrew, T.L., 1992. The design and operation of a wireline pressure core sampler (PCS). *ODP Tech. Note,* 17.

Ravenschlag, K., Sahm, K., and Amann, R., 2001. Quantitative molecular analysis of the microbial community in marine arctic sediments (Svalbard). *Appl. Environ. Microbiol.,* 67:387–395.

Ravenschlag, K., Sahm, K., Knoblauch, C., Jørgensen, B.B., and Amann, R., 2000. Community structure, cellular rRNA content and activity of sulfate-reducing bacteria in marine Arctic sediments. *Appl. Environ. Microbiol.,* 66:3592–3602.

Rider, M., 1996. *The Geological Interpretation of Well Logs* (2nd ed.): Houston (Gulf Publishing Co.).

Rochelle, P.A., Cragg, B.A., Fry, J.C., Parkes, R.J., and Weightman, A.J., 1994. Effect of sample handling on estimation of bacterial diversity in marine sediments by 16S rRNA gene sequence analysis. *FEMS Microbiol. Ecol.,* 15:215–226.

Rochelle, P.A., Fry, J.C., Parkes, R.J., and Weightman, A.J., 1992. DNA extraction for 16S rRNA gene analysis to determine genetic diversity in deep sediment communities. *FEMS Microbiol. Lett.,* 100:59–66.

Sahm, K., MacGregor, B.J., Jørgensen, B.B., and Stahl, D.A., 1999. Sulfate-reduction and vertical distribution of sulfate-reducing bacteria quantified by rRNA slot-blot hybridization in a coastal marine sediment. *Environ. Microbiol.,* 1:65–74.

Schlumberger, 1998. *Log Interpretation Charts:* Houston (Schlumberger).

————, 1989. *Log Interpretation Principles/Applications:* Houston (Schlumberger Educ. Services), SMP–7017.

Serra, O., 1984. *Fundamentals of Well-Log Interpretation* (Vol. 1): *The Acquisition of Logging Data.* Dev. Pet. Sci., 15A.

————, 1986. *Fundamentals of Well-Log Interpretation* (Vol. 2): *The Interpretation of Logging Data.* Dev. Pet. Sci., 15B.

Shepard, F., 1954. Nomenclature based on sand-silt-clay ratios. *J. Sediment. Petrol.,* 24:151–158.

Shipboard Scientific Party, 1988. Explanatory notes. *In* Suess, E., von Huene, R., et al., *Proc. ODP, Init. Repts.,* 112: College Station, TX (Ocean Drilling Program), 25–44.

————, 1992. Explanatory notes. *In* Mayer, L., Pisias, N., Janecek, T., et al., *Proc. ODP, Init. Repts.,* 138 (Pt. 1): College Station, TX (Ocean Drilling Program), 13–42.

————, 2001. Explanatory notes. *In* O'Brien, P.E., Cooper, A.K., Richter, C., et al., *Proc. ODP, Init. Repts.,* 188, 1–66 [CD-ROM]. Available from: Ocean Drilling Program, Texas A&M University, College Station TX 77845-9547, USA.

————, 2003. Explanatory notes. *In* Stephen, R.A., Kasahara, J., Acton, G.D., et al., *Proc. ODP, Init. Repts.,* 200, 1–66 [CD-ROM]. Available from: Ocean Drilling Program, Texas A&M University, College Station TX 77845-9547, USA.

Smith, D.C., and Azam, F., 1992. A simple, economical method for measuring bacterial protein synthesis rates in seawater using ^{3}H-leucine. *Mar. Microb. Food Webs,* 6:107–114.

Smith, D.C., Spivack, A.J., Fisk, M.R., Haveman, S.A., Staudigel, H., and ODP Leg 185 Shipboard Scientific Party, 2000a. Methods for quantifying potential microbial contamination during deep ocean coring. *ODP Tech. Note,* 28 [Online]. Available from the World Wide Web: <http://www-odp.tamu.edu/publications/tnotes/tn28/INDEX.HTM>. [Cited 2002-01-23]

————, 2000b. Tracer-based estimates of drilling-induced microbial contamination of deep sea crust. *Geomicrobiol. J.,* 17:207–219.

Springer, E., Sachs, M.S., Woese, C.R., and Boone, D.R., 1995. Partial gene sequences for the alpha-subunit of methyl-coenzyme M reductase (MCRI) as a phylogenetic tool for the family Methanosarcinaceae. *Internat. J. System. Bacteriol.,* 45:554–559.

Stoeck, T.G., and Duineveld, C.A., 2000. Nucleic acids and ATP to assess microbial biomass and activity in a marine biosedimentary system. *Mar. Biol.,* 137:1111–1123.

Strickland, J.D.H., and Parsons, T.R., 1972. *A Practical Handbook of Seawater Analysis:* Ottawa (Fisheries Research Board of Canada).

Stults, J.R., Snoeyenbos-West, O., Methe, B., Lovley, D.R., and Chandler, D.P., 2001. Application of the 5'-fluorogenic exonuclease assay (TaqMan) for quantitative ribosomal DNA and rRNA analysis in sediments. *Appl. Environ. Microbiol.,* 67:2781–2789.

Suzuki, M.T., Taylor, L.T., and DeLong, E.F., 2000. Quantitative analysis of small-subunit rRNA genes in mixed microbial populations via 5'-nuclease assays. *Appl. Environ. Microbiol.,* 66:4605–4614.

Takai, K., and Horikoshi, K., 1999. Genetic diversity of archaea in deep-sea hydrothermal vent environments. *Genetics,* 152:1285–1297.

————, 2000. Rapid detection and quantification of members of the archaeal community by quantitative PCR using fluorogenic probes. *Appl. Environ. Microbiol.,* 66:5066–5072.

Takai, K., Komatsu, T., Inagaki, F., and Horikoshi, K., 2001. Distribution of Archaea in a black smoker chimney structure. *Appl. Environ. Microbiol.,* 67:3618–3629.

Teske, A., Hinrichs, K.-U., Edgcomb, V., de Vera Gomez, A., Kysela, D., Sylva, S., Sogin, M.L., and Jannasch, H.W., 2002. Microbial diversity of hydrothermal vent sediments: evidence for anaerobic methane-oxidizing microbial communities. *Appl. Environ. Microbiol.,* 68:1994–2007.

Thamdrup, B., Rosselló-Mora, R., and Amann, R., 2000. Microbial manganese and sulfate reduction in Black Sea shelf sediments. *Appl. Environ. Microbiol.,* 66:2888–2897.

Varner, J.E., and Kok, B., 1967. Extraterrestrial life detection based on oxygen isotope exchange reactions. *Science,* 155:1110–1112.

Vester, F., and Ingvorsen, K., 1998. Improved most-probable-number method to detect sulfate-reducing bacteria with natural media and a radiotracer. *Appl. Environ. Microbiol.,* 64:1700–1707.

Von Herzen, R.P., and Maxwell, A.E., 1959. The measurement of thermal conductivity of deep-sea sediments by a needle-probe method. *J. Geophys. Res.,* 64:1557–1563.

Wagner, M., Roger, A.J., Flax, J.L., Brusseau, G.A., and Stahl, D.A., 1998. Phylogeny of dissimilatory sulfite reductases supports an early origin of sulfate respiration. *J. Bacteriol.,* 180:2975–2982.

Wallace, P.J., Dickens, G.R., Paull, C.K., and Ussler III, W., 2000. Effects of core retrieval and degassing on the carbon isotope composition of methane in gas hydrate– and free gas–bearing sediments from the Blake Ridge. *In* Paull, C.K., Matsumoto, R., Wallace, P.J., and Dillon, W.P. (Eds.), *Proc. ODP, Sci. Results,* 164, 101–112 [CD-ROM]. Available from: Ocean Drilling Program, Texas A&M University, College Station, TX 77845-9547, U.S.A.

Warthmann, R., Van Lith, Y., Vasconcelos, C., McKenzie, J.A., and Karpoff, A.M., 2000. Bacterially induced dolomite precipitation in anoxic culture experiments, *Geology,* 28:1091–1094.

Wellsbury, P., Goodman, K., Barth, T., Cragg, B.A., Barnes, S.P., and Parkes, R.J., 1997. Deep marine biosphere fueled by increasing organic matter availability during burial and heating. *Nature,* 388:573–576.

Wellsbury, P., Goodman, K., Cragg, B.A., and Parkes, R.J., 2000. The geomicrobiology of deep marine sediments from Blake Ridge containing methane hydrate (Sites 994, 995, and 997). *In* Paull, C.K., Matsumoto, R., Wallace, P.J., and Dillon, W.P. (Eds.), *Proc. ODP, Sci. Results,* 164: College Station, TX (Ocean Drilling Program), 379–391.

Wentworth, C.K., 1922. A scale of grade and class terms of clastic sediments. *J. Geol.,* 30:377–392.

Whitman, W.B., Coleman, D.C., and Wiebe, W.J., 1998. Prokaryotes: the unseen majority. *Proc. Nat. Acad. Sci. U.S.A.,* 95:6578–6583.

Widdel, F., 1980. Anaerober Abbau von Fettsäuren und Benzoesäure durch neu isolierte Arten sulfatreduzierender Bakterien. [Dissertation], Universität Göttingen.

Widdel, F., and Bak, F., 1992. Gram negative mesophilic sulfate reducing bacteria. *In* Balows, A., et al. (Eds.): *The Prokaryotes* (Vol. 4): New York (Springer-Verlag), 3352–3378.

Widdel, F., Kohring, G.-W., Mayer, F., 1983. Studies on dissimilatory sulfate-reducing bacteria that decompose fatty acids. III. Characterization of the filamentous gliding *Desulfonema limicola* gen. nov. sp. nov., and *Desulfonema magnum* sp. nov. *Arch. Microbiol.,* 134:286–294.

Wiegel, J., 1992. The obligately anaerobic thermophilic bacteria. *In* Kristjansson, J.K. (Ed.), *Thermophilic Bacteria:* Boca Raton, FL (CRC-Press), 105–184.

Wilson, M.S., Bakermans, C., and Madson, E.L., 1999. In situ, real-time catabolic gene expression: extraction and characterization of naphtalene dioxygenase mRNA transcripts from groundwater. *Appl. Environ. Microbiol.,* 65:80–87.

Wilson, W.D., 1960. Speed of sound in seawater as a function of temperature, pressure and salinity. *J. Acoust. Soc. Am.,* 32:641–644.

Woese, C.R., Kandler, O., and Wheelis, M.L., 1990. Towards a natural system of organisms: proposal for the domains Archaea, Bacteria, and Eucarya. *Proc. Nat. Acad. Sci. U.S.A.,* 87:4576–4579.

Wyllie, M.R.J., Gregory, A.R., and Gardner, L.W., 1956. Elastic wave velocities in heterogeneous and porous media. *Geophysics,* 21:41–70.

Zehnder, A.J.B., and Wuhrmann, K., 1976. Titanium(III)citrate as a nontoxic oxidation-reduction buffering system for the culture of obligate anaerobs. *Science,* 194:1165–1166.

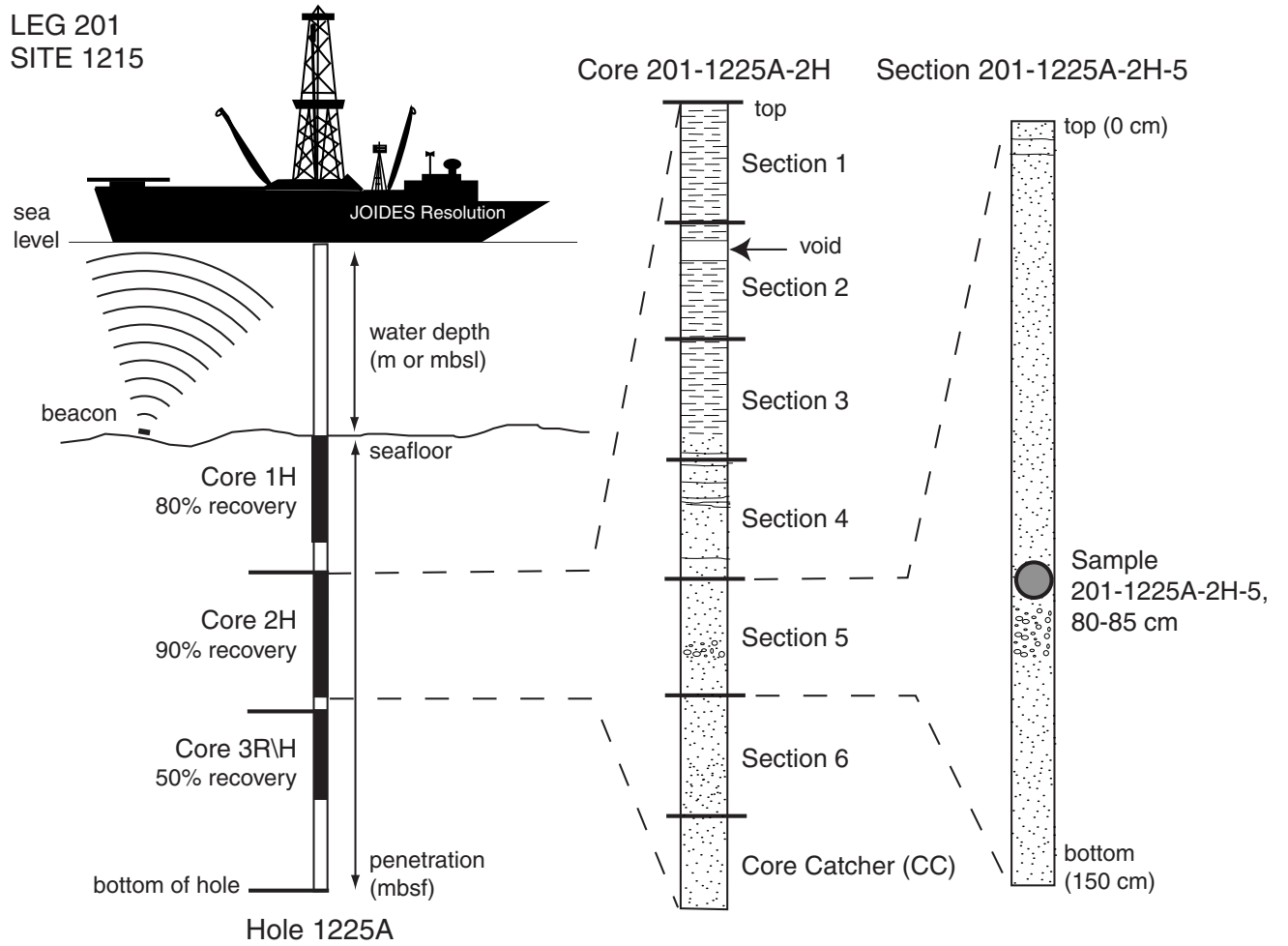**Figure F1.** Example of coring and depth intervals.

Figure F2. Example of the graphical representation of visual core descriptions (barrel sheets) using AppleCORE software.
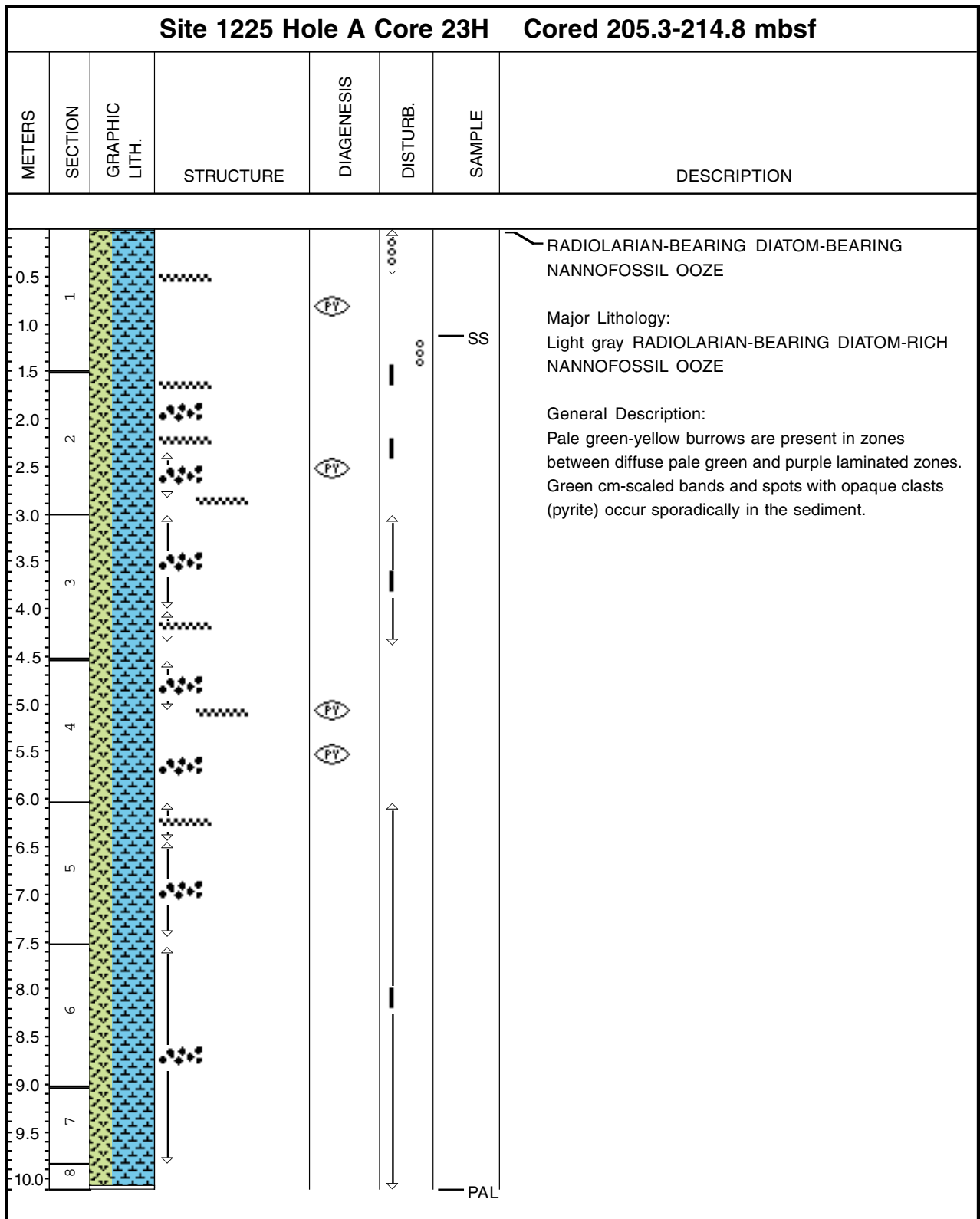

Site 1225 Hole A Core 23H							Cored 205.3–214.8 mbsf
METERS	SECTION	GRAPHIC LITH.	STRUCTURE	DIAGENESIS	DISTURB.	SAMPLE	DESCRIPTION

RADIOLARIAN-BEARING DIATOM-BEARING NANNOFOSSIL OOZE

Major Lithology:
Light gray RADIOLARIAN-BEARING DIATOM-RICH NANNOFOSSIL OOZE

General Description:
Pale green-yellow burrows are present in zones between diffuse pale green and purple laminated zones. Green cm-scaled bands and spots with opaque clasts (pyrite) occur sporadically in the sediment.

Figure F3. Key to patterns and symbols used in Leg 201 barrel sheets.

Lithology

Symbol	Name	Symbol	Name	Symbol	Name	Symbol	Name	Symbol	Name	Symbol	Name
	Nannofossil ooze		Diatom ooze		Chert		Silt		Gravel		Void/No core
	Foraminifer ooze		Radiolarian ooze		Clay		Sandy silt		Volcanic ash or tuff		Whole-round sample
	Nannofossil chalk		Diatom-Rad. Ooze		Silty clay		Clayey sand		Metalliferous sediment		
	Limestone		Diatomite		Sandy clay		Silty sand		Sulfide sand		
	Dolomite		Porcellanite		Clayey silt		Sand		Sulfide silt		

Contacts

Sharp   Undulating   Scoured   Inclined

Structures

- Color band
- Planar lamination
- Low-angle parallel bedding
- High-angle parallel bedding
- Wavy parallel bedding
- Convolute bedding
- Cross-bedding

- Erosion surface
- Mottled
- Normal-graded bedding
- Reverse-graded bedding
- Fining upward
- Coarsening-upward
- Slump

- Sand lamina
- Silt lamina
- Thin ash layer
- Fault
- Microfault (normal)
- Macrofault (normal)
- Fluid escape structure

Diagenesis

- Nodule/concretion, general
- Carbonate nodule/concretion
- Calcite nodule/concretion
- Dolomite nodule concretion
- Phosphate concretion
- Pyrite nodule/concretion

- Calcedony/chert nodule/concretion
- Barite nodule/concretion
- Cement, general
- Calcite cement
- Dolomite cement
- Calcedony/chert cement
- Quartz cement

- Calcareous
- Dolomitic
- Pyrite
- Glauconite
- Magnetite
- Phosphate
- Peloids

Fossils

- Shell fragments
- Fish remains
- Spicules

Ichnofossils

- Planolites
- Skolithos
- *Zoophycos*
- *Chondrites*

Bioturbation

- Bioturbation - minor
- Bioturbation - moderate
- Bioturbation - intense

Drilling Disturbance

- Slightly disturbed
- Moderately disturbed
- Very disturbed
- Soupy
- Biscuit
- Drilling breccia

Samples

PPWR - Physical properties whole round   SS - Smear slide   XRA - X-ray diffraction   IW - Interstitial water   PAL - Paleontology

Figure F4. (**A**) Classification scheme for siliciclastic sediment components and (**B**) an example for naming mixtures of biogenic and siliciclastic sediments. The terms "nannofossil" and "clay" may be replaced by any other name for siliciclastic or biogenic sediment particles (e.g., silt, sand, foraminifers, or diatoms).
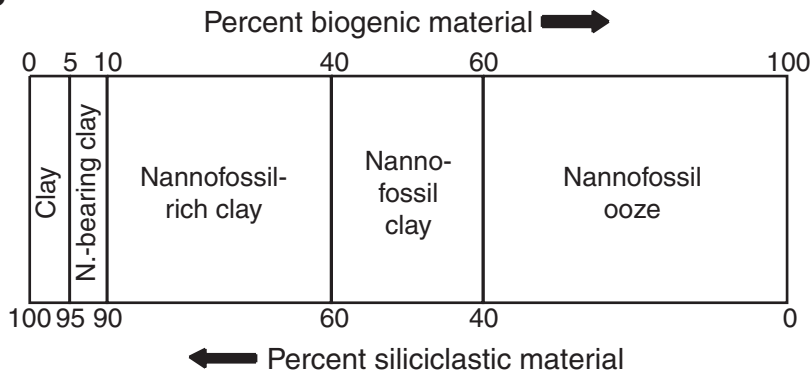
A

B

Figure F5. Grain-size classification diagram for siliciclastic sediments (modified after Wentworth, 1922).

Millimeters (mm)		Micrometers (μm)	Phi (φ)	Wentworth size class		Rock type
	4096		-12.0			
				Boulder		
	256		-8.0 —			
				Cobble	Gravel	Conglomerate/
	64		-6.0 —			Breccia
				Pebble		
	4		-2.0 —			
				Granule		
	2.00		-1.0			
				Very coarse sand		
	1.00		0.0 —			
				Coarse sand		
1/2	0.50	500	1.0 —		Sand	Sandstone
				Medium sand		
1/4	0.25	250	2.0 —			
				Fine sand		
1/8	0.125	125	3.0 —			
				Very fine sand		
1/16	0.0625	63	4.0			
				Coarse silt		
1/32	0.0310	31	5.0 —			
				Medium silt		
1/64	0.0156	15.6	6.0 —		Silt	Siltstone
				Fine silt		
1/128	0.0078	7.8	7.0 —			
				Very fine silt		
1/256	0.0039	3.9	8.0			
	0.00006	0.06	14.0	Clay	Mud	Claystone

Figure F6. Diagram of WRC sectioning for microbiology (MBIO). After taking syringe samples on the catwalk, two complete, sequential, 1.5-m sections were rapidly taken to the cold room (4°–10°C). Typically, Section 3, if not visibly disturbed, was subsampled after cleaning and alcohol wiping. The first cut (bold line) was done with the ODP cutter and separated the section into a portion to be further sectioned cleanly and anoxically in a cutting rig and one to be cut with the ODP cutter. Both sections were handled simultaneously and in the order shown. A sample for interstitial water (IW) was the first section taken and was immediately given to the geochemists for processing (unless already taken on the catwalk from the adjacent section end). The next section was for slurries, if required (nonroutine subsampling). This was rapidly cut, and at the middle cut of the liner the core was broken so that the broken surfaces were pointing downward after breaking (dotted line). The middles of the two broken parts were then immediately subsampled. AODC = acridine orange direct count, PFC = perfluorocarbon tracer, WRC = whole-round core, FISH = fluorescence in situ hybridization, DNA = deoxyribonucleic acid, ATP = adenosine triphosphate, SRR = sulfate reduction rates, DIFF = diffusion experiments, AOM = anaerobic oxidation of methane, MPN = most probable number. CHNS = carbon, hydrogen, nitrogen, sulfur analyses.
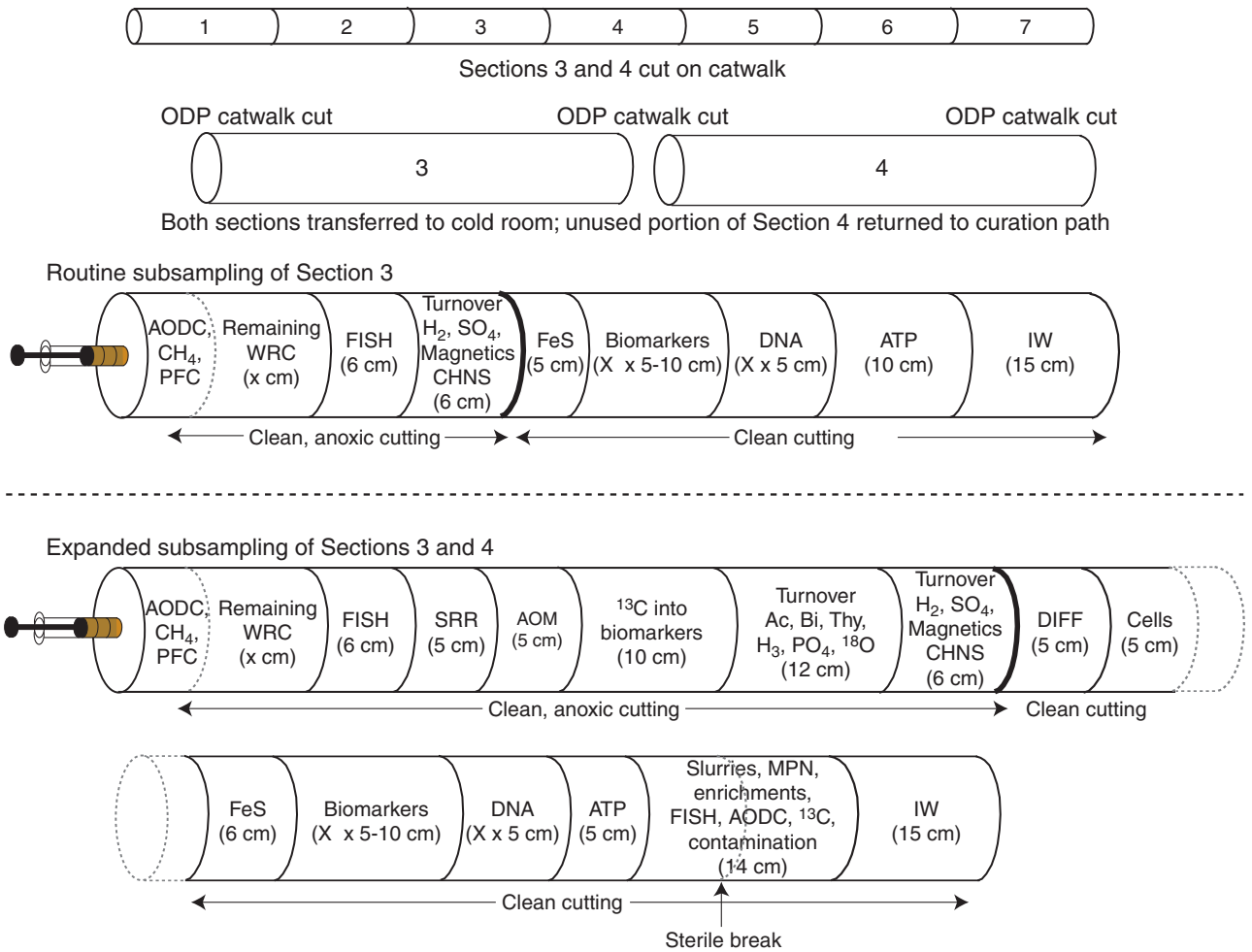
Figure F7. Nitrogen-gassed cutting rig used for cutting whole-round cores (WRCs) in the cold room. The cutting rig and the surface of the WRC are cleaned with alcohol, and the core liner is carefully cut during rotation. Cutting blades can be sterilized. A sterile blade separates a segment from the core. The WRC segment is immediately transferred to the subsampling bucket (see Fig. F8, p. 74).
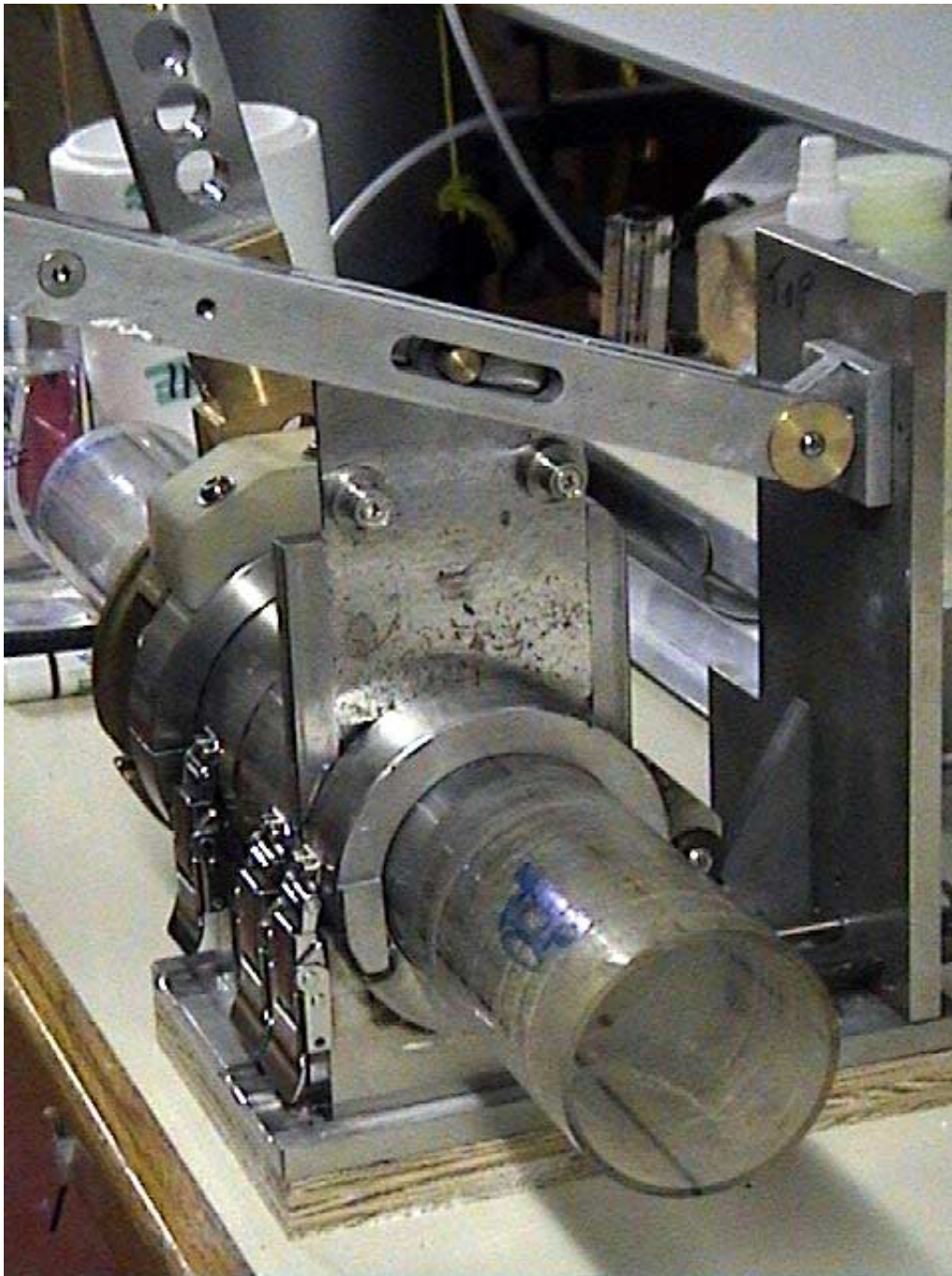
Figure F8. "Bucket" for clean and anoxic subsampling from WRC segments into sterile syringes with the Luer end removed. A 5-cm WRC segment is placed in the middle of the alcohol wiped and flamed bucket in which a steady nitrogen flow maintains anoxic conditions. The uppermost 1 cm is pushed out of the core liner and is cleanly removed. Subcores are then taken from the central part with sterile, cut-off syringes that are subsequently capped with sterile stoppers as shown.
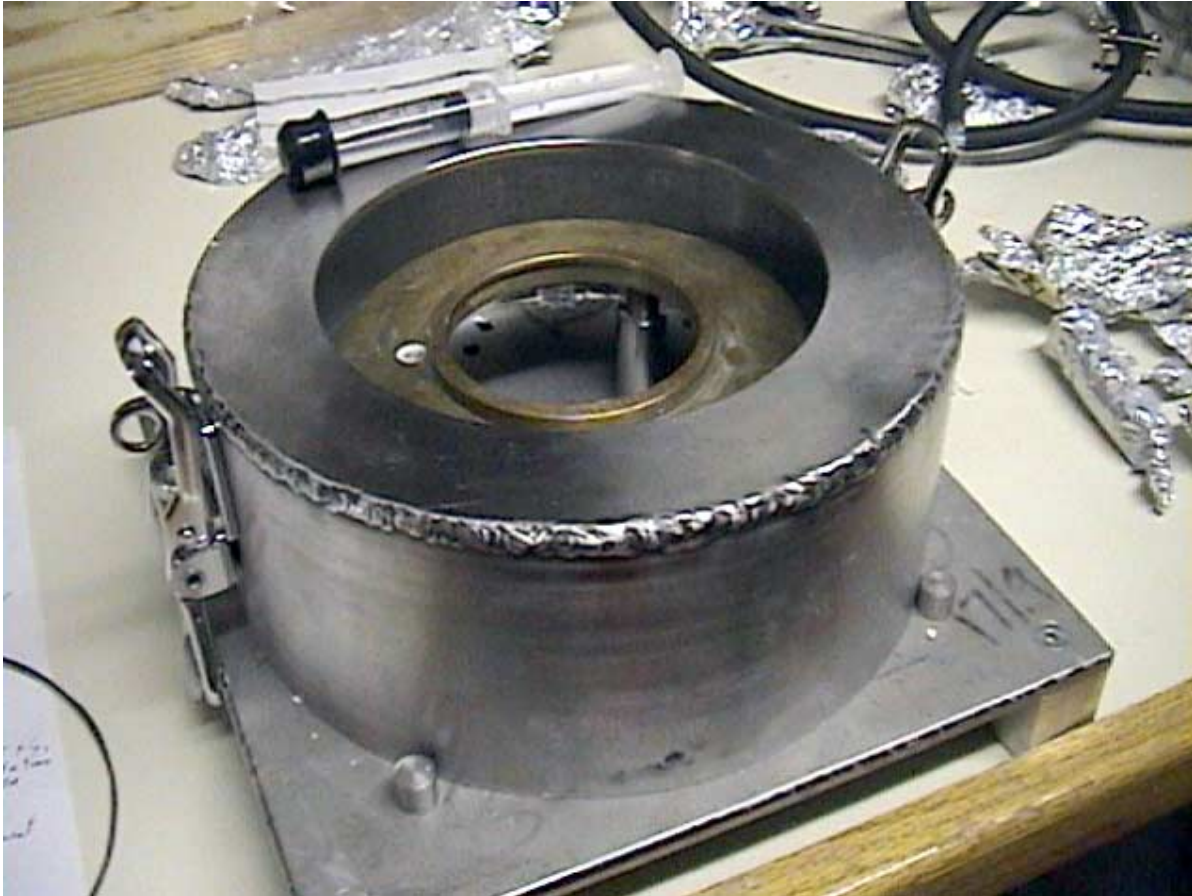
Figure F9. Scheme for inoculation of tubes for most probable number (MPN) counts of prokaryotes. Tubes were filled with 9 mL of sterile medium and were inoculated with either sediment slurry or directly with sediment using a 5-mL syringe with the Luer end removed. The tenfold dilutions were done through three to six steps, sufficient that the last dilutions would probably not contain growing prokaryotes. The tubes showing positive growth after several weeks to months of incubation at a specific temperature were recorded and used to calculate the most probable number of viable cells in the original sample (according to a statistical table). The highest dilutions showing growth were subsequently used as inoculum for new dilution series, with the ultimate purpose of bringing cells into pure culture.
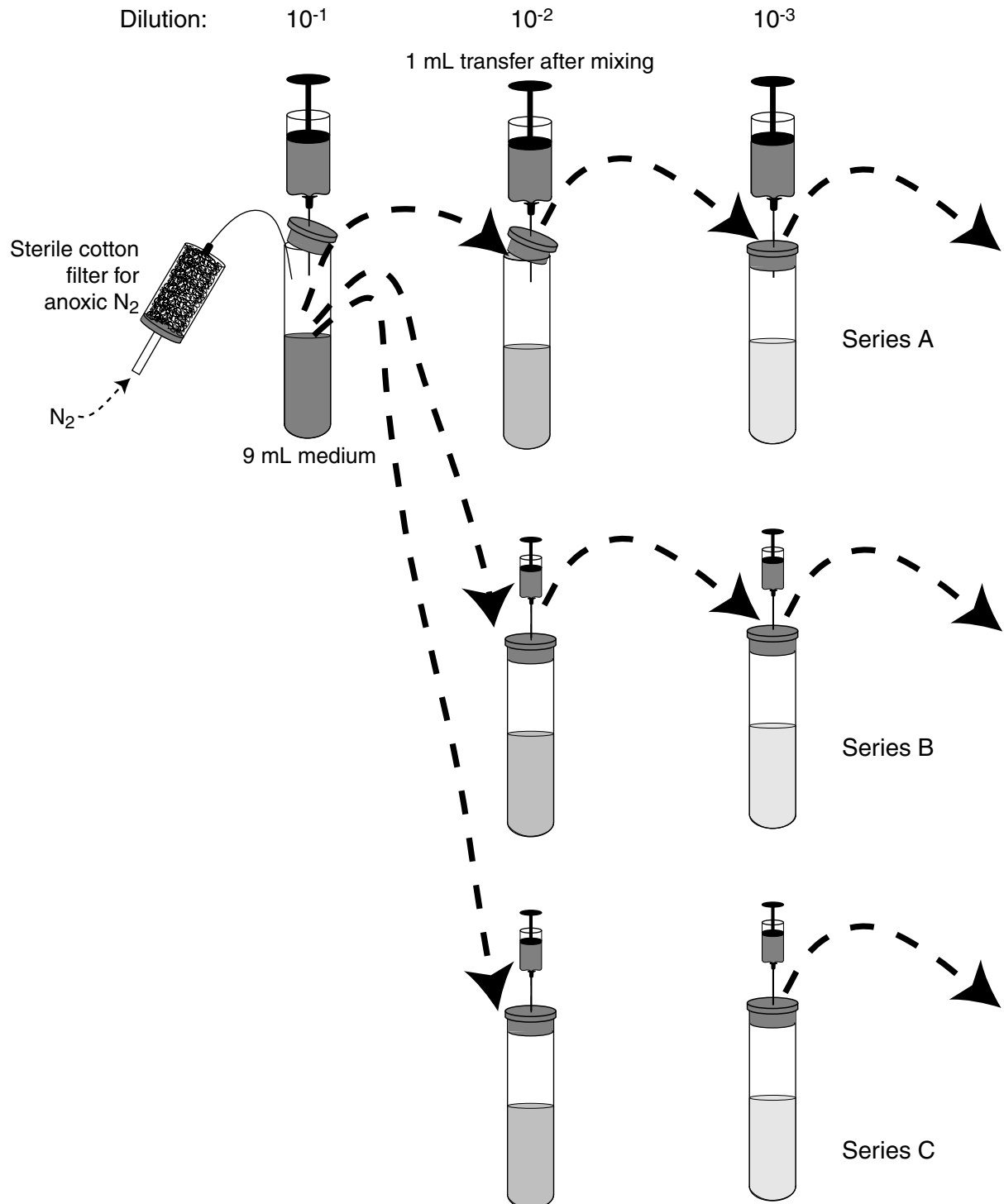
Figure F10. MPN counts with a microtiter plate. On a deep-well microtiter plate, four different slurry samples were diluted in triplicate down to 1:10^6. For each sample, a row remained uninoculated as a control. The wells were sealed with a capmat, and the plate was stored in an anoxic bag with an oxygen-consuming catalyst (Anaerocult A, Merck) and an oxygen indicator.
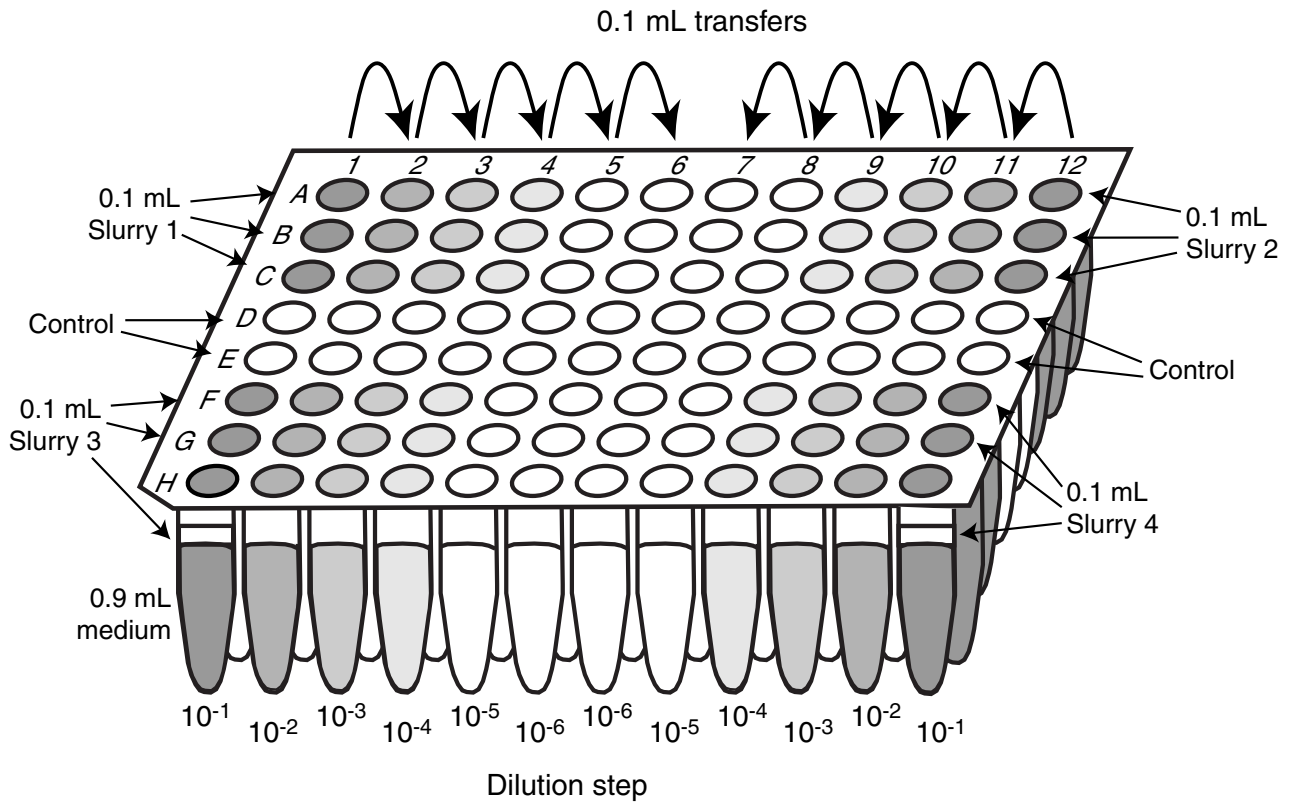
Figure F11. Gradient culture tubes were prepared by fixing 0.5 mL of a monomer medium (Mono) on the bottom with agar. Then, substrate-free mineral medium with agar was added as a spacer, a sediment piece was positioned, and the tube was filled with mineral medium and gassed with nitrogen on ice. MM = marine salts medium.
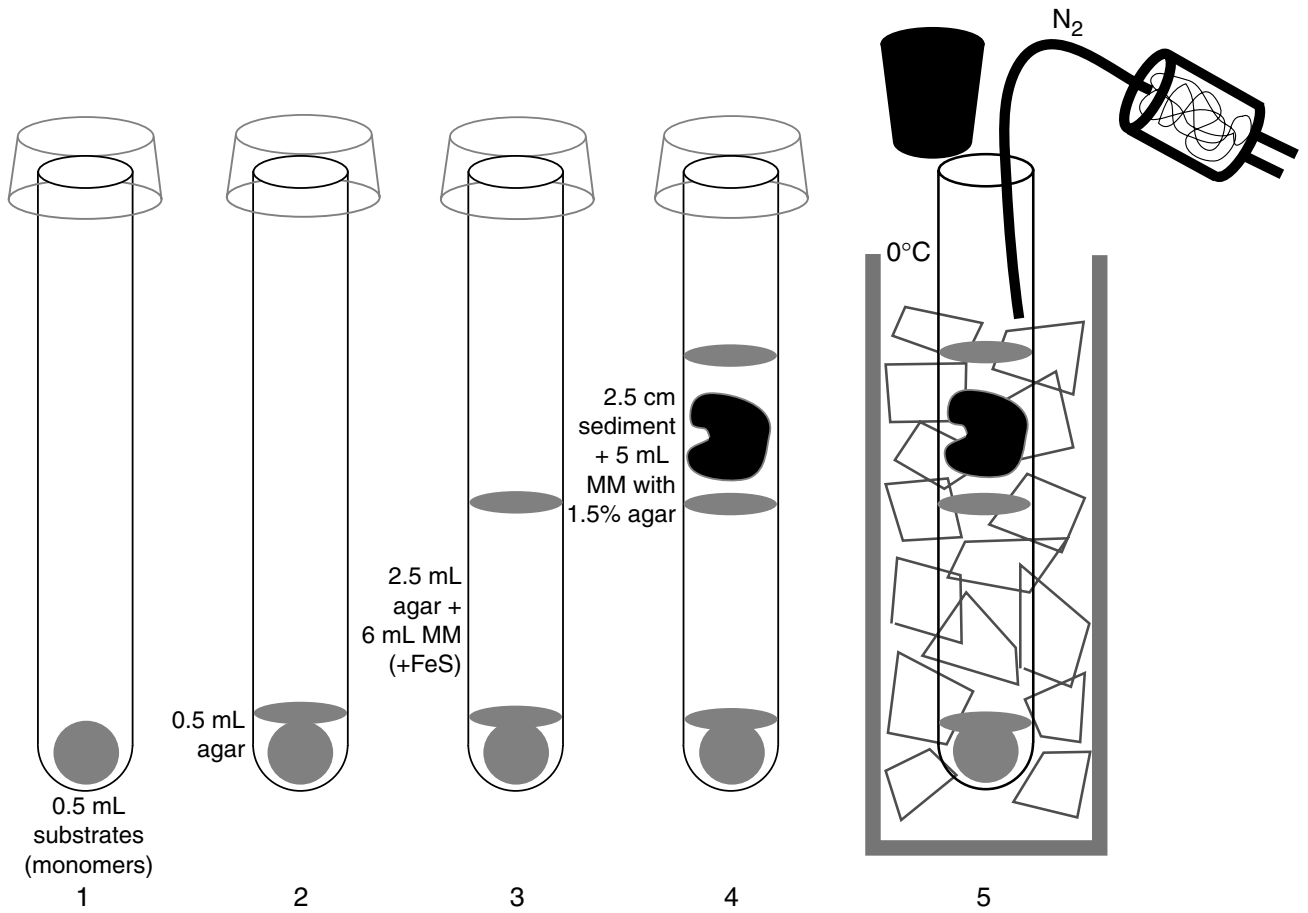
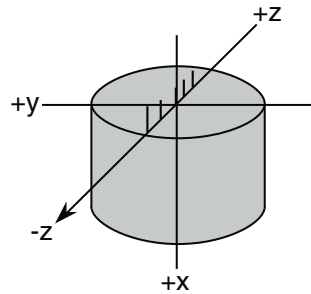**Figure F12.** Infrared thermal imaging camera on cart with reflective shield.

Figure F13. ODP paleomagnetic coordinate system for archive and working halves with radial and vertical overprints shown.

ODP magnetic direction convention
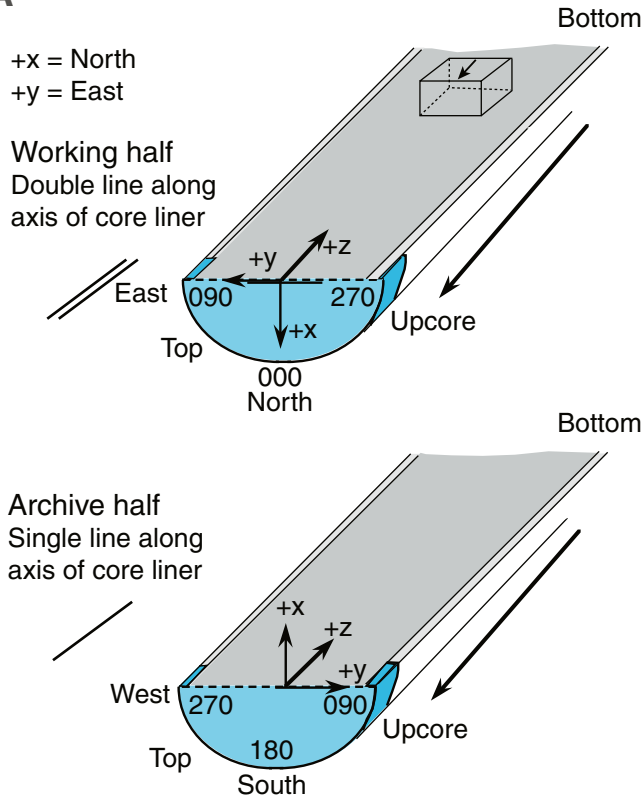
Figure F14. Tool strings used during Leg 201. Close-up of the Formation MicroScanner (FMS) four arms and the 16 individual buttons.
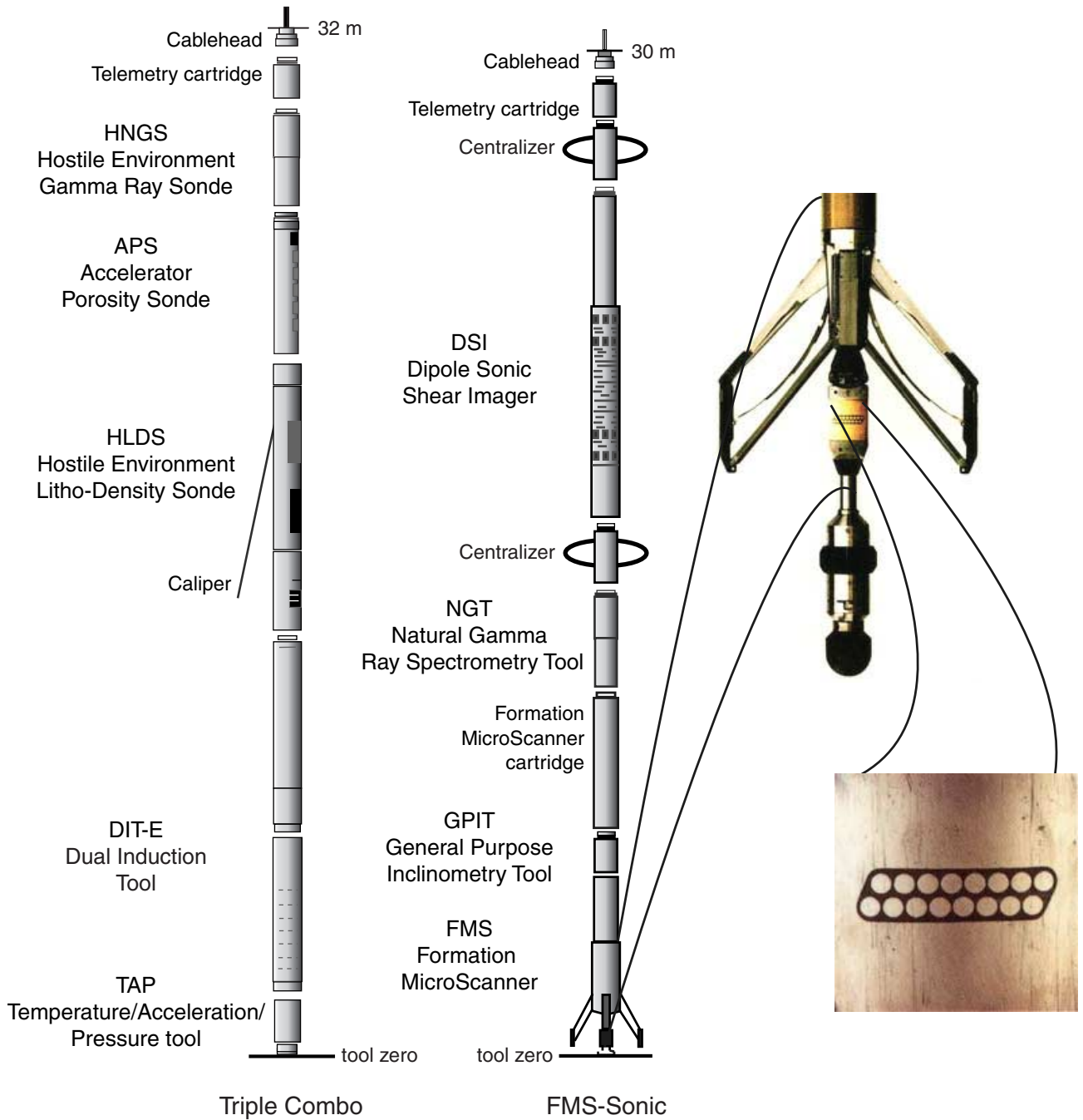
Table T1. Definitions of terms used in microbiology sampling.

Term	Definition
Aseptic	A clinical definition referring to freedom from pathogens. Clinical conditions are not applicable to ODP operations.
Sterile	The most stringent category used during Leg 201. Sterile indicates the absence of contaminating prokaryotic cells that are capable of metabolism and growth and their nucleic acids.
Clean	Defined as giving careful consideration and effort to avoid cross-contamination. May involve ethanol washing, flaming instruments, etc., and may approach sterile conditions.
Anaerobic	A property of organisms indicating the ability to live without oxygen. Also a property of a method ("anaerobic cultivation") or of laboratory cultivation equipment ("anaerobic chambers").
Anoxic	Property of an oxygen-free environment such as used in a glove bag or N_2-flushed sampling bucket.

Table T2. Definitions of sampling codes and packing types.

Codes	Definition
Sampling codes:	
FISH—	FISH and FISH-SIMS
H3S	Tritiated hydrogen turnover experiments
ABTP	Thymidine incorporation, bicarbonate, and acetate turnover rate measurements
O18B	^{18}O stable isotope turnover experiments
PO4B	Determination of ^{18}O in phosphate
SRRF	Sulfate reduction rate measurements
H2S	Hydrogen turnover rate measurements
CNSS	Samples for carbon, nitrogen, and sulfur determination (geochemistry laboratory)
CHNSF	Samples for prokaryotic magnetic particles
BIOM—	Biomarker samples
DIFFF	Core for diffusion experiments
CELLS	Sediment used for isolating individual cells
AODC	Acridine orange direct counts for prokaryotic cell enumeration
FESF	WRC for determination of Fe, Mn, and S solid-phase concentrations, mineralogy, and isotope distributions
SRRWRF	WRC for sulfate reduction, pressure, and temperature experiments
AMO—	Samples for measurements of rates of anaerobic oxidation of methane
HTEW	Enrichments for thermophiles
SLUR	Sediment for master slurry
SLURJ	Enrichments for psychrophilic methanogens
SLURA	Enrichments for psychrophiles
SLURB	Enrichments for sulfate-reducing psychrophiles
FISHWR2	Samples for FISH-SIMS
FISHWR	Samples for FISH-SIMS
DNA—	Samples for microbial molecular analysis
DNAODP	Archived deep-frozen WRC samples for microbial molecular analysis
ATPS	Adenosine triphosphate samples
AIELLO	Residual material from microbiology, used for lithostratigraphic interval and description
PRIEUR	WRC for enrichments
Packing types:	
Polybag	Sterile polyethylene sample bag
Al-bag	Aluminum gas-tight bag
Anaer. jar	N_2-flushed sample jar
Vacuum pack	Air removed from Al bag before heat sealing
Anaerocult A	Small trays of metallic Fe, bicarbonate, and citrate (Merck) that scrub O_2 from a gas-tight bag and produce CO_2 when wetted

Notes: FISH = fluorescent in situ hybridization. SIMS = secondary ion mass spectrometry. WRC = whole-round core. — = additional sample specification may be appended to sample code.

Table T3. Marine medium salts solution used as the basis for psychrophilic and mesophilic media.

Component	Concentration
Distilled water	1000 mL/L
NaCl	24.32 g/L
$MgCl_2 \cdot 6H_2O$	10 g/L
$CaCl_2 \cdot 2H_2O$	1.5 g/L
KCl	0.66 g/L
Na_2SO_4	4.0 g/L
Trace element solution (SL 10)*	1 mL/L
KBr (0.84 M)	1 mL/L
H_2BO_2 (0.4 M)	1 mL/L
$SrCl_2$ (0.15 M)	1 mL/L
NH_2Cl (0.4 M)	1 mL/L
KH_2PO_4 (0.04 M)	1 mL/L
NaF (0.07 M)	1 mL/L
Na_2SeO_3 (10^{-7} M)[†]	1 mL/L
Na_2WoO_4 (10^{-7} M)[†]	1 mL/L

Autoclave, cool under N_2, then add the following from sterile stock solutions:

$NaHCO_3$ (1 M)	30 mL/L
Vitamin solution[‡]	2 mL/L
$FeCl_2$ (1 M) in 0.1-M HCl	0.5 mL/L
Na_2S (1 M)	1.2 mL/L

Notes: Adjust pH to 7.2–7.4 with sterile 1-M HCl or sterile 1-M Na_2CO_3. * = Widdel et al. (1983), † = Widdel (1980). ‡ = mixture of 10 vitamins, concentrated fivefold (after Balch et al., 1979).

Table T4. Media used for cultivation of psychrophiles and mesophiles.

Medium	Components	Concentration	Comments
Mono: monomer	Amino acids: alanine, arginine, asparagine, asparagic acid, cystine, glutamine, glutamic acid, glycine, histidine, isoleucine, leucine, lysine, methionine, phenylalanine, proline, serine, threonine, tryptophane, tyrosine, and valine	0.01 M	Prepare in MM
	Short chain fatty acids (sodium salts): formate, acetate, propionate, butyrate, valerate, and capronate	0.01 M	
	Other organic acids: malate, fumarate, succinate, and lactate	0.01 M	
	n-alcohols: methanol, ethanol, propanol, and butanol	0.01 M	
	Glycerol	0.01 M	
	Glucose	0.01 M	
Poly: polymer	Chitin, xylane, cellulose, and peptone	0.05%	Prepare in MM
Aro: aromatic compounds and long-chain fatty acids	Aromatic compounds (sodium salts): salicylate, 3-OH-benzoate, 3-OH-benzaldehyde, vanillate, vanillin, p-coumarate, ferulate, sinapinate, syringate, and syringaldehyde	0.05 M	Prepare in MM
	Fatty acids (sodium salts): C_{14}–C_{20}	0.05 M	
Lac: lactate	Sodium lactate	5.0 M	Prepare in MM
No SO_4: sulfate-free	Ti(III) citrate	0.5 M	Prepare in MM (omit Na_2SO_4, Na_2S, and $FeCl_2$)
Sed: sediment extract	N-[2-hydroxyethyl]piperazine-N´-[2-ethane-sulfonic acid] buffer	2.38 g/L	Prepare in MM (omit $NaHCO_3$, vitamins, Na_2S, and $FeCl_2$) and adjust pH to 7.2–7.4. Use this solution to extract sediment at 80°C (see **"Enrichments near In Situ Temperatures,"** p. 29).
	To sediment extract, after heating add the following: Vitamins, Na_2S, and $FeCl_2$		
	$NaHCO_3$	0.2 g/L	
A-bas: autotrophic basalt	NaCl	24 g/L	Dissolve salts in deionized water, and autoclave 20 min at 121°C
	$MgCl_2 \cdot 6H_2O$	10 g/L	
	KCl	0.5 g/L	
	Na_2SO_4	4 g/L	
	NH_4Cl	0.25 g/L	
	$CaCl_2$	1.5 g/L	
	KH_2PO_4	0.2 g/L	
AmOx: ammonium oxidizing medium	NH_4Cl	0.64 g/L	Dissolve 10 mg $FeCl_3 \cdot 6H_2O$ in 0.3 mL 1-N HCl, add 10 mL deionized water, and then add and dissolve 60 mg EDTA.*
	KH_2PO_4	0.1 g/L	
	$MgCl_2 \cdot 6H_2O$	0.2 g/L	
	$CaCO_3$	2.0 g/L	
	$FeCl_3 \cdot 6H_2O$ solution	1 mL/L	
NiOx: nitrite-oxidizing medium	$NaNO_2$	0.76 g/L	$NaNO_2$ is used instead of NH_4Cl; the preparation is the same as for AmOx.*
	NH_4Cl	0.64 g/L	
	KH_2PO_4	0.1 g/L	
	$MgCl_2 \cdot 6H_2O$	0.2 g/L	
	$CaCO_3$	2.0 g/L	
	$FeCl_3 \cdot 6H_2O$ solution	1 mL/L	
Methylo: methylotrophs	Agar	15 g/L	Dissolve chemicals in 1 L filtered seawater and autoclave for 20 min at 121°C. After cooling to ~60°C, add 5 mL of sterile-filtered methanol. Pour on agar plates; store plate, wrapped in parafilm, at 4°C to minimize evaporation. Plates are inoculated with 0.1-mL aliquots from sample dilution series made using sterile-filtered seawater.
	NH_4Cl	0.4 g/L	
	KH_2PO_4	0.6 g/L	
	$Na_2HPO_4 \cdot 7H_2O$	1.8 g/L	
	$CaCl_2$	30 mg/L	
	$FeCl_3 \cdot 6H_2O$	1 mg/L	

Notes: MM = marine medium salts solution (see Table **T3,** p. 83). EDTA = disodium ethylenediaminetetraacetate. * = for AmOx and NiOx the chemicals were dissolved in 1 L filtered seawater and the pH was adjusted with HCl or NaOH. The solution was sterilized by autoclaving for 20 min at 121°C. After cooling, 1 mL of sterile-filtered iron(III) solution was added. Sterile tubes with 9 mL medium each were inoculated with 1 mL of a nitrite-oxidizing medium (NiOx).

Table T5. Media used for cultivations at 25°, 50°, and 80°C. (**See table notes.** Continued on next page.)

Medium	Components	Concentration (% wt/vol)	Comments
201-1: Heterotrophic sulfur reducer medium	Yeast extract Peptone Glucose Na_2S Elemental sulfur Wolfe's vitamin solution*	0.1 0.1 0.05 0.05 3	Prepare in MJ under N_2 headspace
201-2: Heterotrophic Fe(III) reducer medium	Yeast extract Peptone Glucose Na_2S Ferrihydrite Magnetite Wolfe's vitamin solution*	0.1 0.1 0.05 0.05 1 1	Prepare in MJ under N_2 headspace
201-3: Heterotrophic nitrate reducer medium	Yeast extract Peptone Glucose Na_2SO_4 $NaNO_3$ Wolfe's vitamin solution*	0.1 0.1 0.05 0.05 1	Prepare in MJ under N_2 headspace
201-4: Heterotrophic sulfate reducer medium	Sodium lactate Sodium acetate Sodium formate Sodium fumarate Glucose Na_2SO_4 Na_2S Cystein-HCl Wolfe's vitamin solution*	0.05 0.05 0.05 0.05 0.05 0.1 0.05 0.05	Prepare in MJ under N_2 headspace
201-5: Autotrophic H_2-oxidizing sulfate reducer medium	$NaHCO_3$ Na_2SO_4 Na_2S Cystein-HCl Wolfe's vitamin solution*	0.15 0.1 0.05 0.05 0.15	Prepare in MJ under 80% H_2 + 20% CO_2 headspace
201-6: Autotrophic $HS^-/S_2O_3^{2-}/S^0$ oxidizing Fe(III) or nitrate reducer medium	$NaHCO_3$ $Na_2S_2O_3$ Elemental sulfur Ferrihydrite $NaNO_3$ Na_2S Wolfe's vitamin solution*	0.15 0.1 3 0.05 0.05 0.025	Prepare in MJ under 70% N_2 + 30% CO_2 headspace
201-7: Micro-aerobic, autotrophic $HS^-/S_2O_3^{2-}/$ S^0 oxidizing Fe(III)/NO_3^- reducer medium	$NaHCO_3$ $Na_2S_2O_3$ Elemental sulfur Ferrihydrite $NaNO_3$ Na_2S Wolfe's vitamin solution*	15 0.1 3 0.05 0.05 0.025	Prepare in MJ under 68.5% N_2 + 28.5% CO_2 + 3% O_2 headspace
201-8: Methanogen medium	$NaHCO_3$ Sodium acetate Sodium formate Methanol Na_2S Cystein-HCl Magnetite Wolfe's vitamin solution*	0.15 0.05 0.05 0.05 0.05 0.05 0.05	Prepare in MJ under 80% H_2 + 20% CO_2 headspace
201-9: Autotrophic NH_4^+ oxidizing Fe(III)/ NO_3^- reducer medium	$NaHCO_3$ NH_4Cl Ferrihydrite $NaNO_3$ $CuSO_4$ Wolfe's vitamin solution*	0.15 0.1 0.1 0.1 0.05	Prepare in MJ under 70% N_2 + 30% CO_2 headspace
201-10: Micro-aerobic, autotrophic NH_4^+ oxidizing Fe(III)/NO_3^- reducer medium	$NaHCO_3$ NH_4Cl Ferrihydrite	0.15 0.1 0.1	Prepare in MJ under 68.5% N_2 + 28.5% CO_2 + 3% O_2 headspace

Table T5 (continued).

Medium	Components	Concentration (% wt/vol)	Comments
	NaNO$_3$	0.1	
	CuSO$_4$	0.05	
	Wolfe's vitamin solution*		
201-11: Extremely halophilic archaea (genus *Haloarcula*) medium	NaCl	20.8	Prepare in MJ under air headspace; pH (25°C) = 7.2
	Yeast extract	1.0	
	MgSO$_4$·7H$_2$O	4.7	
	CaCl$_2$	0.05	
	MnCl$_2$	0.013	
	Wolfe's vitamin solution*		

Notes: MJ = artificial seawater solution (see Table **T6,** p. 87). * = added at 1 mL/L; Freier et al., 1988.

Table T6. MJ solution* used as the basis for 25°, 50°, and 80°C cultivation media.

Component	Concentration
NaCl	30 g/L
Na_2HPO_4	0.14 g/L
$CaCl_2·2H_2O$	0.14 g/L
$MgCl_2·6H_2O$	7.58 g/L
NH_4Cl	0.25 g/L
KCl	0.33 g/L
$Na_2SeO_3·5H_2O$	0.5 mg/L
$Fe(NH_4)_2(SO_4)_2·6H_2O$	0.01 g/L
Wolfe's trace mineral solution[†]	10 mL/L

Notes: MJ = artificial seawater solution. * = Leg 201 version. Adjust pH to 7.2 at 25°C with NaOH. † = Balch et al. (1979).

Table T7. Media used for cultivations at 60°C.

Medium	Components	Concentration	Comments
Ferm: heterotrophic fermenter	Na_2S Cystein HCl A) glucose, fructose, and mannose B) xylose and ribose C) xylose and ribose + 25 mM $NaS_2O_3^{2-}$	2 mM 2 mM 0.2%, wt/vol each 0.2%, wt/vol each 0.2%, wt/vol each	Prepare in MSSM under N_2 headspace MPNs pH$^{60°C}$ = 7.95 Enrichments pH$^{60°C}$ = 8.8
H_2/HCO_3^-: acetogenic/methanogenic	Na_2CO_3	15 mM (total 25–30 mM with near-equal amount from sea salt)	Prepare in MSSM under 100% H_2 headspace MPNs pH$^{60°C}$ = 7.95 (8.0) Enrichments pH$^{60°C}$ = 8.8
H_2/HCO_3^-/FeIII: iron(III) reducer	Na_2CO_3 Fe(III)	15 mM (total 25–30 mM with near-equal amount from sea salt) 90 mM	Prepare in MSSM under 100% H_2 headspace MPNs pH$^{60°C}$ = 7.8 Enrichments pH$^{60°C}$ = 8.3
H_2/HCO_3^-/MnIV: manganese(IV) reducer	Na_2CO_3 $Mn(IV)(HO,O)_x$	15 mM (total 25–30 mM with near-equal amount from sea salt) 15 mM	Prepare in MSSM under 100% H_2 headspace MPNs pH$^{60°C}$ = 7.8 (Site 1231 only) Enrichments pH$^{60°C}$ = 7.8 (selected sites)
C-18 lipo: lipolytic microorganism	Cystein HCl Yeast extract (total of 0.2%) Na_2SO_4 Olive oil	0.15 g 0.15% 10 mM 20 ml	Prepare in MSSM under N_2 headspace MPNs pH$^{60°C}$ = 7.8 Enrichments pH$^{60°C}$ = 9
SRB: heterotrophic sulfate reducer	Na_2SO_4 Cystein HCl A) Lactate Acetate Propionate Butyrate B) Benzoate (only pH = 8)	20 mM 2 mM 25 mM 25 mM 5 M 5 mM 10 mM	Prepare in MSSM under N_2 headspace Enumerations pH$^{60°C}$ = 8.0 Enrichments pH$^{60°C}$ = 8.6 Enumerations pH$^{60°C}$ = 8.0
Chlor: chlorate reducer	Na_2CO_3 (total bicarbonate/carbonate to be determined later) Na chlorate	15 mM (total 25 mM + equal unknown amount from the salt) 5 mM	Prepare in MSSM under 100% H_2 headspace
methylamine: methylamine-utilizing methanogens	Na_2S Cystein HCl Methylamine Trimethylamine	2 mM 2 mM 2.5 mM 2.5 mM	Prepare in MSSM under 100% N_2 headspace MPNs pH$^{25°C}$ = 8.4 Enrichments pH$^{25°C}$ = 8.4 Site 1229 only; use at 60° and 25°C
CH_4-ace: acetate-utilizing methanogens	Na_2S Cystein HCl Acetate	2 mM 2 mM 5 mM	Prepare in MSSM under 100% N_2 headspace MPNs pH$^{25°C}$ = 8.3 Enrichments pH$^{25°C}$ = 8.3 Site 1229 only; use at 60° and 25°C

Notes: MSSM = marine sea-salt media (see Table T8, p. 89). * = Freier et al., 1988. pH$^{25°C}$ = pH meter was calibrated with the electrode and buffer equilibrated at room temperature. No correction for the sea salt concentration was made. pH$^{60°C}$ = pH meter, with temperature probe connected, was calibrated with the electrode and buffer equilibrated for 30 min at 60°C. Buffer values were temperature corrected. No correction was made for the sea salt.

Table T8. MSSM used as the basis for 60°C cultivations.

Component	Concentration
Sigma sea salt	40 g/L
$Na_2HPO_4 \cdot H_2O$	2 mM/L
Modified (Ni, W) Wolfe's mineral	0.25 mL/L
Wolfe's vitamin solution*	5 mL/L
Yeast extract	0.5%/L
NH_4Cl	0.1%/L
Na_2CO_3	25 mM/L

Notes: MSSM = marine sea-salts media. Prepare solution in deionized, distilled water. * = Freier et al., 1988. pH (25°C) was adjusted to 8.5 and 10.0, respectively, before autoclaving. The pH after autoclaving and at 60°C is ~0.5 to 1.2 pH units (depending on media supplements) more acidic.

Table T9. Media definitions.

Medium	Definition	pH
Sed	Sediment extract medium	
Mono	Medium with 36 monomers as substrate	
Poly	Medium with polymers	
Aro	Medium with aromatic compounds and long-chain fatty acids	
B-sed	Medium with sediment extract and sulfate-reducing bacteria in the background	
B-poly	Medium with polymers and sulfate-reducing bacteria in the background	
Rad	Radiotracer MPN with sediment extract medium and labeled sulfate	
Grad	Gradient culture with monomers as substrate	
FERM-Glyc: 8.0	Heterotrophic full-strength seawater medium containing 0.2% glucose, fructose, and mannose as substrate	8.0
FERM-Glyc: 8.8	Heterotrophic full-strength seawater medium containing 0.2% glucose, fructose, and mannose as substrate	8.8
FERM-Xyl: 8.0	Heterotrophic full-strength seawater medium containing 0.2% (wt/vol) each xylose and ribose as substrate	8.0
FERM-Xyl: 8.8	Heterotrophic full-strength seawater medium containing 0.2% (wt/vol) each xylose and ribose as substrate	8.8
SRB: 8.0	Heterotrophic (lactate/acetate) sulfate reducing medium	8.0
SRB: 8.6	Heterotrophic (lactate/acetate) sulfate reducing medium	8.6
SRB benz: 8.0	Heterotrophic (benzoate) sulfate reducing medium	8.0
$H_2/HCO_3^-/FeIII$: 7.9	H_2-containing medium with Fe(III) as electron acceptor for chemolithoautotrophic iron reducers	7.9
$H_2/HCO_3^-/FeIII$: 8.5	H_2-containing medium with Fe(III) as electron acceptor for chemolithoautotrophic iron reducers	8.5
$H_2/HCO_3^-/MnIV$: 7.8	H_2-containing medium with Mn(IV) as electron acceptor for chemolithoautotrophic manganese reducers	7.8
H_2/HCO_3^-: 7.8	Chemolithoautotrophic medium for methanogens and acetogens	7.8
H_2/HCO_3^-: 8.8	Chemolithoautotrophic medium for methanogens and acetogens	8.8
C-18-lipo: 7.8	Olive oil-containing media for lipolytic bacteria	7.8
C-18-lipo: 9.0	Olive oil-containing media for lipolytic bacteria	9.0
Chlor: 7.8	Acetate- and chlorate-containing medium for chlorate reducers	7.8
201-1	Heterotrophic sulfur reducer medium	
201-2	Heterotrophic Fe(III) reducer medium	
201-3	Heterotrophic nitrate reducer medium	
201-4	Heterotrophic sulfate reducer medium	
201-5	Autotrophic H_2-oxidizing sulfate reducers medium	
201-6	Autotrophic $HS^-/S_2O_3^{2-}/SE$–oxidizing Fe(III) or nitrate reducer medium	
201-7	Microaerobic autotrophic $HS^-/S_2O_3^{2-}/SE$–oxidizing Fe(III)/NO_3^- reducer medium	
201-8	Methanogen medium	
201-9	Autotrophic NH_4^+-oxidizing Fe(III)/NO_3^- reducer medium	
201-10	Microaerobic autotrophic NH_4^+-oxidizing Fe(III)/NO_3^--reducer medium	
201-11	Extremely halophilic archaea (genus Haloarcula) medium	
AmOx	Aerobic chemolithoautotrophic ammonia-oxidizing nitrifying bacteria	
NiOx	Aerobic chemolithoautotrophic nitrite-oxidizing nitrifying bacteria	
Methylo	Aerobic Cl^- compound utilizing methylotrophic bacteria	
Methylamine	Methylamine-utilizing methanogen medium	
Fe(III) red	Acetate-containing medium with Fe(III) as electron acceptor for heterotrophic iron reducer	
Mn(IV) red	Acetate-containing medium with Mn(IV) as electron acceptor for heterotrophic manganese reducer	
CH_4-ace	Methanogen meduim with acetate	
Sed-SO_3	SO_3^{2-} supplemented Sed, Mono, Poly	
Mono-SO_3	SO_3^{2-} supplemented Sed, Mono, Poly	
Poly-SO_3	SO_3^{2-} supplemented Sed, Mono, Poly	
Past-Sed	Pasteurized medium for spore-forming bacteria	
Past-Mono	Pasteurized medium for spore-forming bacteria	
Mono-O_2	Aerobic mono	

Table T10. Enrichment inoculations, Holes 1225A and 1226B.

Enrichment	Comments
Sample 201-1225A-35H-CC, incubated at 10°C:	
Tube 1: with $Fe(OH)_3$ and MnO_2	Control
Tube 2: no $Fe(OH)_3$ and MnO_2	Control
Tube 3: with $Fe(OH)_3$ and MnO_2	Basalt piece taken directly from the sample, not washed, not crushed
Tube 4: with $Fe(OH)_3$ and MnO_2	First basalt piece washed with salt solution, crushed in chips
Tube 5: no $Fe(OH)_3$ and MnO_2	First basalt piece washed with salt solution, crushed in chips
Tube 6: with $Fe(OH)_3$ and MnO_2	Second basalt piece washed with salt solution, crushed in chips
Tube 7: no $Fe(OH)_3$ and MnO_2	Second basalt piece washed with salt solution, crushed in chips
Tube 8: with $Fe(OH)_3$ and MnO_2	First basalt piece washed with salt solution, additional washing with 3-M HCl for 1 min, crushed in chips
Tube 9: no $Fe(OH)_3$ and MnO_2	First basalt piece washed with salt solution, additional washing with 3-M HCl for 1 min, crushed in chips
Tube 10: with $Fe(OH)_3$ and MnO_2	First basalt piece washed with salt solution, crushed in very small chips
Tube 11: no $Fe(OH)_3$ and MnO_2	First basalt piece washed with salt solution, crushed in very small chips
Core 201-1226B-47X, incubated at 23°C:	
Tube 1: with $Fe(OH)_3$ and MnO_2	Control
Tube 2: no $Fe(OH)_3$ and MnO_2	Control
Tube 3: with $Fe(OH)_3$ and MnO_2	Sediment, FISH WRC
Tube 4: no $Fe(OH)_3$ and MnO_2	Sediment, FISH WRC
Tube 5: with $Fe(OH)_3$ and MnO_2	Basalt piece washed
Tube 6: no $Fe(OH)_3$ and MnO_2	Basalt piece washed
Tube 7: with $Fe(OH)_3$ and MnO_2	Basalt piece washed with salt solution, additional washing with 3-M HCl for 1 min
Tube 8: no $Fe(OH)_3$ and MnO_2	Basalt piece washed with salt solution, additional washing with 3-M HCl for 1 min
Tube 9: with $Fe(OH)_3$ and MnO_2	Control
Tube 10: no $Fe(OH)_3$ and MnO_2	Control
Tube 11: with $Fe(OH)_3$ and MnO_2	Washing solution
Tube 12: no $Fe(OH)_3$ and MnO_2	Washing solution

Note: WRC = whole-round core, FISH = fluorescent in situ hybridization.

Table T11. Sample preparation and fixation for FISH analysis.

Solution	Components	Concentration	Comments
Phosphate buffered saline (PBS):	NaCl	8 g/L	Prepare in 1L of sterile-filtered water; adjust pH to 7.2–7.5
	KCl	0.2 g/L	
	KH_2PO_4	0.2 g/L	
	$Na_2HPO_4 \cdot 2H_2O$	1.44 g/L	
4% Formaldehyde/PBS buffer:	A) PBS buffer:	25 mL/L	Prepare at least once per week; adjust pH to 7.2–7.5
	37% formaldehyde solution	2.7 mL	
	B) PBS buffer:	25 mL	Heat to 60°C
	Paraformaldehyde	1 g/L	White powder (toxic)
	NaOH	A few microliters	To dissolve paraformaldehyde

Fixation procedure	Comments
Add 1.5 mL 4% formaldehyde/PBS buffer to 0.5-cm sample or cell suspension in a 2-mL screwtop microfuge tube.	Samples are taken in 5-mL syringes from cold room on a regular basis and are fixed immediately.
Keep cold on ice for 1–24 hr.	This can also be done at 4°C or room temperature.
Centrifuge at 13,000 rpm in the table-top centrifuge.	Optimally at 4°C.
Remove supernatant, add 1.5 mL PBS buffer, and suspend cells/sediment on whirl mixer.	
Repeat these two washing steps to remove formaldehyde.	
Centrifuge at 13,000 rpm in the table-top centrifuge.	Optimally at 4°C.
Remove supernatant and add 1.5 mL of 1:1 mix of PBS buffer/100% ethanol.	
Resuspend sample on whirl mixer.	Use samples directly for FISH or keep at –20°C for a maximum of several months. The mixture should remain liquid and therefore must not be frozen at –80°C. Storage at 4°C is also possible for some time.

Note: FISH = fluorescence in situ hybridization.

Table T12. Hybridization procedure for FISH analysis.

Solution	Components	Volume	Final concentration
Hybridization buffer:	5-M NaCl	360 µL	900 mM
	1-M Tris/HCl (pH = 7.5)	40 µL	20 mM
	Formamide	Vol% depending on probe	
	Distilled H$_2$O	Add to 2 mL	
	10% SDS	2 µL	0.1%
Washing buffer:	5-M NaCl	Depending on %*	900 mM
	Formamide in hybridization buffer (see above)	*	
	1-M Tris/HCl (pH = 7.5)	1 mL	20 mM
	0.5-M EDTA	500 µL	5 mM
	Distilled H$_2$O	Add to 50 mL	
	10% SDS	50 µL	0.01%

Hybridization procedure	Comments
Resuspend sample and transfer 20–100 µL of aliquot to 500 µL of a 1:1 mix of PBS/ethanol in a 2-mL microfuge tube.	Optional dilution step.
Sonicate aliquot for 20–30 s at low intensity using 1-s sonication pulses. If required, the sonicated sample can be further diluted.	For fine-particle sediments, vortexing is fine.
Place GTTP filter (pore size = 0.2 µm) on glass filter surface (shiny side on top). Add 10–100 µL of fixed suspension to 5–10 mL of PBS buffer into the filter tower and filter this volume onto the membrane filter.	
Air-dry filters can be stored in Petri dishes at –20°C until hybridization.	The procedure can be paused here if shipboard schedule demands it.
Prepare 2 mL of hybridization buffer in a microfuge tube (see above).	
For the hybridization mixtures, add 2 µL of probe working solution (50–200 ng probe/µL) to 18 µL of hybridization buffer in a 0.5-mL microfuge tube.	Keep probe solutions dark and on ice.
Cut filter in quarters with razor blade and place the pieces on a glass slide, upside facing up.	Do not touch filter surface with fingers. Several filters can be placed on one slide and simultaneously hybridized with the same probe. Quarters may be marked with incisions if different probes will be applied.
Put a piece of blotting paper into a 50-mL polyethylene tube and soak it with the remaining hybridization buffer.	*JOIDES Resolution* toilet paper can serve as blotting paper.
Add hybridization mix on the samples, one 20-µL drop per filter section, and place the slide with filter sections into the polyethylene tube in a horizontal position.	Make sure the hybridization mix does not run off.
Incubate 1.5–2 hr at 46°C.	Do not exceed 3 hr.
Prepare 50 mL of washing buffer (see above) in a polyethylene tube and pre-warm at 48°C in a water bath.	
Quickly transfer filter sections into preheated washing buffer and incubate for 15 min at 48°C.	
Pour washing buffer with filter sections into a Petri dish. Pick filter sections and rinse them by placing them into a Petri dish with distilled H$_2$O for several seconds, then let them air-dry on blotting paper.	
For counterstaining, put filter sections on glass slides (side with bacterial cells facing up), cover with 50 µL DAPI solution (1 mg/L), and incubate for 3 min. Afterward, rinse filter sections briefly in distilled H$_2$O, wash them for several seconds in 80% ethanol to remove unspecific DAPI staining, and air-dry.	
Filters on glass slide are embedded in a 4:1 mix of Citifluor and Vecta Shield and are covered with a cover slide. The filter sections have to be completely dried before embedding; otherwise, a fraction of cells will detach during inspection.	It is also possible to use Citifluor or Vecta Shield without a coverslip.
Double-stained and air-dried preparations as well as filters mounted on slides can be stored in the dark at –20°C for several months without substantial loss of probe fluorescence.	
Probe-conferred fluorescence fades much more rapidly than DAPI fluorescence in the microscopic image. For counting, it is therefore safer to first quantify specifically stained cells in green excitation and subsequently all cells from the same field in UV excitation (DAPI).	

Notes: FISH = fluorescence in situ hybridization. PBS = phosphate buffered saline, DAPI = 4′,6-diamindino-2-phenylindole, Tris = tris(hydroxymethyl)amino methane, SDS = sodium dodecyl sulfate, EDTA = disodium ethylenediaminetetraacetate, UV = ultraviolet. * = concentrations of NaCl in washing buffer (48°C) are given at different concentrations of formamide in hybridization buffer (46°C). The first number of each pair is the formamide concentration in the buffer (vol%) and the second number is the NaCl concentration in the washing buffer (mM): 1, 900; 5, 636; 10, 450; 15, 318; 20, 225; 25, 159; 30, 112; 35, 80; 40, 56; 45, 40; 50, 28; 55, 20; 60, 14; 65, 10; 70, 7; 75, 5; 80, 3.5.

Table T13. Sample preparation and ^{13}C experiments for FISH-SIMS.

Sample preparation:

   A 5-cm^3 subcore was injected into a sterile 50-mL centrifuge tube containing 10 mL 1:1 ethanol/PBS solution; the
      suspension was stored at –20°C.

   At select sites:

      1) A 5-cm^3 subcore was fixed in 3.7% formaldehyde in PBS for 1–24 hr.

      2) The sample was washed twice with PBS (using standard FISH protocols; see Table T11, p. 92, FISH fixation).

      3) After washing, the sample was stored at –20°C in a sterile 50-mL centrifuge tube containing 10 mL 1:1 ethanol/PBS.

   The residual round core from which the subcores had been removed was frozen at –80°C for storage.

Experiments on incorporation of ^{13}C-labeled substrates:

   1) Sterile bottles with 10 mL of reduced DGH media (see below) and a labeled substrate were sealed in an 80% N_2/20%
      CO_2 atmosphere during precruise preparation. In some cases, the headspace also included 20 mL of nonlabeled
      methane.

   2) For each sample, 10 mL of 25% sediment slurry was injected into an experiment bottle and incubated at 4°C.

   3) To terminate incubation, 40 mL of headspace gas was removed (at the rear of the ship to avoid ^{13}C contamination of
      geological samples), and 20 mL of filtered ethanol was injected into the bottle. Samples were then stored at –20°C.
      Postcruise, samples will be fixed in 3.7% formaldehyde, washed with filtered PBS buffer, and ultimately stored in a 1:1
      ethanol/PBS solution at –20°C.

Each bottle had one of three possible ^{13}C labeled substrates: glucose, acetate, or methane. Glucose and acetate
   concentrations were 1 mg/mL of media with half of the substrate ^{13}C labeled, whereas methane concentrations were 20
   mL/per serum bottle with one-fourth of the methane ^{13}C labeled.

DGH media preparation*:

Component:	NaCl	Concentration:	10 g/500 mL
	Na_2SO_4		1.5 g/500 mL
	KH_2PO_4		0.1 g/500 mL
	NH_4Cl		0.15 g/500 mL
	KCl		0.15 g/500 mL
	$CaCl_2 \cdot H_2O$		0.1 g/500 mL
	$MgCl_2 \cdot 6H_2O$		0.15 g/500 mL
	Wolfe trace elements		
	0.2% $(NH_4)_2Fe(SO_4)_2$		0.5 mL/500 mL
	10% NaOH[†]		1.5 mL/500 mL
	ddH_2O		500 mL/500 mL

Notes: DGH media were prepared prior to the cruise. * = 0.25 g NaS was added to reduce the media. The
   media was dispensed in an anoxic environment with 10 mL added to each 125-mL serum vial. † = media
   was degassed with N_2/CO_2, neutralizing the NaOH and resulting in a final pH of 6.8.

Table T14. Procedure for sulfate reduction measurements.

1) In the cold room, whole-round cores were cleanly and anoxically cut and transferred into an N_2-gassed (filtered) sampling bucket. After removing 1 cm of surface sediment, four 5-cm^3 subsamples were taken with sterile syringes with the Luer end removed.

2) The syringes were closed gas-tight with sterile butyl rubber and placed in a N_2-filled aluminum bag for transport.

3) After transfer to the radioisotope van, the syringe samples were kept at in situ temperature in a thermostated incubator to equilibrate before further processing.

4) To start the experiment, 10 μL of a $^{35}SO_4^{2-}$ solution was injected by microsyringe into three of the four parallel syringes through the butyl rubber stopper and along a 1- to 2-cm line in the middle of the sediment. The radiotracer stock solution for injections was made up as $^{35}SO_4^{2-}$ in sterile saline solution (containing sulfate concentrations appropriate for the site and depth) by diluting a commercial stock solution (Perkin-Elmer/NEN, 185 MBq).

5) Three types of blank measurements were performed:
   a. From each vial of radiolabeled solution, a 10-μL aliquot was fixed in Zn acetate solution.
   b. At selected depths, a "time-zero" control was performed on a syringe subsample. The radiolabeled sulfate was injected into the sediment and allowed to incubate for ~30 min (<1% of the total incubation time), after which time it was fixed in Zn acetate solution.
   c. A third "killed" control consisted of adding the sediment to the Zn acetate solution. After 30 min, 10 μL of $^{35}SO_4^{2-}$ was then added to the Zn acetate-sediment slurry.
   All controls are distilled and counted as for live samples.

6) The radiolabeled syringe samples were placed in N_2-filled gas bags. Two squares of an oxygen scrubber tray (Anaerocult A; Merck) were added to the bag and wetted. The bags were sealed and placed in the appropriate incubator.

7) At the conclusion of the incubation period, ranging from 7 to 42 days, the bacterial activity was stopped by mixing the sediment into pre-tared 50-mL Corning screw-top vials containing 14 mL of 20% (w/v) zinc acetate solution. The zinc solution kills the bacteria and preserves any free sulfides by precipitating them as ZnS.

8) These fixed samples were transported frozen to the shore-based institute in Bremen, Germany, for further processing. For safe handling and transport, all vials were packed break-proof in original styrofoam, double-bagged, and packed in a International Air Transport Association approved carton (shipped as UN2910-Radioactive material, excepted package—limited quantity of material).

9) The processing (as modified from Fossing and Jørgensen, 1989) involves the separation of the injected $^{35}SO_4^{2-}$ and the reduced ^{35}S-sulfide (in total reduced inorganic sulfides) in chromous acid solution by cold distillation of the released $H_2^{35}S$ into Zn-acetate traps. By measurement of the $^{35}SO_4^{2-}$ and $Zn^{35}S$ radioactivities on a liquid scintillation counter, the fraction of sulfate reduced during the experiment can be determined. This is converted to total amount of sulfate reduced per unit time (nmol $SO_4^{2-}/cm^3/day$) based on the interstitial water concentration of sulfate, the porosity, and the incubation time (cf. Jørgensen, 1978).

Table T15. Procedure for methanogenesis and acetate turnover (^{14}C tracer) experiments.

---

1) Syringe subsamples (5 mL) sealed with a butyl suba-seal were stored in an N_2-flushed anaerobic jar during storage in the constant temperature room.

2) These subsamples were transferred to the isotope van and kept at in situ temperature in an appropriate incubator to equilibrate.

3) The control sample for each sediment depth was prechilled (4°C) prior to injection with the isotope.

4) An injection microsyringe was flushed thoroughly with the isotope (at least five times), ensuring that there were no air bubbles. The subsample was placed in the injection rig, followed by the injection microsyringe, by inserting the needle through the suba-seal. An exact amount of isotope was delivered evenly along the length of the sediment in the sample by pulling back the barrel of the microsyringe completely to the stop. When removing the microsyringe from the rig, the volume injected was checked.

5) Volumes of radiotracer injected into each syringe subsample and for each individual tracer was 7.2 µL (4.8 µCi) of sodium ^{14}C-bicarbonate solution (Amersham, UK; diluted with filter-sterilized [0.2 µm], degassed distilled water) or 7.4 µL (1.5 µCi) of undiluted [1-(2)^{14}C] acetate; Amersham UK).

6) After injections, all controls were immediately frozen while all other samples were incubated in gas-tight aluminum bags containing an oxygen scrubber (Anaerocult A, Merck) for a set time (2 hr to 7 days for acetate, 0.75–35 days for bicarbonate) before activity was stopped by freezing.

7) At the conclusion of the injections, the microsyringe was thoroughly rinsed with distilled water (10 times) to remove residual isotope.

8) Frozen samples were transported frozen to the shore-based institute in Bristol, UK, for further processing.

Table T16. Procedure for leucine ^{3}H tracer experiments.

1) Using cut-off syringes, the sediment cores were subsampled cleanly while maintaining anoxic conditions in the cold room. The cleanly stoppered syringes were transported cold to the radioisotope van.

2) The ^{3}H-leucine ([L-(3,4,5-^{3}H[N])]; Perkin Elmer, NET-460A) was injected. Formalin was injected into one core prior to the radiotracer as a time-zero control.

3) After incubation, the sediment was extruded into a vial containing a 2% formalin solution and stored cold.

4) The fixed samples were transported to the Graduate School of Oceanography, University of Rhode Island, for processing for both protein production and microautoradiography.

5) Protein will be extracted using 5% trichloroacetic acid (TCA). After extraction, the samples will be rinsed with 5% TCA followed by 80% ethanol using centrifugation (Smith and Azam, 1992).

6) The samples will be radioassayed.

Microautoradiography:

7) Prokaryotes in the fixed samples will be separated from the bulk sediment by sonicating samples with sodium pyrophosphate and/or Tween-80.

8) The supernatant containing the cells will be filtered onto 0.2-μm polycarbonate filters and placed on a glass microscope slide covered with photographic emulsion (Kodak NTB-2).

9) The emulsion will be exposed to the radioactive samples for a period of weeks to months and processed.

10) The samples will be counterstained with acridine orange and observed with transmitted light and epifluorescence microscopy. The comparison of images for bacterial and silver grain distributions will show which cells have actively incorporated radiolabeled leucine.

Table T17. Procedure for H_2 turnover experiments (^3H tracer).

---

1) Tritiated sodium borohydride ($NaBH_4$) was used to generate tritiated hydrogen gas (HT). Sodium borohydride [$^3H^-$] (NET-023A; Perkin Elmer) was dissolved into 0.1-N NaOH. $NaBH_4$ is stable in alkaline conditions and decomposes upon acidification. 1.8 nmol of $NaBH_4$ was transferred to 20-mL headspace vials and sealed (crimp cap). The solution was acidified by injecting H_2SO_4 through the septum.

2) Syringe subsamples of sediment cores were placed into 2.0-mL headspace vials. After sealing, the vials were flushed with He gas and transferred to the radioisotope van.

3) Tritiated H_2 gas ($\times$ 400 μL) was injected into the vials through the septum.

4) The vials were incubated at near in situ temperature in the radioisotope van.

5) The incubations were terminated by injecting $HgCl_2$ and returned for shore-based processing.

Table T18. Radioisotopes used during Leg 201.

Radioisotope	Strength (MBq)
^{35}S-labeled SO$_4^{2-}$	500
^{14}C-labeled HCO$_3^-$	185
^{14}C-labeled acetate	74
^{3}H-labeled thymidine	555
^{3}H-labeled NaBH$_4$ for H$_2$	740

Table T19. Spill control and decontamination procedure.

Spill control:

1) Notify individuals in the area of the spill's occurrence, location, size, and nature.

2) Wash your hands if they have become contaminated as part of the spill incident.

3) Put on personal protective equipment including gloves, lab coat, and eyewear to prevent contamination of the hands, body, and clothes.

4) Define and confine the spill zone. Mark off the spill area with chalk, markers, tape, etc., and restrict traffic to that area.

5) Individuals in the spill zone must stay within the zone until monitored for contamination, then decontaminated and/or established as free of contamination. Individuals within the spill zone should move to the area of lowest exposure.

6) If the spill is of dry material, dampen the spill slightly. This will avoid the spill's spread due to air currents. Be careful not to spread the spill area unnecessarily. If the spill is liquid material, cover the liquid with absorbent material to limit the spread of contamination.

7) Shut off fans or air circulation devices. Direct exhaust ventilation should be left operating.

8) Notify the resident marine technician, the Laboratory Officer, and/or the Staff Scientist.

9) Once the spill zone is controlled, then emphasis shifts to decontamination procedures. Begin decontamination procedures as soon as possible. Cleaning agents are in the spill kit in the radioisotope van. Start at the periphery of the contaminated area and work inward. Systematically reduce the contaminated area. Avoid using large circular cleaning motions, as this practice will increase the spill's surface area. Mitigation of liquid ^{14}C spills can be enhanced by rinsing the area with acid. This should only be done in a well-ventilated area.

10) Put all contaminated disposable materials into plastic bags for appropriate disposal later. Contaminated equipment should be bagged or set aside in dish pans for later decontamination.

11) Survey meter and/or wipe tests should be used to monitor the progress of the decontamination.

Personal decontamination:

1) Administer first aid if necessary.

2) Be aware of personal and ethnic privacy issues when decontaminating personnel.

3) Define the area of contamination. Note the quantity of contamination, size, and location.

4) Begin decontamination procedures with the mildest form of cleansing. Skin should be decontaminated using mild soap and water. The decontamination should progress to using soap with a mild abrasive, soft brush, and water, then to a mild organic acid (citric acid or vinegar). Nails or hair may need to be trimmed to complete decontamination. Decontamination procedures should not break the skin.

5) Shoe bottoms can be decontaminated by lifting off the contamination with adhesive tape. Duct tape works especially well for decontaminating the soles of shoes.

6) Survey meter and/or wipe tests should be used to monitor the progress of the decontamination.

7) Record the size, location, and degree of contamination. Give this information to the radiation safety officers and notify them of the spill. Notify the resident marine technician, the Laboratory Officer, and/or the Staff Scientist.

8) Put all contaminated disposable materials into plastic bags for appropriate disposal later.

9) Clothing may need to be removed or changed. Contaminated clothing may be bagged and retained for decay or disposal.

Table T20. Expected depths of significant gas at proposed Leg 201 drill sites.

Site	Proposed site	Previous site	Hole depth (mbsf)	>1000 μL/L headspace CH$_4$ (mbsf)	Gas voids (mbsf)
1225	EQP-1A	851	320	—	—
1226	EQP-2A	846	420	—	—
1227	PRB-2A	684	160	40–base	—
1228	PRU-1A	680	200	—	—
1229	PRU-2A	681	200	30–90	58–62
1330	PRU-3A	685	300	10–base	30 and lower
1331	PRU-4A	321	114	—	—

Note: — = significant gas not expected.

Table T21. Measurements made by wireline tool strings.

Tool string	Tool	Measurement	Sampling interval (cm)	Approximate vertical resolution (cm)
Triple combination	HNGS	Spectral gamma ray	15	51
	APS	Porosity	5 and 15	43
	HLDS	Bulk density	2.5 and 15	38
	DITE	Resistivity	15	150/90/60
	TAP	Temperature	1 per s	NA
		Tool acceleration	4 per s	NA
		Pressure	1 per s	NA
Formation MicroScanner	NGT	Natural gamma ray	15	46
(FMS)-sonic combination	GPIT	Tool orientation	0.25 and 15	NA
	DSI	Acoustic velocity	15	61–120*
	FMS	Microresistivity	0.25	0.5

Notes: * = depending on mode. All tool and tool string names (except the TAP tool) are trademarks of Schlumberger. For additional information about tool physics and use consult ODP Logging Services at **www.ldeo.columbia.edu/ BRG/ODP.** See Table **T4,** p. 84, for explanations of acronyms used to describe tool strings and tools. NA = not applicable.

Table T22. Acronyms and units used for wireline tools.

Tool	Output	Description	Units
DIT-E		Dual Induction Tool	
	IDPH	Deep induction phasor-processed resistivity	Ωm
	IMPH	Medium induction phasor-processed resistivity	Ωm
	SFLU	Shallow spherically focused resistivity	Ωm
DSI		Dipole Sonic Imager	
	DTCO	Compressional wave delay time (Δt)	ms/ft
	DTSM	Shear wave delay time (Δt)	ms/ft
	DTST	Stoneley wave delay time (Δt)	ms/ft
FMS		Formation MicroScanner	
	C1, C2	Orthogonal hole diameters	in
	P1AZ	Pad 1 azimuth	Degrees
		Spatially oriented resistivity images of borehole wall	
GPIT		General Purpose Inclinometer Tool	
	DEVI	Hole deviation	Degrees
	HAZI	Hole azimuth	Degrees
	F_x, F_y, F_z	Earth's magnetic field (three orthogonal components)	Degrees
	A_x, A_y, A_z	Acceleration (three orthogonal components)	m/s^2
HLDS		Hostile Environment Litho-Density Sonde	
	RHOM	Bulk density	g/cm^3
	PEFL	Photoelectric effect	b/e$^-$
	LCAL	Caliper (measure of borehole diameter)	in
	DRH	Bulk density correction	g/cm^3
HNGS		Hostile Environment Gamma Ray Sonde	
	HSGR	Standard (total) gamma ray	API units
	HCGR	Computed gamma ray (HSGR minus uranium contribution)	API units
	HFK	Potassium	wt%
	HTHO	Thorium	ppm
	HURA	Uranium	ppm
NGT		Natural Gamma Ray Spectrometry Tool	
	SGR	Standard total gamma ray	API units
	CGR	Computed gamma ray (SGR minus uranium contribution)	API units
	POTA	Potassium	wt%
	THOR	Thorium	ppm
	URAN	Uranium	ppm
TAP		Temperature/Acceleration/Pressure tool	°C, m/s^2, psi